

NORTHWESTERN UNIVERSITY

Pedunculo pontine Glutamatergic Input to Substantia Nigra Pars
Compacta Dopamine Neurons

A DISSERTATION

SUBMITTED TO THE GRADUATE SCHOOL
IN PARTIAL FULFILLMENT OF THE REQUIREMENTS

for the degree

DOCTOR OF PHILOSOPHY

Field of Neuroscience

By

Daniel James Galtieri

Evanston, Illinois

December 2017

Abstract

Pedunculopontine Glutamatergic Input to Substantia Nigra Pars Compacta Dopamine Neurons

Daniel James Galtieri

In vivo, substantia nigra pars compacta (SNc) dopaminergic neurons exhibit three spiking patterns – irregular, regular, and bursting. These distinct modes of activity are thought to underlie the different roles that dopamine (DA) plays in target structures within the basal ganglia. In particular, burst spiking in SNc DA neurons is thought to be a key signaling event in the circuitry controlling goal-directed behavior. The spontaneous transitions from single-spike mode to burst-spiking observed *in vivo* are lost, however, in *ex vivo* brain slices. Rather, a regular 1-4 Hz firing modes dominates SNc neuron activity in *in vitro* preparations. This change has been attributed to the loss of afferent input to SNc cells that would otherwise be present in an intact animal. Synaptic glutamatergic activity is thought to be especially important for burst generation, with much of the literature focusing on the interaction between N-methyl-D-aspartate receptors (NMDARs) and the intrinsic oscillatory activity in SNc neurons as a mechanism that promotes burst firing.

To date, however, the role of specific neural networks in shaping spike patterning in SNc DA neurons has gone largely unstudied, due in part to the inability to selectively activate different inputs to the SNc. To begin filling this gap, SNc glutamatergic synapses arising from pedunculopontine nucleus (PPN) neurons were characterized using a mixture

of optical and electrophysiological approaches. We found that PPN glutamatergic synapses are made primarily on the soma and proximal dendritic tree of these cells, placing these inputs in an ideal location to influence spike generation. Indeed, optogenetic stimulation of PPN axons reliably evoked spiking in SNc DA neurons that was dependent upon AMPA receptors but not NMDA receptors. Moreover, burst stimulation of PPN axons was faithfully followed by SNc DA neurons, suggesting that PPN-evoked burst spiking of SNc neurons *in vivo* may not only be extrinsically triggered but extrinsically patterned as well.

Acknowledgements

I would first like to express my sincere gratitude to my Ph.D. advisor, Dr. D. James Surmeier, for his support and mentorship throughout my time at Northwestern. I am continuously amazed by Jim's work ethic and scientific knowledge and will forever be grateful for the opportunity to work with him. I would also like to thank the rest of my thesis committee – Drs. Mark Bevan, Geoffrey Swanson, and Paul Schumacker – for their insights and guidance throughout my dissertation work.

I would like to thank the Surmeier lab at large for their time, their enthusiasm, and most importantly their friendship over these last many years. On this last point I cannot strongly enough express how much I have enjoyed the time spent discussing science, along with so many other things, with those in the lab. Graduate school can be a very lonely place at times, but it was often the interactions with those around me that made the long days less daunting. For this I would like to particularly thank the other graduate students with whom I overlapped – Drs. Garry Cooper, Chad Estep, and Allie Melendez – as well as Drs. David Wokosin, Javier Sanchez, and Enrico Zampese, all of whom have been instrumental to my successes in graduate school.

I am further grateful for the many years of kind words and support I have received from my friends and family. In particular, I thank my parents, who have been an unwavering source of encouragement all of my life. They have been a constant point of reassurance to counter any moments of frustration and doubt experienced over these

several years. I truly could not have asked for two more loving, caring individuals in my life, and for that I am eternally grateful.

Finally, I cannot begin to express my appreciation for all of the love and support provided by my girlfriend, Kate Hinckley, over these last several years. She has endured far too many late nights and weekends with me at the lab or otherwise working and yet has remained a constant source of positivity and optimism throughout our time together. It's finally over! What's next?

Special Contributions

I would like to additionally thank Drs. Chad Estep and David Wokosin for their assistance in the work presented here. Both provided numerous pieces of scientific and technical knowledge and guidance throughout this project, without which this work would not have been possible.

List of Abbreviations

1P	One-photon
2PLSM	Two-photon laser-scanning microscopy
AAV9	Adeno-associated virus serotype 9
AC	Adenylyl cyclase
aCSF	Artificial cerebrospinal fluid
AHP	Afterhyperpolarization
AIS	Axon initial segment
AMPA	Alpha-amino-3-hydroxy-5-methyl-4-isoxazolepropionic acid
AMPAR	Alpha-amino-3-hydroxy-5-methyl-4-isoxazolepropionic acid receptor
AP	Action potential
BG	Basal ganglia
BK	Large-conductance, calcium-activated potassium channel
cAMP	Cyclic adenosine monophosphate
ChR2	Channelrhodopsin-2
CB1	Cannabinoid receptor 1

ChAt	Choline acetyltransferase
CNO	Clozapine-N-oxide
DA	Dopamine
DAT	Dopamine transporter
DBS	Deep-brain stimulation
DREADD	Designer receptors exclusively activated by designer drugs
dV/dt	Change in voltage / change in time
EC	Endocannabinoid
f	Fluorescence
f_{max}	Maximum Fluorescence
FI	Frequency-current
GABA	Gamma-Aminobutyric acid
GAD	Glutamic acid decarboxylase
GaAsP	Gallium arsenide phosphide
GECI	Genetically-encoded calcium indicator
GPCR	G-protein coupled receptor
GPE	Globus pallidus, external segment

GPI	Globus pallidus, internal segment
HCN	Hyperpolarization-activated, cyclic nucleotide-gated channel
hSyn	Human synapsin I
I _A	A-type potassium current
ISI	Interspike interval
IV	Current-voltage
K _d	Dissociation constant
K _{ir}	Inward-rectifying potassium channel
LC	Locus Coeruleus
LDT	Laterodorsal tegmental nucleus
L-NAME	L-N ^G -nitroarginine methyl ester
LTD	Long-term depression
LTP	Long-term potentiation
LTS	Low-threshold spike
mAHP	Medium afterhyperpolarization
MLR	Mesencephalic locomotor region
NAc	Nucleus accumbens

NMDA	N-methyl-D-aspartate
NMDAR	N-methyl-D-aspartate receptors
NOS	Nitric oxide synthase
PBS	Phosphate buffered saline
PD	Parkinson's disease
PFA	Paraformaldehyde
PKA	Protein kinase A
PMT	Photomultiplier tube
PPN	Pedunculo pontine nucleus
PPR	Paired-pulse ratio
RAS	Reticular activating system
REM	Rapid-eye movement
R_f	Retention Value
RMS	Root mean square
RPE	Reward prediction error
RRF	Retrosubthalamic field
RuBi	Ruthenium-bipyridine-trimethylphosphine

SC	Superior colliculus
sCRACM	Subcellular channelrhodopsin assisted circuit mapping
SK	Small-conductance, calcium-activated potassium channel
SNc	Substantia nigra pars compacta
SNr	Substantia nigra pars reticulata
SPN	Spiny projection neuron
STEP	Striatal-enriched phosphatase
STN	Subthalamic nucleus
TH	Tyrosine hydroxylase
TTX	Tetrodotoxin
VGCC	Voltage-gated calcium channel
VGLUT2	Vesicular glutamate transporter-2
V _m	Membrane Voltage
VTA	Ventral tegmental area

Dedication

To my parents

Table of Contents

ABSTRACT	2
ACKNOWLEDGEMENTS	4
LIST OF ABBREVIATIONS	6
DEDICATION	11
LIST OF FIGURES	13
CHAPTER 1: Background	14
Anatomy of the Basal Ganglia	14
The role of dopamine in the dorsal striatum	19
Activity patterns in dopamine neurons	23
Synaptic connectivity in the SNc	29
The Pedunculo pontine Nucleus	34
CHAPTER 2: Pedunculo pontine glutamatergic neurons control spike patterning in substantia nigra dopaminergic neurons	47
Introduction	47
Results	50
Discussion	70
Future Directions	76
MATERIALS AND METHODS	82
REFERENCES	89
APPENDIX A: Additional Projects	126
APPENDIX B: Development of Analysis Tools	131

List of Figures

2.1: Optogenetic stimulation of PPN afferents evokes glutamatergic responses in SNc DA neurons.....	51
2.2: ChR2 is functionally expressed in PPN neuron	52
2.3: Electrical stimulation of PPN glutamatergic afferents to SNc.....	53
2.4: Glutamatergic receptors at the PPN-SNc synapse are composed of GluA2-containing AMPARs and GluN2B/D-containing NMDARs	55
2.5: PPN glutamatergic synapses preferentially target proximal portions of the SNc dendritic tree	58
2.6: Validation of the spatial resolution for sCRACM functional mapping	59
2.7: Evoked-spike probability is related to stimulus intensity	61
2.8: PPN glutamatergic input is capable of generating burst firing in SNc DA neurons	62
2.9: Features of PPN-evoked spikes depend on the phase of SNc DA neuron pacemaking cycle	65
2.10: Effect of SK inhibition on PPN stimulation of SNc DA neurons.....	67
2.11: PPN-evoked spikes reliably invade the axon.....	70
A.1: Data visualization with PVDataTools.....	130
A.2: Pacemaking analysis with PVDataTools.....	131
A.3: PyMinis workflow	132
A.4: Application for calcium oscillation analysis	134
A.5: Application for FI and IV analysis	135

Chapter 1: Background

Dopamine (DA) has been identified as a critical signal for a range of behaviors, including motor control, action selection, reward, and reinforcement learning, with pathology in the DA system being implicated in neuropsychiatric and neurodegenerative diseases ranging from schizophrenia to Parkinson's disease. As such, it is one of the most widely studied neuromodulators in the brain, having stimulated tens of thousands of studies since its discovery as a neurotransmitter by Arvid Carlsson in the 1950s (Carlsson, 1959; Benes, 2001). Many of these studies are concerned with elucidating how the activity in the neural systems that generate this signal is governed. This subsequently necessitates both an understanding of the circuitry in which DA transmission plays an important role as well as an examination of the underlying physiology of the cells that produce this important messenger.

Anatomy of the Basal Ganglia

General Overview

The basal ganglia (BG) are composed of a series of highly interconnected nuclei through which cortical and thalamic information is filtered in order to generate appropriate, task-oriented behavioral responses to intrinsic and extrinsic stimuli (Albin et al., 1989; Cisek and Kalaska, 2010; Redgrave et al., 2010; Schultz, 2016a). This flow of information begins at the striatum, which acts as the primary input structure for the BG circuit (McGeer et al., 1977; Gerfen and Wilson, 1996; Smith et al., 1998; Bolam et al.,

2000). The striatum is composed almost entirely (~90%) of medium-sized, densely spined GABAergic cells called spiny projection neurons (SPNs) that act as the sole output of the striatum to the other BG nuclei (Gerfen and Wilson, 1996; Smith et al., 1998; Gerfen and Surmeier, 2011).

SPNs are subdivided into two main groups based, in part, on expression of either dopamine D₁ or D₂ receptors (Gerfen et al., 1990; Le Moine et al., 1991; Surmeier et al., 1996; Gertler et al., 2008). In the canonical model of the BG these two subpopulations make up distinct pathways based upon their projection targets: The D₁-class SPNs, forming the direct pathway, send projections to the BG output structures of the GPI (globus pallidus internal segment) and SNr (substantia nigra pars compacta), while D₂-class SPNs project to the GPE (globus pallidus external segment) as part of the indirect pathway (Albin et al., 1989; Gerfen and Wilson, 1996; Smith et al., 1998; Surmeier et al., 2007). As the name implies, D₁ SPNs have a direct influence on BG output by inhibiting GABAergic projections from the GPI and SNr to the thalamus, thereby disinhibiting thalamic projections to areas of the cortex, particularly motor cortex (Albin et al., 1989; Nakano, 2000; Surmeier et al., 2007; Kravitz et al., 2010). In contrast, information passing through the indirect pathways requires multiple steps before reaching the BG output structures. Activation of D₂ SPNs results in inhibition of the GABAergic GPE, which projects to the STN (subthalamic nucleus). This subsequently disinhibits the STN, which sends glutamatergic projections to the GPI and SNr (Miller and DeLong, 1987; Bergman et al., 1994; Bevan et al., 2002). The total effect, then, of indirect pathway activation is an increase in BG output, resulting in a decrease in thalamic input to cortical motor areas (Albin et al., 1989; Nakano, 2000;

Surmeier et al., 2007, p. 200; Kravitz et al., 2010). These dichotomous effects have coined the terms “Go” and “No-go” for these two pathways, as the direct pathway is generally associated with the production of appropriate actions while the indirect pathway is attributed with suppressing unwanted behaviors (Albin et al., 1989; Nakano, 2000; Surmeier et al., 2007).

Included in this canonical model of BG circuitry are the midbrain DA nuclei of the substantia nigras pars compacta (SNc) and ventral tegmental area (VTA), whose activity serves to modulate the striatal SPNs (Albin et al., 1989; Nicola et al., 2000; Surmeier et al., 2007; Gerfen and Surmeier, 2011). While the VTA primarily projects to ventral striatum as well as portions of the prefrontal cortex, the SNc provides the majority of DA input to the dorsal striatum (Andén et al., 1966; Björklund and Dunnett, 2007), and is subsequently the primary focus for the work discussed here.

The substantia nigras pars compacta

The SNc exists as part of a continuous group of dopaminergic nuclei in the mesencephalon that also includes the retrorubral field (RRF) and ventral tegmental area (Dahlstroem and Fuxe, 1964; German and Manaye, 1993; Nelson et al., 1996). The majority of DA signaling in the brain originates from this relatively small region, historically referred to as the mesotelencephalic dopamine system (White, 1996; Gardner and Ashby, 2000).

Anatomically the SNc resides along the dorsal edge of the SNr (Hardman et al., 2002). The rostral portion of the SNc is bounded by the STN, while caudally it is bordered by the RRF. Medially the SNc is bounded by the VTA and the medial lemniscus. In rodents,

each unilateral SNc is composed of approximately 7,000 – 9,000 tyrosine hydroxylase (TH; rate limiting enzyme in DA synthesis) positive neurons (Oorschot, 1996; Nair-Roberts et al., 2008; Baquet et al., 2009). The SNc also has a sizable population of GABAergic neurons, which account for approximately 29% of the cell population in the nucleus (Nair-Roberts et al., 2008). Studies have also observed the presence of VGLUT2 (vesicular glutamate transporter-2) positive neurons in the most medial and caudal portions of the SNc (Yamaguchi et al., 2013). In contrast to the VTA, where a subpopulation of TH+ neurons also express VGLUT2 (Kawano et al., 2006; Yamaguchi et al., 2011; Li et al., 2013), there is virtually no overlap of TH+ and VGLUT2+ cells in the SNc (Yamaguchi et al., 2013).

The SNc can be subdivided along both dorsal-ventral and medial-lateral axes based on cellular morphology and expression patterns of various proteins, particularly the calcium binding protein calbindin-D28k. The most ventral SNc DA neurons tend to be the largest, with soma sizes ranging between 20 and 30 μm . These cells generally have 3-5 primary dendrites, at least one of which extends deeply into the SNr (Gerfen, 1984; González-Hernández and Rodríguez, 2000; Yetnikoff et al., 2014). Having a larger portion of their dendritic tree within the SNr, ventral tier SNc DA neurons also exhibit a higher percentage of GABAergic to glutamatergic synapses than dorsal tier SNc DA neurons (Henny et al., 2012). Ventral tier cells also show a complete lack of calbindin expression, although some have been shown to express the calcium binding protein parvalbumin (German et al., 1992; Fu et al., 2012). In contrast, dorsal tier SNc neurons are somewhat smaller, with somas ranging between 15 and 20 μm in diameter and dendrites that largely remain within the SNc (Grace and Onn, 1989). A low percentage ($\sim 2\%$, in mouse) of dorsal

tier neurons are calbindin positive (Fu et al., 2012). More medial portions of the SNc show a much higher fraction (~21%, in mouse) of calbindin positive neurons (Gerfen et al., 1985; Gerfen, 1992; Barrot et al., 2000; Fu et al., 2012).

The axons of SNc DA neurons are unmyelinated, with a diameter of $<0.5 \mu\text{m}$ (Grace and Onn, 1989; Smiley et al., 1992; Matsuda et al., 2009). They are found to originate both from the soma as well as from primary dendrites, sometimes many dozens of microns away from the soma (Grace and Onn, 1989; Häusser et al., 1995; Blythe et al., 2009; Matsuda et al., 2009). Projections from the SNc form the nigrostriatal pathway, through which the SNc provides the bulk of the dopaminergic input to the dorsal striatum (Lavoie and Parent, 1991; Gerfen and Wilson, 1996). On their way to their target SNc axons follow a somewhat tortuous path, often passing through portions of the SNr and STN before finally traveling through the internal capsule and entering the striatum (Grace and Onn, 1989; Matsuda et al., 2009). Along this path SNc axons form virtually no local collaterals, with the exception being for short collaterals formed within the GPe (Matsuda et al., 2009). Once in the striatum, though, SNc axons form extensive arborizations. Analysis of the axonal arbors of individual SNc has found the total axonal length for these cells within striatum to range between approximately 40 to 60 cm, with the arbor of a single cell occupying a maximum of 5.7% of the total striatal volume (Matsuda et al., 2009). Estimates place the number of synapses formed by these collaterals at upwards of 400,000, with an individual SNc DA neuron influencing, on average, 75,000 striatal neurons (Wickens and Arbuthnott, 2005; Matsuda et al., 2009; Moss and Bolam, 2009). This number of synapses is many times that of other individual cells in the BG, including even neighboring VTA neurons, which each

form an estimated 12,000-30,000 synapses within target structures (Moss and Bolam, 2009; Bolam and Pissadaki, 2012). In addition to this massive divergence in input from the SNc, there is a significant amount of overlap in terms of the number of DA neurons, estimated at anywhere between 90 and 200, from which a single striatal cell may receive input (Matsuda et al., 2009). The resulting synaptic architecture is one in which every glutamatergic synapse in the striatum is in a position to be influenced by a site of DA release (Moss and Bolam, 2008, 2009). These structural properties are crucial to the important modulatory role DA plays in the physiology of the striatum.

The role of dopamine in the dorsal striatum

In the broadest sense, the purpose of DA signaling in the striatum is to facilitate action selection and goal-directed behavior (Schultz, 2007, 2016a). This is accomplished through bi-directional modulation of the striatal direct and indirect pathways (Nicola et al., 2000; Surmeier et al., 2007; Gerfen and Surmeier, 2011). Dopamine's dichotomous role in the striatum is mediated by the expression of different DA receptors, which have opposing effects on both the intrinsic excitability and synaptic gain in D₁-class and D₂-class SPNs.

In contrast to neurotransmitters that directly affect the activity of neurons through the opening of ion channels (ionotropic receptors), all DA receptors are metabotropic; i.e. they are coupled to intracellular signaling cascades that subsequently modulate the excitability of the cell (Kebabian and Greengard, 1971; Cools and Rossum, 1976; Greengard, 2001). D₁- and D₂-family receptors couple to G-proteins (G_s/G_{olf} and G_i, respectively) that have opposing effects on the same signaling pathway: D₁ (and D₅) receptors increase the

activity of adenylyl cyclase (AC), thereby increasing cyclic adenosine monophosphate (cAMP) levels which then activates protein kinase A (PKA), while D₂ (and D₃, D₄) receptors decrease PKA activity through inhibiting AC and subsequently cAMP production (Kebabian, 1978; Onali et al., 1985; Monsma et al., 1990; Senogles, 1994; Vallone et al., 2000). In D₁ expressing SPNs the consequence of DA receptor activation is an increased propensity to fire action potentials (APs) due to an increase in depolarizing currents through L-type calcium channels and a decrease in outward, hyperpolarizing potassium currents (Surmeier and Kitai, 1993; Surmeier et al., 1995; Galarraga et al., 1997; Vilchis et al., 1999). In contrast, in indirect pathways SPNs D₂ activation results in a suppression of firing through inhibition of sodium and L-type Ca²⁺ channels and an increase in outwards K⁺ currents (Surmeier and Kitai, 1993; Greif et al., 1995; Schiffmann et al., 1998; Hernández-López et al., 2000; Olson, 2005; Day et al., 2008; Higley and Sabatini, 2010).

DA signaling also plays an important role in modulating the glutamatergic cortical and thalamic input to striatal SPNs. The elevation of cytosolic PKA levels associated with D₁ receptor activation can regulate the trafficking of glutamate receptors by acting on proteins such as Fyn (a tyrosine kinase), STEP (striatal-enriched phosphatase), and DARPP-32 (Snyder et al., 2000; Flores-Hernández et al., 2002; Dunah et al., 2004; Sun et al., 2005; Braithwaite et al., 2006; Hallett et al., 2006). D₁ signaling has also been shown to enhance NMDA currents in SPNs, likely through enhancement of L-type calcium channels (Cepeda et al., 1993; Nicola and Malenka, 1998). Conversely, D₂ receptor activation has been shown to decrease the amplitude of AMPA currents, and reduces presynaptic release of glutamate (Cepeda et al., 1993; Bamford, 2004; Hernández-Echeagaray et al., 2004).

In addition to this acute regulation of glutamatergic input to SPNs, DA signaling is also critical for plasticity at these synapses. Antagonism of D₁ receptors has been shown to occlude long-term potentiation (LTP; i.e. the increase in strength of a particular synapse) at corticostriatal synapses in direct pathway SPNs, although the particular mechanisms for this are not well understood (Pawlak and Kerr, 2008; Shen et al., 2008). Similarly, D₂ receptors are thought to mediate long-term depression (LTD; i.e. the decrease in strength of a particular synapse) in indirect pathway SPNs (Wang et al., 2006; Kreitzer and Malenka, 2007; Shen et al., 2008). This LTD is dependent upon postsynaptic production of endocannabinoids (EC), which then bind to presynaptic CB1 receptors in order to decrease glutamate release probability (Kreitzer and Malenka, 2007; Shen et al., 2008). D₂ receptor activation facilitates this EC production, potentially through suppression of adenosine A_{2a} receptor signaling (Fuxe et al., 2007; Shen et al., 2008; Higley and Sabatini, 2010; Lerner et al., 2010). This dynamic potentiation and depotentiation of, in particular, the corticostriatal synapses has been proposed to be an important mechanism underlying the types of motor learning and behavioral conditioning for which the striatum is known to be a central player (Balleine et al., 2007; Kreitzer and Malenka, 2008; Cisek and Kalaska, 2010; Gerfen and Surmeier, 2011).

Tonic vs. phasic dopamine signaling

In order to both ensure proper functioning of striatal circuits as well as signal behaviorally relevant events, DA transmission in the striatum operates on two relatively distinct timescales. There exists a tonic background level of DA (approximately 5-20 nM) that does not directly correlate with movement initiation or external stimuli (Dugast et al.,

1994; Garris and Wightman, 1994; Wightman and Robinson, 2002). Despite the lack of obvious temporal association with any particular behavior, this tonic signal is crucial to maintaining normal SPN physiology and the overall integrity of the BG, a point that is best illustrated in cases where this background DA activity is absent. With the loss of striatal DA associated with the degeneration of SNc DA neurons seen in Parkinson's disease (PD) comes a bevy of pathologies related to striatal dysfunction (Albin et al., 1989; DeLong, 1990; Redgrave et al., 2010). The most obvious of these are the cardinal motor symptoms of PD, all of which are associated with an inability to generate movement (Jankovic, 2008). This hypokinesia is predictably explained by a bias towards activity in the "No-go" pathway and away from the "Go" pathway resulting from the loss of dopaminergic tone at D₂ and D₁ SPNs respectively (Albin et al., 1989; DeLong, 1990; Redgrave et al., 2010).

Layered on top of this background DA activity are transient changes in striatal DA concentrations that signal the occurrence of salient events of either positive or negative behavioral value (Schultz, 2002; Bromberg-Martin et al., 2010). DA levels in the striatum have been suggested to rise as high as 1 μM in response to primary rewards and conditioned stimuli in a variety of sensory modalities (Gonon, 1988; Dugast et al., 1994; Garris et al., 1997; Dreyer et al., 2010). These phasic events occur in close temporal approximation to the presentation of the stimulus and are graded based upon the salience of the reward (Schultz, 1998, 2002, 2016a). This signal subsequently links, likely through the induction of LTP and LTD at direct and indirect pathway corticostriatal synapses respectively, a behavioral response to the outcome of the action taken, thereby either

increasing or decreasing the future likelihood of repeating that response (Reynolds et al., 2001; Yin et al., 2009; Gerfen and Surmeier, 2011).

These two elements of DA signaling are directly tied to the activity of the cells from which it originates – i.e. the DA cells of the SNc. As such, a great deal of energy has been expended on elucidating the mechanisms underlying the firing patterns of these neurons.

Activity patterns in dopamine neurons

Initially described in a series of papers by Grace and Bunney, the firing patterns of SNc DA neurons *in vivo* can be roughly categorized into one of two groups: a low frequency, regular or irregular, single spike pattern and a higher-frequency “burst” pattern (Grace and Bunney, 1984a, 1984b; Hyland et al., 2002). Broadly speaking, the regular single spike pattern is derived from intrinsic mechanisms, involving a series of ion channels that work in concert to generate the necessary oscillatory activity underlying pacemaking behavior. In contrast, while the exact mechanisms underlying the transient high-frequency spiking observed in SNc DA neurons is less clear, it is generally agreed that this behavior is derived from synaptic input to these cells, as disruption of that input occludes the occurrence of these events.

Intrinsically derived, low-frequency pacemaking activity

SNc DA neurons are autonomously active cells capable of generating action potentials in the absence of any synaptic input (Shepard and Bunney, 1991; Chan et al., 2007; Guzman et al., 2009; Kimm et al., 2015). This pacemaking activity is characterized by broad (> 2 ms) spikes, with firing rates being in the range of 1-9 Hz (Grace and Bunney,

1984a; Grace and Onn, 1989; Nedergaard et al., 1993). *In vivo* single spiking tends to occur in both regular and irregular patterns, as defined by the shape of autocorrelograms of spiking data (Lee and Tepper, 2009). This is likely due to the influence of synaptic input on the spike generation mechanism, as this irregularity is mostly absent in *in vitro* preparations where the microcircuits of synaptic input to DA neurons have been disrupted (Puopolo et al., 2007; Guzman et al., 2009; Khaliq and Bean, 2010).

The depolarizing phase of the pacemaking mechanism primarily engages sodium and calcium channels. In particular, a persistent sodium current and a low-voltage activated L-type voltage-gated calcium channel (VGCC) activated in subthreshold voltage ranges are thought to be the primary driver of the cell to threshold (Chan et al., 2007; Puopolo et al., 2007; Ding et al., 2011). Hyperpolarization-activated, cyclic nucleotide-gated (HCN) channels have also been identified as a potential depolarizing drive, in likely what is a form of redundancy in the pacemaking mechanism (Neuhoff et al., 2002; Guzman et al., 2009; Amendola et al., 2012). This is illustrated by the fact that in the presence of antagonists for the L-type VGCC pacemaking persists unless HCN channels are also blocked (Guzman et al., 2009). Antagonism of HCN channels alone, though, also fails to disrupt DA neuron spiking (Chan et al., 2007; Puopolo et al., 2007; Guzman et al., 2009).

The repolarizing phase of the pacemaking oscillation involves several different potassium channels. Calcium entry through VGCCs during spike generation results in the activation of small-conductance, calcium-activated potassium (SK) channels that act to both deepen and broaden the AP afterhyperpolarization (AHP). SK channels have also been shown to play an important role in the regularity of SNc DA firing, with antagonism of SK

channels promoting irregular and burst firing (Ping and Shepard, 1996, 1999; Wolfart et al., 2001; Sarpal et al., 2004; Deignan et al., 2012; Ramírez-Latorre, 2012). The A-type $K_v4.3$ voltage-gated K^+ channel has also been identified as an important regulator of firing rate in SNc neurons, with antagonism producing higher firing rates (Liss and Roeper, 2001; Hahn et al., 2003; Segev and Korngreen, 2007). The interaction between K_v2 and large-conductance, Ca^{2+} activated K^+ (BK) channels has also been recently identified as a source of regulation for AP frequency and shape in SNc neurons (Kimm et al., 2015).

Extrinsically derived, episodic high-frequency “burst” firing

SNc DA neurons have been observed to burst both spontaneously and in response to the presentation of an unexpected reward (Schultz, 1998, 2002, 2016a). This behavior has been observed in *in vivo* preparations of both anaesthetized and awake-behaving mice, rats, and non-human primates (Ljungberg et al., 1992; Schultz et al., 1993; Horvitz et al., 1997; Hyland et al., 2002; Bayer and Glimcher, 2005; Pan et al., 2005; Kobayashi and Schultz, 2014). Importantly, though, in *in vitro* preparations spontaneous bursts are rarely observed, indicating the need for intact neural circuitry for the generation of these events (Overton and Clark, 1992, 1997; Paladini and Roeper, 2014). These bursts are composed of, on average, 2-3 spikes, although as many as 10 spikes within a burst have been recorded (Grace and Bunney, 1984b; Hyland et al., 2002). Intraburst frequency ranges between 20-50 Hz, with bursts associated with a reward generally having a higher average frequency than spontaneous bursts (Grace and Bunney, 1983a, 1984b; Hyland et al., 2002; Pan et al., 2005). While initial studies in anaesthetized animals observed significant spike frequency adaptation (i.e. an increase in interspike interval, ISI, across the burst), more recent work

in awake animals suggests this may be less common than originally thought (Grace and Bunney, 1984b; Hyland et al., 2002).

The mechanism by which SNc neurons transition from single-spike mode to burst firing is still poorly understood. It has been suggested that N-methyl-D-aspartate (NMDA) glutamate receptors play a critical role in burst induction (Overton and Clark, 1992; Chergui et al., 1993; Lee and Tepper, 2009; Zweifel et al., 2009; Morikawa and Paladini, 2011). *In vivo* studies have shown, for example, that blockade or knockout of NMDARs reduces burst firing in SNc neurons (Charley et al., 1991; Overton and Clark, 1992; Smith and Grace, 1992; Chergui et al., 1993; Zweifel et al., 2009). Similarly, *in vitro* preparations have shown that NMDAR signaling is necessary for synaptically evoked bursts in SNc neurons (Wilson and Callaway, 2000; Kuznetsov, 2005; Deister et al., 2009; Kuznetsova et al., 2010; Ha and Kuznetsov, 2013). The proposed mechanism for this is one in which oscillations in the dendrites of SNc neurons are the primary driver of spiking irregularity and burst firing. Several papers have suggested a model in which the soma and dendrites oscillate at different frequencies; this is attributed to differences in clearance of intracellular calcium due to a smaller vs. larger ratio of surface area: volume in somatic vs. dendritic compartments (Wilson and Callaway, 2000; Kuznetsov, 2005; Deister et al., 2009). Under basal conditions the somatic oscillation dominates the overall pacemaking cycle (Wilson and Callaway, 2000; Kuznetsov, 2005; Deister et al., 2009; Ha and Kuznetsov, 2013). This balance, however, is pushed in favor of the dendritic oscillator upon activation of NMDARs signaling, which, due to their strong voltage dependence associated with

magnesium block, amplify the dendritic oscillations, subsequently causing the transition to burst firing (Wilson and Callaway, 2000; Kuznetsov, 2005; Deister et al., 2009).

There exists several pieces of experimental data, however, that contradict these hypotheses. In contrast with the proposition that the locus of spike generation changes in single spiking vs. burst spiking mode, it has been repeatedly shown that APs are initiated within the axon initial segment (AIS) of DA neurons (Häusser et al., 1995; Blythe et al., 2009). Recordings from somatic and dendritic compartments adjacent-to and distal-from the AIS have consistently observed the presence of the spike at the AIS first, followed by some delay before the AP propagates in to the other regions in the cell (Häusser et al., 1995; Blythe et al., 2009). Furthermore, antagonism of the calcium oscillations that are proposed to underlie the dendritic oscillations does not occlude burst generation (Blythe et al., 2009). Finally, it has been shown the inhibition of α -amino-3-hydroxy-5-methyl-4-isoxazolepropionic acid (AMPA) receptors, which lack the voltage dependence of NMDARs, can also occlude burst firing in DA neurons (Georges and Aston-Jones, 2002; Blythe et al., 2007).

Reward prediction error in dopamine neurons

These episodic bursts observed in SNc DA neurons correspond to the previously discussed phasic increase in striatal DA levels. The information being encoded by these events is referred to as reward prediction error (RPE) – i.e. the difference between the reward received and the reward expected from a particular behavior (Schultz, 1998, 2002, 2016b). Rewards that are either unexpected or are better than expected result in a positive

prediction error, while a worse or absent expected reward results in a negative prediction error. A reward that is predicted perfectly (i.e. the received reward is exactly equal to the expected reward) produces zero prediction error. This concept of prediction error is critical to learning, as it provides a mechanism by which an animal can determine whether the performed behavior resulted in the expected outcome or not.

This reward prediction error has been found to be directly encoded by activity within SNc neurons (Schultz et al., 1997). A positive prediction error results in a burst of activity within DA neurons, and consequently a rise in striatal DA levels that promotes both the acute and future performance of behavior similar to what just produced the reward. In contrast, a negative prediction error produces a pause in SNc neuron firing and a concomitant fall in striatal DA, thereby disfavoring the associated behavior. Finally, a zero prediction error produces no change in SNc neuron firing, as would be expected of a behavior of no putative learning value.

The response of DA neurons to a stimulus can be divided into two temporal components. The first component, which begins within 60-90 ms of stimulus presentation and lasts between 50-100 ms, occurs regardless of the valence (positive, negative, or neutral) of the stimulus (Steinfels et al., 1983; Romo and Schultz, 1990; Horvitz et al., 1997; Tobler et al., 2003). Rather, the degree of response in DA cells is dependent upon the intensity of the sensory stimulus, indicating that this early activation phase corresponds to the salience of the stimulus (Fiorillo et al., 2013; Kobayashi and Schultz, 2014). The second component encodes the RPE of the stimulus. Depending on the complexity of the required

task this second component may begin during the first component or may directly follow it (Nomoto et al., 2010; Schultz, 2016a).

The observation that burst firing in DA neurons is dependent upon synaptic input raises the question of where the synaptic drive underlying these reward-associated bursts originates. Given that these two distinct aspects of the DA activation in response to a rewarding stimulus encode different pieces of information, it may be the case that multiple synaptic inputs work in concert to shape the DA response.

Synaptic connectivity in the SNc

SNc DA neurons receive GABAergic, glutamatergic, and neuromodulatory input from a variety of brain areas (Watabe-Uchida et al., 2012). The densest of these connections arise from other nuclei within the BG (Watabe-Uchida et al., 2012). In particular, SNc DA neurons receive substantial GABAergic input from both the dorsal striatum and GPe, representing reciprocal connections from the primary projection targets for the SNc (Grofová, 1975; Hattori et al., 1975; Bunney and Aghajanian, 1976; Tulloch et al., 1978; Ribak et al., 1980; Williams and Faull, 1985; Chang, 1988; Bolam and Smith, 1990; Zahm et al., 2011; Watabe-Uchida et al., 2012). The SNc also receives GABAergic input from the SNr and, to a lesser extent, the GPi (Grofova et al., 1982; Tepper et al., 1995; Paladini et al., 1999; Lee et al., 2004; Watabe-Uchida et al., 2012). All of these nuclei primarily project to the ipsilateral SNc, where they form symmetrical synapses on both the dendrites and somata of SNc neurons (Bolam and Smith, 1990; Smith et al., 1998). In addition to this

GABAergic input, the SNc receives glutamatergic input from the BG via projections from the STN (discussed below).

While generally less dense, the SNc also receives input from a number of nuclei outside the BG. The SNc receives limited projections from both the hippocampus and the amygdala (Zahm et al., 2011; Watabe-Uchida et al., 2012). The largest of these is a significant projection from the central nucleus of the amygdala (Watabe-Uchida et al., 2012). While the neurochemical identity of these synapses has not been described, they are likely GABAergic afferents given that the majority of projections from the central nucleus are GABAergic (Sah et al., 2003). The SNc is also only sparsely connected to the thalamus and hypothalamus, with the paraventricular nucleus representing the densest projection from these two regions (Watabe-Uchida et al., 2012). The SNc receives input from a number of other midbrain nuclei as well. In particular, the dorsal raphe has been shown to provide a prominent serotonergic input to SNc neurons (Fibiger and Miller, 1977; Dray et al., 1978; Gervais and Rouillard, 2000), while the pedunculo-pontine nucleus is the primary source of cholinergic input to SNc DA cells (Clarke et al., 1987; Lavoie and Parent, 1994a; Futami et al., 1995; Xiao et al., 2016).

Glutamatergic input

While overall the bulk of the innervation to SNc DA neurons is GABAergic, comprising between 40-70% of the synaptic contacts in SNc DA neurons (Henny et al., 2012), SNc neurons also receive glutamatergic input from several brain regions.

Cortex

The SNc receives synaptic input from rostral portions of the cortex, particularly from primary motor and premotor (M1 and M2, respectively) cortex as well as primary somatosensory cortex (Watabe-Uchida et al., 2012). To a lesser extent, the SNc also receives input from prefrontal areas such as frontal association and orbitofrontal cortex (Carter, 1982; Usunoff et al., 1982; Kornhuber et al., 1984; Naito and Kita, 1994; Watabe-Uchida et al., 2012). There are virtually no projections from caudal cortical regions to the SNc (Watabe-Uchida et al., 2012). While no physiological data exists for these connections, anatomical studies have shown these synapses are asymmetrical and are likely glutamatergic (Carter, 1982; Usunoff et al., 1982).

Superior Colliculus

Both anterograde and retrograde tracing studies have shown a significant projection from the superior colliculus (SC) to SNc DA neurons (Comoli et al., 2003; McHaffie et al., 2006; May et al., 2009). Afferents from the SC have been shown to form both symmetrical and asymmetrical synapses on SNc neurons, with the latter constituting the majority of the connections (Comoli et al., 2003). This connection has been shown to be preserved in both cats and non-human primates as well (McHaffie et al., 2006; May et al., 2009).

Chemical stimulation of the SC increases firing rate and burst activity within midbrain DA neurons (Coizet et al., 2003). One of the hallmark features of RPE in SNc neurons is the rapid (< 100 ms) response to the presentation of the stimulus (Schultz,

1998, 2002). It has been argued that the SC represents the source of short-latency visual information for the SNc, as the SC has been shown to respond to similar stimuli at shorter latencies than the SNc (Comoli et al., 2003; Dommett et al., 2005). Furthermore, Comoli *et al.* (2003) showed that amplification of the SC response to visual stimuli produces a concomitant increase in the SNc response to those same stimuli, while inhibition of SC response resulted in a reduction in the SNc response.

Subthalamic Nucleus

As part of the indirect pathway, the STN sends a substantial projection to the substantia nigra (Kanazawa et al., 1976; Deniau et al., 1978; Van Der Kooy and Hattori, 1980; Carpenter et al., 1981; Smith et al., 1990). While the majority of these afferents terminate within the SNr, a subset have been shown to also synapse on DA neurons in the SNc (Chang et al., 1984; Kita and Kitai, 1987; Smith et al., 1998). The STN forms asymmetrical glutamatergic synapses on these projection targets, with afferents originating primarily from the ipsilateral STN (Chang et al., 1984; Kita and Kitai, 1987; Smith et al., 1998). Recent retrograde tracing has confirmed monosynaptic connections between the STN and SNc DA neurons (Watabe-Uchida et al., 2012).

The impact of the STN glutamatergic input to SNc DA neurons remains largely unclear. Studies using both electrical and chemical stimulation of the STN have shown mixed results with regards to the effect on SNc neuron firing. In some experiments, both brief electrical stimulation as well as prolonged chemical stimulation have produced excitatory responses, including increased burst activity, in SNc neurons (Hammond et al.,

1978; Robledo and Féger, 1990; Smith and Grace, 1992; Chergui et al., 1994). These effects were shown to be partially attenuated by blockade of NMDARs (Overton and Clark, 1992; Smith and Grace, 1992; Chergui et al., 1994). Furthermore, it has been observed that inhibition of the STN reduces burst activity within the SNc (Smith and Grace, 1992). Other work, however, has instead observed an overall inhibitory effect of STN stimulation on SNc firing (Robledo and Féger, 1990; Féger and Robledo, 1991; Iribe et al., 1999). This is explained as a polysynaptic effect resulting from the excitation of the GABAergic input to the SNc from the SNr (Robledo and Féger, 1990; Iribe et al., 1999).

Pedunculopontine Nucleus

In addition to the already mentioned cholinergic projection, the PPN also sends glutamatergic afferents to the SNc (Lavoie and Parent, 1994a; Futami et al., 1995; Charara et al., 1996; Smith et al., 1996). While these projections primarily originate from the ipsilateral PPN, some contralateral projections have been observed (Lavoie and Parent, 1994a; Charara et al., 1996). The majority of projections from the PPN form asymmetrical synapses on SNc neurons, with roughly 40% of boutons being identified as glutamatergic (Charara et al., 1996).

The PPN has been reliably shown to be able to elicit excitatory responses in SNc DA neurons. Electrical stimulation of the rostral PPN in *in vitro* preparations has been shown to evoke glutamate-mediated excitatory post-synaptic potentials (EPSPs) in SNc neurons (Futami et al., 1995). *In vivo*, PPN stimulation produces short latency responses in SNc neurons that are largely attenuated by non-NMDAR glutamatergic antagonists (Scarnati et

al., 1986, 1987; Di Loreto et al., 1992). This stimulation has further been shown to elicit burst firing within the SNc (Scarnati et al., 1984; Lokwan et al., 1999; Hong and Hikosaka, 2014).

Like the SC, the PPN responds to sensory stimuli at latencies that precede a response in the SNc (Pan and Hyland, 2005). Furthermore, the PPN has been shown to encode different components of the reward-prediction response (Kobayashi and Okada, 2007; Okada et al., 2009; Norton et al., 2011; Hong and Hikosaka, 2014). It therefore represents a putative source of information for the generation of RPE in SNc DA neurons.

The Pedunculopontine Nucleus

The PPN was originally described as one of the brainstem cholinergic centers that, as part of the reticular activating system (RAS), are critical for the maintenance of arousal and the sleep to wakefulness transition (Steriade, 1996). With time and further examination, however, the PPN was found to contain a diverse population of cells and has been implicated in a wide array of behaviors. In particular, the PPN has dense interconnectivity with the structures of the BG, to the point that some have argued that the PPN should be included in the list of BG nuclei (Mena-Segovia et al., 2004).

Cytoarchitecture

As mentioned, the PPN was initially thought to be composed largely, if not entirely, of cholinergic cells (Mesulam et al., 1983; Rye et al., 1987; Mesulam et al., 1989; Côté and Parent, 1992). These cells, which are identified by their strong immunoreactivity to antibodies for choline acetyltransferase (ChAT; enzyme response to catalyzes formation of

acetylcholine from choline and acetyl-CoA), range in size from 20 to 40 μm . Larger cells generally have a fusiform or triangular soma with 3-6 primary dendrites, while more medium-sized cells are round in shape and give rise to 2-3 primary dendrites (Rye et al., 1987; Lavoie and Parent, 1994b; Ford et al., 1995; Takakusaki et al., 1997; Wang and Morales, 2009). In addition to these cells, however, the PPN has been shown to contain a large population of GABAergic and glutamatergic cells, as identified by the expression of glutamic acid decarboxylase (GAD) and VGLUT2, respectively (Ford et al., 1995; Mena-Segovia et al., 2009; Wang and Morales, 2009; Martinez-Gonzalez et al., 2012). Both GABAergic and glutamatergic cell populations tend to be smaller, with round somas in the range of 10-20 μm in diameter.

Due to the historical focus on its cholinergic cell population, the PPN borders are defined by the location of these ChAt+ cells (Mesulam et al., 1983, 1984; Rye et al., 1987). Rostrally it is bordered by the substantia nigra and RRF, while being bounded caudally by the parabrachial nucleus (Rye 1987). Its medial border is formed by the superior cerebellar peduncle and midbrain extrapyramidal area, while the lateral border is formed by lateral lemniscus. The dorsal and ventral borders are made up by the cuneiform nucleus and pontine tegmental field, respectively. The PPN is further subdivided into two regions – pars dissipata, located rostrally, and the pars compacta, located caudally – based on the density of cholinergic cells within these areas (Olszewski and Baxter, 1982; Rye et al., 1987). This rostral portion receives a larger portion of BG input than the caudal region (Charara and Parent, 1994; Lavoie and Parent, 1994c; Oakman et al., 1995; Takakusaki et al., 1996;

Oakman et al., 1999; Dautan et al., 2014). Furthermore, the majority of input from the PPN to the SNc arises from cells within the pars dissipata (Takakusaki et al., 1996).

More recently these functionally distinct rostral and caudal regions have been redefined based upon the GABAergic, rather than cholinergic, cell population within the PPN (Mena-Segovia et al., 2009). GABAergic neurons are most abundant in the rostral PPN, representing 40-45% of the cells in this area. In contrast, GABAergic cells are the minority population in the caudal PPN, being outnumbered by cholinergic cells roughly 3:1 (Mena-Segovia et al., 2009). VGLUT2 positive cells also follow a gradient opposite that of the GABAergic population, representing approximately 50% and 37% of the cells in the pars compacta and pars dissipata, respectively (Wang and Morales, 2009). Interestingly, the most recent estimates put the cholinergic cells as the least populous group in the PPN, constituting roughly 25-30% of the overall cell population in the PPN (Wang and Morales, 2009). Rather, glutamatergic cells represent the majority population, making up between 40-45% of the total population in the PPN, while GABAergic cells compose between 30-34% of the total number of PPN neurons (Wang and Morales, 2009).

Cellular physiology

The diversity in cell types in the PPN is paralleled by a diversity in their physiology. Early groups identified different subsets of PPN neurons based on properties such as spontaneous activity, spike waveform, and the presence of certain currents. Leonard and Llinás (1990, 1994) identified three primary subtypes, two of which were observed to fire spontaneously while the third responded to current injections with a train of spikes. Two of

these populations, one being the group lacking spontaneous activity, were shown to have a calcium-mediated low-threshold spike (LTS), while the other spontaneous population contained an A-type potassium current (I_A) (Leonard and Llinás, 1990, 1994). Largely in agreement with this work, Kang and Kitai (1990) classified PPN neurons into three groups: Type I, II, and III. Type I were identified based on the presence of a calcium-dependent LTS; Type II contained an A-type potassium current; and Type III lacked both LTS and I_A (Kang and Kitai, 1990). Based on subsequent work, Type II neurons likely correspond to cholinergic cells in the PPN (Takakusaki et al., 1997).

More recently, it has been observed that cholinergic and GABAergic cells in the PPN can be largely distinguished based on the presence or absence, respectively, of the M-type potassium current (Bordas et al., 2015). Cholinergic cells were further shown to have a slower basal firing rate and a larger AHP than GABAergic cells in the PPN (Bordas et al., 2015; Petzold et al., 2015). The presence of an M-current is also tied to a more prominent spike-frequency adaption in cholinergic neurons, as well as the presence of a tetrodotoxin (TTX) sensitive, high-threshold membrane oscillation observed in cholinergic neurons but not GABAergic neurons (Bordas et al., 2015). While not directly assessed, glutamatergic neurons in the PPN also likely lack this M-type current.

A number of *in vivo* studies have also sought to classify PPN neurons based on their activities profiles during different brain states. Cholinergic cells have been repeatedly shown to increase their activity prior-to, and during, waking and REM-sleep state transitions from a sleeping-state (Steriade et al., 1990a, 1990b; Mena-Segovia et al., 2008; Boucetta and Jones, 2009; Boucetta et al., 2014; Cox et al., 2016). The response profiles of

non-cholinergic cells is more heterogenous, with some showing a similar increase in firing rate in response to arousal, while others show an opposite pattern in which they are primarily active in the sleeping-state and are inhibited during the aroused state (Boucetta and Jones, 2009; Roš et al., 2010; Boucetta et al., 2014; Petzold et al., 2015). Within the non-cholinergic group of cells that are activated in the aroused state, further subpopulations have been described showing a preferential activation during waking or REM-sleep states (Boucetta et al., 2014). While some have argued that the cholinergic population can be distinguished from non-cholinergic cells based on a phasic vs. tonic or inhibitory response to cortical activation (Petzold et al., 2015), others indicate too great of an overlap in activity profiles to reliably separate cholinergic, glutamatergic, and GABAergic populations in the PPN from physiology data alone (Boucetta et al., 2014).

Connectivity

The PPN sends cholinergic, glutamatergic, and GABAergic projections to a number of brain areas. The longest range afferents arise from the cholinergic cells, which on average give rise to five collaterals that primarily ascend to target areas of the BG and limbic system (Semba and Fibiger, 1992; Lavoie and Parent, 1994c; Takakusaki et al., 1996; Mena-Segovia et al., 2008; Dautan et al., 2014, 2016a). GABAergic and glutamatergic cells in the PPN, in contrast, produce on average two axon collaterals that primarily project to more local targets within the midbrain and brainstem (Bevan and Bolam, 1995; Ford et al., 1995; Mena-Segovia et al., 2008; Roš et al., 2010). Ascending projections are topographically organized, with projections to the motor structures such as the SNc and dorsal striatum originating in the rostral PPN while afferents from the caudal PPN primarily project to

limbic structures (Jackson and Crossman, 1983; Lavoie and Parent, 1994c; Oakman et al., 1995; Martinez-Gonzalez et al., 2011; Dautan et al., 2014). Overall every nuclei within the BG receives some combination of input from cells within the PPN. The thalamus is also heavily innervated by the PPN, with the majority of the projections arising from cholinergic cells in the caudal PPN (Sugimoto and Hattori, 1984; Smith et al., 1988; Steriade et al., 1988, 1990a; Kobayashi and Nakamura, 2003; Kobayashi et al., 2007; Parent and Descarries, 2008). Both the superior and inferior colliculus also receive projections from the PPN (Beninato and Spencer, 1986; Hall et al., 1989; Mena-Segovia et al., 2008; Motts and Schofield, 2009).

The PPN also sends a number of descending projections to structures within the brainstem and spinal cord. The descending cholinergic fibers arise as collaterals from the ascending axons, while the descending non-cholinergic fibers exist as both collaterals from ascending projections as well as single descending axons (Mena-Segovia et al., 2008; Roš et al., 2010; Martinez-Gonzalez et al., 2014). The brainstem projection targets include the pontine reticular formation, gigantocellular reticular nucleus, and portions of the medulla (Mitani et al., 1988; Rye et al., 1988; Nakamura et al., 1989; Skinner et al., 1990b; Grofova and Keane, 1991; Takakusaki et al., 1996; Garcia-Rill et al., 2001; Martinez-Gonzalez et al., 2014). Projections to the spinal cord arise primarily from the non-cholinergic cells in the PPN (Rye et al., 1988; Spann and Grofova, 1989; Skinner et al., 1990a).

Afferent input to the PPN has been less well described, particularly with regards to input to specific neurochemical subpopulations within the PPN. It is clear, however, that the PPN receives reciprocal connections from the BG output nuclei (GPi, SNr) as well as the

STN and GPe (Kita and Kitai, 1987; Scarnati et al., 1987; Granata and Kitai, 1989; Nakamura et al., 1989; Spann and Grofova, 1991; Semba and Fibiger, 1992; Saitoh et al., 2003; Florio et al., 2007). The PPN also receives DA input from both the VTA and SNc (Haber et al., 1990; Semba and Fibiger, 1992; Grofova and Zhou, 1998; Rolland et al., 2009). Tracing studies have also identified afferents from cortical areas including frontal motor regions, medial prefrontal cortex and primary auditory cortex (Sesack et al., 1989, 1989; Semba and Fibiger, 1992; Schofield and Motts, 2009). Both the inferior and superior colliculus send projections to the PPN, as do the deep cerebellar nuclei and laterodorsal tegmental nucleus (LDT) (Sato and Fibiger, 1986; Woolf and Butcher, 1986; Redgrave et al., 1987; Hazrati and Parent, 1992; Semba and Fibiger, 1992; Steininger et al., 1992). The PPN also receives input from several brainstem nuclei including the dorsal raphe and locus coeruleus (Jones and Yang, 1985; Vertes, 1991; Semba and Fibiger, 1992; Steininger et al., 1997).

Function

Arousal

The cholinergic neurons in the PPN and neighboring LDT were originally described in the context of the RAS, which had been identified as a critical structure for the transitioning between states of arousal (Steriade et al., 1991; Steriade, 1996). The abundant projections from the PPN to the thalamus, which in turn projects to regions throughout the cortex, were suggested to provide a means by which the RAS could activate the cortex and promote wakefulness (Smith et al., 1988, 1988). This hypothesis is supported by the observation that cells within the PPN show higher average activity levels

during waking and REM-sleep states (Steriade et al., 1990a; Datta and Siwek, 2002; Mena-Segovia et al., 2008; Boucetta and Jones, 2009). Furthermore, both electrical and pharmacological stimulation of the PPN has been repeatedly shown to induce transitions from the sleep to the waking state (Moruzzi and Magoun, 1949; Jones, 1991; Datta and Siwek, 1997; Datta, 2002, 2007).

Despite this work, lesions to the PPN have largely failed to show a disruption to the overall sleep-wake cycle (Shouse and Siegel, 1992; Deurveilher and Hennevin, 2001; Lu et al., 2006). Similarly, studies employing techniques to selectively activate PPN cholinergic cells have produced mixed results. While optogenetic activation of these cells has been shown to induce the transition to rapid-eye movement (REM)-sleep (Van Dort et al., 2015), prolonged chemogenetic stimulation of PPN cholinergic cells failed to increase time spent in the awake state (Kroeger et al., 2017). Furthermore, *in vivo* recordings of PPN cholinergic neurons show transient increases in firing rate preceding the transition from a sleep to waking state (Mena-Segovia et al., 2008; Boucetta et al., 2014), arguing against a role for these cells in the maintenance of arousal (Mena-Segovia and Bolam, 2017). In contrast, chemogenetic activation glutamatergic PPN neurons, subpopulations of which show prolonged activation following state transitions (Roš et al., 2010), produces significant increases in wakefulness (Kroeger et al., 2017).

Nevertheless, cholinergic activity in the thalamus has been shown to be associated with the desynchronization of cortical slow-wave activity and the transition to high-frequency gamma oscillations associated with wakefulness (Steriade et al., 1990a, 1991; Williams et al., 1994; Mena-Segovia et al., 2008). Specific activation of PPN cholinergic cells

has similarly been shown to induce cortical gamma oscillations (Furman et al., 2015). By acting upon muscarinic receptors in the thalamus, even transient activation of cholinergic PPN neurons may exert long-lasting effects on the activity of thalamocortical neurons (Dossi et al., 1991; McCormick, 1993; Steriade, 1993). The role that non-cholinergic PPN neurons play in regulating thalamocortical projections remains largely unclear, however.

Movement

The PPN has also long been included as a part of the mesencephalic locomotor region (MLR), which, upon repeated stimulation, is capable of generating spontaneous movement, particularly stepping behavior (Shik et al., 1966; Mori et al., 1978; Garcia-Rill et al., 1987; Lai and Siegel, 1990; Skinner et al., 1990a). In contrast, other stimulation patterns within reticular structures such as the PPN have been shown to induce atonia, as experienced during REM sleep, through inhibition of spinal motoneurons (Chase et al., 1986; Chase and Morales, 1990; Takakusaki et al., 2016). Furthermore, degeneration of PPN cholinergic neurons has been suggested to play a particularly important role in falls associated with postural instability seen in PD (Rinne et al., 2008; Weinberger et al., 2008; Bohnen et al., 2009), which has led to the targeting of PPN for deep-brain stimulation (DBS) in PD patients (Pahapill and Lozano, 2000; Hamani et al., 2011; Garcia-Rill et al., 2015).

Recent work in decerebrate cats by Takakusaki *et al.* (2016) has demonstrated dichotomous roles for cholinergic and non-cholinergic (presumed glutamatergic) signaling originating from the PPN with regards to movement. Stimulation of the PPN was shown to produce inhibition of brainstem motor regions and spinal motoneurons, as well as a

concomitant decrease in muscle tone, all of which were sensitive to block by muscarinic antagonist atropine. In contrast, a non-atropine sensitive excitatory response in these same areas was also observed (Takakusaki et al., 2016). Selective stimulation of glutamatergic PPN neurons in mice has also been shown to more robustly induce locomotion than selective stimulation of the cholinergic cells in PPN (Roseberry et al., 2016).

These findings contrast with other reports that activation of PPN cholinergic neurons increases motor activity in mice (Dautan et al., 2016b; Xiao et al., 2016). An important distinction between these studies and the work by Takakusaki *et al.* (2016), however, is the preservation of forebrain connections, particularly to midbrain DA structures. It is therefore possible that the observed increased in locomotor activity upon PPN cholinergic stimulation can be attributed to increased activity in BG motor circuits (Mena-Segovia and Bolam, 2017). Overall, the current literature suggests that the inclusion of PPN in the MLR can most likely be attributed to activity of the glutamatergic population of PPN neurons, while PPN cholinergic neurons likely underlie the role of PPN in postural muscle tone (Mena-Segovia and Bolam, 2017).

Reinforcement Learning

In addition to its canonical role in arousal and movement, the PPN has more recently been suggested to play a significant part in a variety of learning paradigms. Lesions of the PPN disrupt learning acquisition for both classical and operant conditioning tasks (Inglis et al., 2000; Alderson et al., 2001, 2002, 2003, 2004, 2006, 2008; Bortolanza et al., 2010; Syed et al., 2016). More selective lesions targeting either the anterior or posterior

PPN, which preferentially target the SNc and VTA respectively, have also been shown to affect different aspects of a reinforcement learning task, with the latter primarily impairing learning the task (lever pressing) while the former disrupted response control (Wilson et al., 2009). In agreement with these studies, stimulation of the PPN *in vivo* produces a significant, transient increase in DA levels in the nucleus accumbens (NAc; structure within the ventral striatum primarily targeted by VTA DA neurons) due to increased burst activity within the VTA (Floresco et al., 2003). Moreover, recent work employing techniques to selectively stimulate neuron sub-populations within the PPN has found that activation of the PPN glutamatergic cells is reinforcing in a self-administration paradigm (Yoo et al., 2016). Similarly, bidirectional control (activation or inhibition) of the cholinergic PPN population is capable of conditioning an animal to prefer one chamber over another in a conditioned placed-preference task (Xiao et al., 2016).

Despite this evidence, the specific information encoded by the PPN with regards to these learning tasks remains largely unclear. Studies have found significant heterogeneity within the response profiles of PPN neurons to different behavioral cues. Some cells, for example, have been shown to respond to sensory stimuli independent of any reward value associated with the stimulus (Pan and Hyland, 2005). The responses of these cells were themselves heterogeneous with regards to preference for sensory modality and overall structure (i.e. duration and direction of response). In contrast, a number of studies have observed PPN neurons that show differential responses based on a presented reward or reward-predicting stimulus (Dormont et al., 1998; Okada et al., 2009; Okada and Kobayashi, 2013; Hong and Hikosaka, 2014). These studies have largely identified two

separate populations that respond either to the onset of the reward-predicting stimulus or to the delivery of the reward (Okada et al., 2009). The responses were generally observed as an increase in the tonic firing rate of the cells, with the response duration and amplitude (firing rate) being graded by the magnitude of the reward (Okada et al., 2009; Norton et al., 2011). While some cells show some aspect of prediction error based on the grading of the response, overall the response profiles of PPN neurons do not resemble the direct encoding of RPE observed in DA neurons (Okada et al., 2009; Norton et al., 2011; Okada and Kobayashi, 2013; Hong and Hikosaka, 2014). In all of these examples, the response within the PPN generally occurred at shorter latency to the expected (or observed) DA neuron response latency, indicating that PPN neurons are a potential driver of the subsequent activity observed in the DA cells. Lacking from this work, however, is any neurochemical identification of the cells involved in these signals.

Summary

Overall the physiological and anatomical characteristics of the PPN, particularly its dense connectivity with the BG, place it in a position to influence a variety of behaviors. It has recently been suggested that the primary purpose of the PPN is to provide the BG with information about changing behavioral states in response to environmental events (Mena-Segovia and Bolam, 2017). This perspective primarily focuses on the role of cholinergic neurons within the PPN, noting that the role of the non-cholinergic population is still largely unclear (Mena-Segovia and Bolam, 2017). With regards to the SNc, the PPN likely represents an important input structure, particularly as a source of excitatory signaling. Despite the neurochemical heterogeneity within the PPN, the majority of the literature that

has examined PPN-SNc connectivity has done so largely with respect to the cholinergic innervation of SNc neurons by the PPN. The work presented here therefore aims to expand this literature with a detailed neurophysiological examination of the PPN glutamatergic input to SNc DA neurons.

Chapter 2: Pedunculopontine glutamatergic neurons control spike patterning in substantia nigra dopaminergic neurons

Introduction

SNc dopaminergic (DA) neurons play a central role in modulating goal directed actions and habits, which are under the control of the basal ganglia. As such, a great deal of effort has been devoted to understanding what governs the activity of SNc DA neurons. The spiking behavior of these cells can be placed into one of two broad categories – a single spiking, low-frequency (< 10Hz) mode and a multi-spike, higher frequency, “burst” mode (Grace and Bunney, 1984a, 1984b; Hyland et al., 2002). The single spike mode is critical for maintaining ambient levels of DA in target structures, while the burst mode is thought to be a fundamental signal for action selection and reward-based learning (Schultz, 2007; Tsai et al., 2009; Schultz, 2016a).

The single spiking mode of SNc neurons is generated by an intrinsic pacemaking mechanisms involving the cooperation of a number of Na⁺, K⁺, and Ca²⁺ ion channels (Shepard and Bunney, 1988; Nedergaard et al., 1993; Chan et al., 2007; Puopolo et al., 2007; Guzman et al., 2009; Ding et al., 2011; Kimm et al., 2015). This behavior is preserved in the absence of synaptic input, and is observed in both dissociated and *ex vivo* brain slice preparations (Chan et al., 2007; Puopolo et al., 2007; Guzman et al., 2009; Ding et al., 2011). In contrast, burst spiking is lost in preparations lacking functionally intact synaptic connectivity (Shepard and Bunney, 1991; Johnson and Wu, 2004; Blythe et al., 2007) and is

disrupted *in vivo* by local application of glutamatergic receptor antagonists (Grace and Bunney, 1984b; Charley et al., 1991; Overton and Clark, 1992; Smith and Grace, 1992; Chergui et al., 1993), demonstrating the necessity of synaptic activity for the production of these events.

Because local infusion of NMDAR antagonists *in vivo* reduced burst activity in anesthetized rodents (Overton and Clark, 1992; Chergui et al., 1993), subsequent studies have focused on the potential mechanisms by which NMDARs might generate naturally occurring bursts. Indeed, NMDARs can amplify intrinsic oscillatory activity and promote the transition from slow, single spike pacemaking to a burst pattern (Wilson and Callaway, 2000; Kuznetsov, 2005; Deister et al., 2009; Kuznetsova et al., 2010; Ha and Kuznetsov, 2013). In contrast, α -amino-3-hydroxy-5-methyl-4-isoxazolepropionic acid (AMPA) receptors (AMPA), the other ionotropic glutamate receptor found at SNc glutamatergic synapses, appear unable to produce burst activity like that observed *in vivo* (Shepard and Bunney, 1991; Johnson and Wu, 2004; Deister et al., 2009). However, local electrical stimulation of glutamatergic axons can induce burst-like spiking in SNc DA neurons that is dependent upon AMPARs (Georges and Aston-Jones, 2002; Blythe et al., 2007).

One of the missing pieces in this story is an interrogation of specific glutamatergic inputs to SNc DA neurons. Rabies virus tracing studies have identified a handful of glutamatergic neurons that synapse on SNc DA neurons, including those in the subthalamic nucleus (STN), cerebral cortex, the superior colliculus and the pedunculo-pontine nucleus (PPN) (Watabe-Uchida et al., 2012). Of these, the PPN is of particular interest because of the strength of its projection to SNc and its connectivity with the rest of the basal ganglia

(Clarke et al., 1987; Lavoie and Parent, 1994c, 1994a; Charara et al., 1996; Mena-Segovia et al., 2004; Martinez-Gonzalez et al., 2011). Interestingly, PPN neurons respond to environmental events in a way that resembles SNc DA neurons, including burst spiking in response to salient and rewarding stimuli (Condé et al., 1998; Kobayashi et al., 2002; Pan and Hyland, 2005; Norton et al., 2011; Thompson and Felsen, 2013; Hong and Hikosaka, 2014). Moreover, activation of the PPN *in vivo* can evoke repetitive spiking in SNc DA neurons (Scarnati et al., 1984; Lokwan et al., 1999; Floresco et al., 2003; Hong and Hikosaka, 2014), and ablation of the PPN disrupts learning operant tasks (Inglis et al., 2000; Wilson et al., 2009; Bortolanza et al., 2010; Syed et al., 2016).

Taken together, these observations suggest that PPN glutamatergic neurons might be able to generate patterned activity in SNc DA neurons, particularly bursts. To isolate the influence of PPN glutamatergic neurons on SNc, a combination of optogenetic and pharmacological tools were used. Subcellular optogenetic mapping revealed that PPN glutamatergic synapses were focused on the soma and proximal dendrites, near the axon initial segment. Indeed, stimulation of PPN axons reliably evoked spikes within SNc neurons at a variety of firing rates, including those observed in *in vivo* bursts. The ability of PPN axons to drive burst firing was dependent solely upon AMPARs, not NMDARs. Thus, in addition to NMDAR-dependent forms of burst spiking, where the pattern of activity is dependent upon an interaction between synaptic and intrinsic mechanisms, the pattern of PPN-evoked burst spiking may be extrinsically determined.

Results

PPN-SNc glutamatergic synapses had Ca²⁺ impermeable AMPARs and GluN2D containing NMDARs

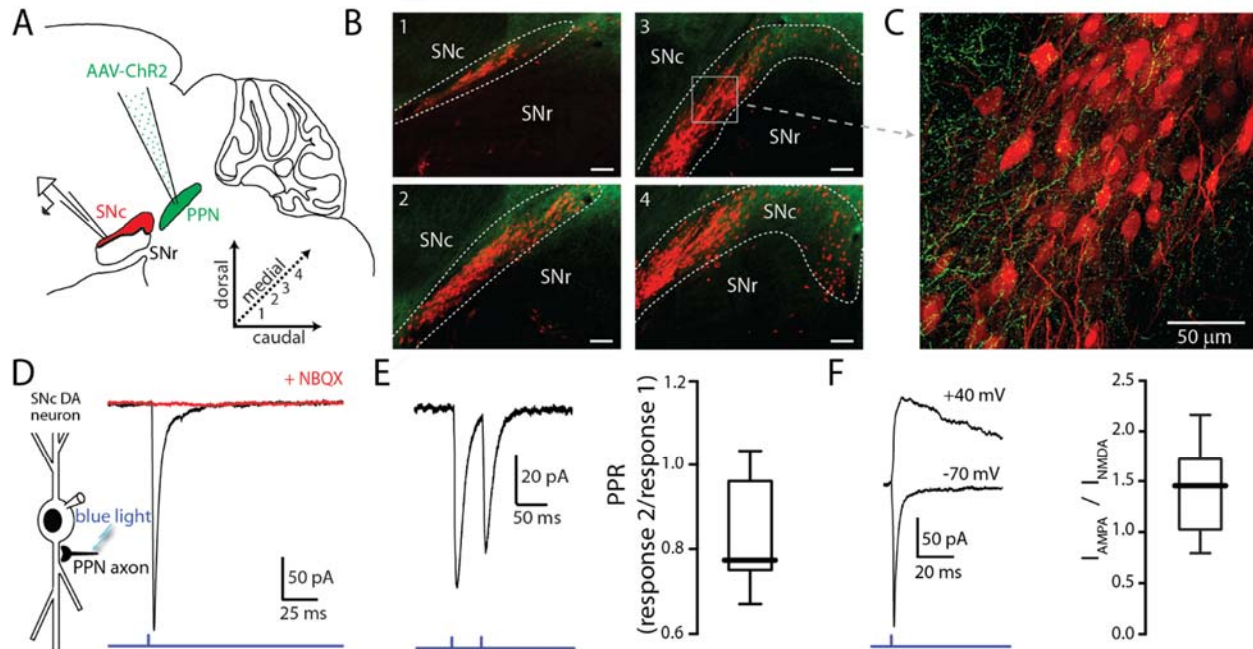
Injections of adeno-associated virus serotype 9 (AAV9) ChR2-eYFP driven by the human Synapsin I (hSyn) promoter were made into the PPN of wildtype or DAT-Cre/Ai14-tdTomato mice (Figure 1A). Projections from the PPN to SNc were visualized ten days after injection (Figure 1B-C). To confirm functional expression of ChR2 in PPN neurons, whole-cell patch clamp recordings were performed on ChR2 expressing cells in the PPN (Figure 2). Photo-stimulation of these cells with full-field (~360 μm diameter) blue light (473 nm) LED illumination reliably evoked photocurrents and associated action potentials (Figure 1 B-C).

SNc neurons were identified in coronal or parasagittal *ex vivo* brain slices based on their morphology, location within the slice, and regular pacemaking activity (Lacey et al., 1989; Mercuri et al., 1994; Chan et al., 2007; Guzman et al., 2009). Glutamatergic responses were isolated by antagonizing GABA_A (10 μ M gabazine) and nicotinic cholinergic receptors (10 μ M mecamylamine). Synaptic responses evoked with 1 ms full-field photo-stimulation of PPN ChR2 expressing afferents were recorded in SNc neurons held at -70 mV in the whole-cell patch-clamp configuration (Figure 1D). Paired-pulse stimulation (20 Hz) evoked responses with amplitude ratios less than one (Figure 1E; PPR = 0.83 ± 0.13 , n=10), indicating that the PPN glutamatergic synapse had a high release probability. This was confirmed with electrical stimulation of PPN afferents using a bipolar electrode placed in

Figure 1. Optogenetic stimulation of PPN afferents evokes glutamatergic responses in SNc DA neurons

(A) Stereotaxic injections of AAV9.hSyn.hChR2 were made in to the PPN of DAT-Cre/Ai14-tdTomato or wildtype mice. (B) Representative images taken from four sagittal sections from one DAT-Cre/Ai14-tdTomato mouse 10 days following injection of hSyn-ChR2-eYFP in to PPN. Scale bars represent 100 μ m. (C) Expanded view of section (gray box) from (B3) showing ChR2-expressing PPN fibers (green) intermingled with SNc DA neurons (red). (D) Blue light LED stimulation produced an inward current in SNc DA neurons held at -70 mV that was abolished by the AMPAR antagonist NBQX (10 μ M) (E) A 20 Hz paired-pulse stimulation protocol produced a depressing synaptic response in SNc DA neurons. (Right) Summary of PPR responses (0.83 ± 0.13 , n=10) (F) To determine AMPA:NMDA ratio cells were initially held at -70 mV to determine the timing of the AMPA peak (bottom trace), after which cells were depolarized to +40 mV to relieve Mg²⁺ block of the NMDA receptor. The NMDA peak was calculated 40 ms after the AMPA peak. (Right) Summary of AMPA peak current vs. NMDA peak current (1.43 ± 0.42 , n=13)

the rostral portion of PPN (Figure 3; PPR = 0.70 ± 0.16 , n=19). To determine the



AMPA/NMDA ratio at these synapses, cells were first held at -70 mV to determine the time of the AMPA peak, and then held at +40 mV to relieve NMDAR Mg^{2+} block. The NMDA current was measured 40 ms after the AMPA peak (Figure 1F). Measured in this way, the NMDAR current was roughly half that of the AMPAR current (peak AMPAR current/peak NMDAR current = 1.43 ± 0.42 , $n=13$).

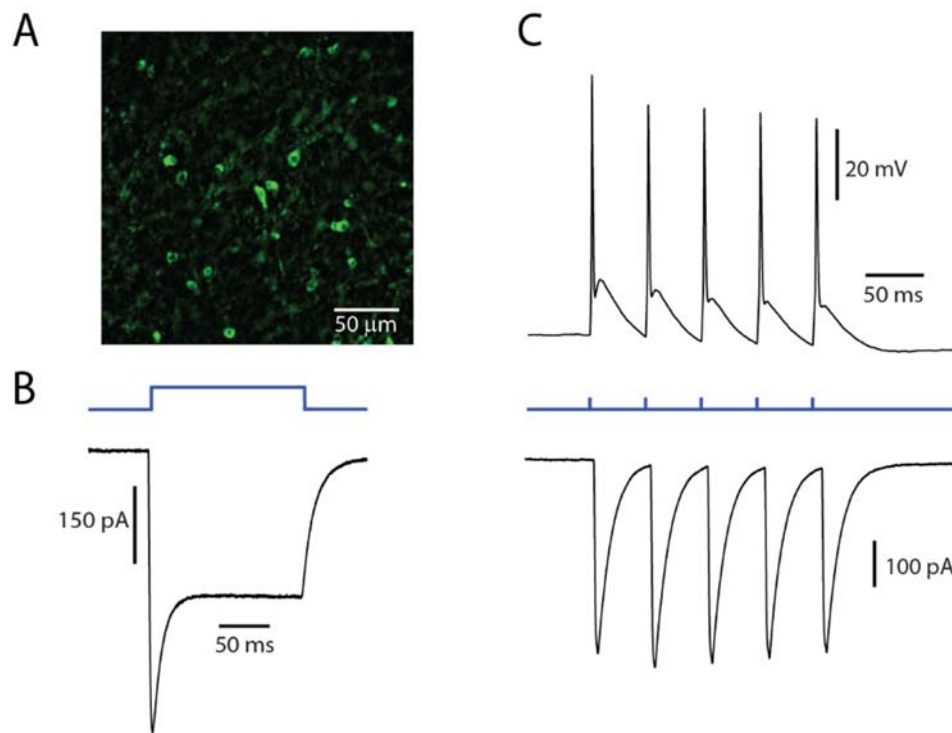


Figure 2. ChR2 is functionally expressed in PPN neurons

(A) Representative image of PPN cells expressing ChR2-eYFP. (B) Example of a prototypical photocurrent, produced by a 150 ms continuous pulse of blue LED light. (C) Evoked action potentials (Top) and associated currents (Bottom) from a train of 5 stimuli at 20 Hz. The cell reliably follows the stimulation pattern

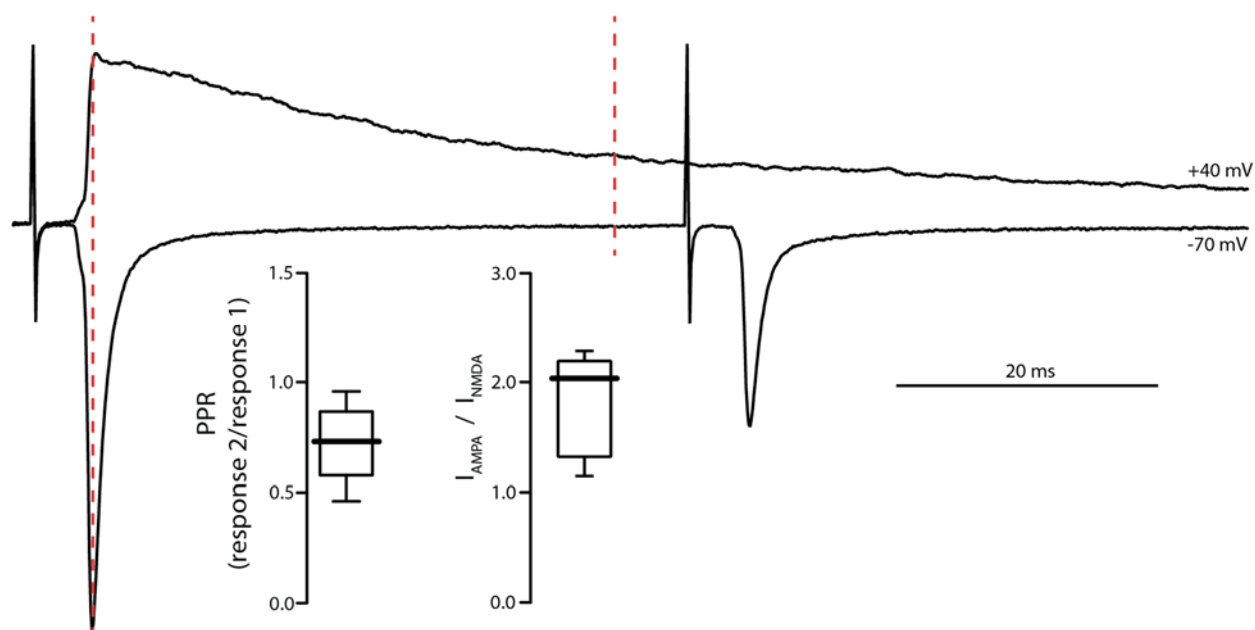


Figure 3. Electrical stimulation of PPN glutamatergic afferents to SNc

Example traces of (Top) electrical stimulation with SNc DA neuron held at +40 mV to alleviate Mg²⁺ block and (Bottom) 20 Hz PPR stimulation of SNc DA neuron held at -70 mV. The AMPA component of the current measured at +40 mV is determined based on the peak of the first current in the pair measured at -70 mV (left-most red dashed line). The NMDA component is then measured 40 ms after the AMPA component. Both PPR (0.70 ± 0.16 , $n=19$) and AMPA:NMDA ratio (2.13 ± 0.78 , $n=10$) determined with electrical stimulation are similar to those established with optogenetic stimulation of PPN afferents.

Next, the receptor subunit composition of the AMPARs and NMDARs was assessed. The majority of AMPARs in the brain contain edited GluA2 subunits, making them essentially impermeable to Ca²⁺ (Kawahara et al., 2003; Wright and Vissel, 2012; Henley and Wilkinson, 2016). In contrast to AMPARs lacking edited GluA2 subunits, these AMPARs do not rectify at depolarized membrane potentials (Koike et al., 1997; Washburn et al., 1997). At PPN synapses on SNc dopaminergic neurons, there was no discernible rectification at depolarized membrane potentials (Figure 4A), suggesting AMPARs at this synapse had

edited GluA2 subunits. Furthermore, the polyamine toxin philanthotoxin-74, which preferentially antagonizes GluA2-lacking (GluA1 and GluA3 homomeric) AMPARs (Poulsen et al., 2014), failed to significantly reduce the AMPAR currents (Figure 4B), again indicating the presence of the GluA2 receptor subunit.

NMDARs are obligate heteromers composed of two GluN1 and two GluN2 subunits. The identity of the two GluN2 subunits significantly impacts properties of the receptor, such as sensitivity to Mg^{2+} block and relative Ca^{2+} permeability. While the majority of NMDARs in the brain contain a combination of GluN2A and GluN2B subunits (Monyer et al., 1994; Wyllie et al., 2013), previous work has shown that NMDARs in SNc DA neurons contain GluN2B and GluN2D subunits (Jones and Gibb, 2005; Brothwell et al., 2007; Suárez et al., 2010; Huang and Gibb, 2014), with the latter conferring reduced Mg^{2+} sensitivity and Ca^{2+} permeability (Retchless et al., 2012; Huang and Gibb, 2014). However, none of this work was done at identified synapses. To determine the subunit composition of the NMDARs at PPN synapses, currents were evoked by a single 1 ms full-field LED pulse with SNc cells held at -60 mV in the nominal absence of extracellular Mg^{2+} . In agreement with previous work, both the GluN2B specific antagonist ifenprodil (Williams, 1993) and the GluN2C/D specific potentiator CIQ (Mullasseril et al., 2010) altered the amplitude of the evoked NMDAR currents (Figure 4C-D; ifenprodil % change: -43.31 ± 16.89 , $n=6$, $p = 0.0313$; CIQ % change: 86.22 ± 56.54 , $n=6$, $p = 0.0313$). In contrast, the GluN2A specific antagonist TCN 201 (Edman et al., 2012) had no effect on NMDAR currents (Figure 4C-D; % change: 7.76 ± 18.40 , $n=6$, $p = 0.4375$).

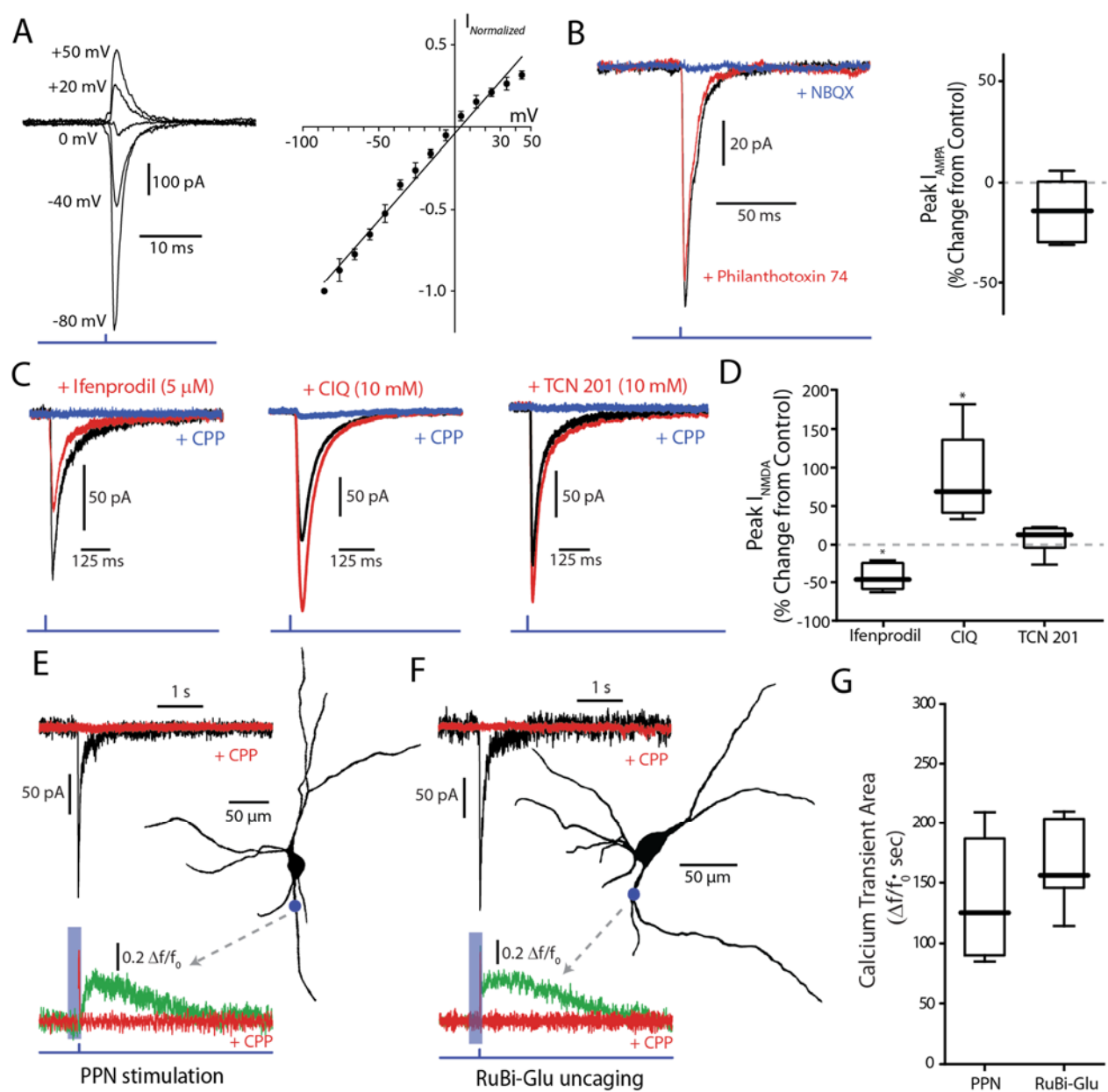


Figure 4. Glutamatergic receptors at the PPN-SNc synapse are composed of GluA2-containing AMPARs and GluN2B/D-containing NMDARs

(A) Example traces of isolated AMPA currents evoked with the cell held at different membrane potentials. (Right) Summary current-voltage (IV) relationship, where the currents at the different membrane potentials for each cell have been normalized to the current measured at -80 mV for that cell. A linear fit was applied to the data points (represented as mean \pm standard deviation). No obvious rectification is observed at positive membrane potentials. (B) Example traces of AMPA currents recorded from a DA neuron held at -70 mV before and after pharmacological manipulation. Application of philanthotoxin-74 (5 μ M; red) did not attenuate the measured current as compared to control (black). NBQX (10 μ M; blue) was applied to confirm the identity of the current. (Right) Summary of the effect of philanthotoxin-74 application ($-13.17\% \pm 14.67\%$, $n=6$). Summary data represented as mean \pm standard deviation. No significant effect was observed ($p = 0.1563$). (C) Example traces of isolated NMDA currents measured from DA neurons held at -60 mV in aCSF containing 0 Mg^{2+} before and after application of receptor-subunit specific pharmacological agents. (Left) The Glu2NB-selective antagonist ifenprodil attenuated the observed NMDA current, while (Middle) the Glu2NC/D-selective potentiator CIQ increased the peak of the measured current. (Right) The GluN2A-selective antagonist TCN 201 failed to attenuate the measured current. In all examples the nonspecific NMDAR antagonist CPP (5 μ M) abolished the current, confirming its identity. (D) Summary of the effect, relative to control, on isolated NMDA currents of the GluN2B-selective antagonist ifenprodil ($-43.31 \pm 16.89\%$, $n=6$), the GluN2C/D-selective potentiator CIQ ($86.22 \pm 56.54\%$, $n=6$), and the GluN2A selective antagonist TCN201 ($7.76 \pm 18.40\%$, $n=6$). Summarized data shown as mean \pm standard deviation. Statistical tests were two-tailed Wilcoxon signed rank tests. * $p < 0.05$ (E) 2PLSM calcium imaging of a PPN-evoked NMDA current and the associated calcium transient produced by that current. (Top) Example trace of a somatically recorded NMDA current produced by blue laser stimulation of a region of dendrite, visualized after filling the cell with a red indicator dye. (Right) Reconstructed cell generated, with a blue dot indicating both the point of stimulation and the general region where imaging data was acquired. (Bottom) Normalized ($\Delta f/f_0$) calcium transient associated with somatic NMDA current. Shaded blue area represents region where green PMT was shuttered. Application of CPP (5 μ M; red) abolished both the somatically recorded NMDA current (top) and the associated calcium transient (bottom). (F) Similar to (E), with the primary difference being that the evoked response is produced by the uncaging of focally applied RuBi-glutamate (2 mM) by blue laser light. (G) Summary of calcium transient areas from PPN-evoked ($139.26 \pm 56.40 \Delta f/f_0$ * sec, $n=5$) and uncaged RuBi-glutamate mediated ($165.94 \pm 40.27 \Delta f/f_0$ * sec, $n=5$) NMDA currents. No significance difference was found between the two data sets ($p = 0.4206$). Summary data presented as mean \pm standard deviation. Statistical test used was a two-tailed Mann-Whitney test.

To determine whether Ca^{2+} entry through synaptic NMDARs differed from those that could be activated at neighboring dendritic regions, two-photon-excitation laser-scanning microscopy was used to image SNc dopaminergic neurons loaded with either 100 μM Fura-2 or Fluo-4 calcium indicator dye. The fluorescent transient evoked by focal, dendritic optogenetic stimulation of PPN axons was compared to the transient evoked by uncaging of RuBi-glutamate in the same dendritic region (Figure 4E, F). The Ca^{2+} signal evoked by these two stimuli were not significantly different (Figure 2G).

PPN glutamatergic synapses preferentially targeted proximal dendrites

To determine the dendritic location of PPN synapses, the sCRACM approach was used (Petreanu et al., 2009; Fieblinger et al., 2014). Briefly, in *ex vivo* brain slices from mice in which ChR2 was expressed in PPN and where conducted activity was blocked by tetrodotoxin (1 μM), a focused laser (473 nm) spot was moved in 8-10 μm increments along dendrites while using the somatic electrode to monitor for synaptically evoked currents (Figure 5A-C). Spatial resolution was assessed by walking the stimulation spot away from dendrite (Figure 6). Neurons with dendrites above or below the focal plane were excluded from study to minimize the chances that synaptically evoked activity originated from a site other than the one visualized. In these experiments, photo-stimulation of proximal dendrites (within ~ 70 μm of the soma) reliably evoked responses from PPN ChR2-expressing terminals, whereas photo-stimulation of more distal dendrites almost always failed to evoke a response (Figure 5A, E).

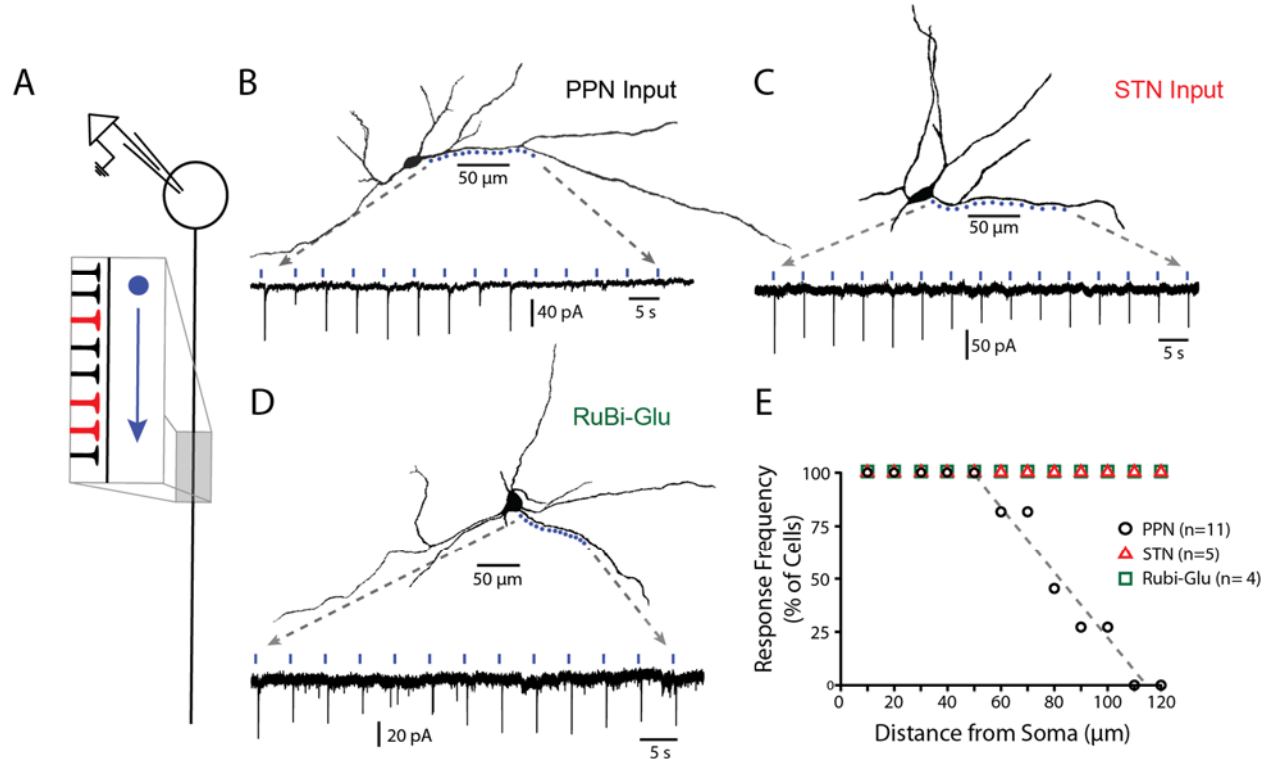


Figure 5. PPN glutamatergic synapses preferentially target proximal portions of the SNc dendritic tree

(A) Schematic of the experimental procedure. Spots along a section of dendrite, visualized with 2PLSM imaging of dye-filled cells, were assessed for responses to focal spot-laser stimulation using the sCRACM technique. (B) Example reconstructed SNc DA neuron (top) with stimulation spots placed in approximately 10 μm along a section of dendrite that was wholly visualized in the same focal plane. (Bottom) Somatically recorded currents produced by focal stimulation of PPN synapses at the spots displayed above. Responses were elicited in the first 9 spots (~ 0 to 80 μm from soma), while more distal spots (> 100 μm) failed to elicit responses. (C) Similar to (B), with the primary being that the afferents expressing ChR2 in this example originated from the STN, rather than the PPN. In contrast to (B) responses were reliably elicited at both proximal and distal locations. (D) Similar to (B) and (C), with the primary difference being that evoked responses were produced by uncaging of focally applied RuBi-glutamate (2 mM). Similar to (C), and in contrast to (B), response were elicited at in both proximal and distal dendritic regions. (E) Summary response frequency at points along the dendrite, measured as the fraction of cells that showed a synaptic response at a particular distance from the soma. Responses recorded from DA neurons in slices expressing ChR2 in PPN afferents (n=11) showed a location-dependent decrement in response frequency that was not observed in STN-ChR2 evoked responses (n=5) or RuBi-glutamate mediated responses (n=4).

Two additional experiments were performed to provide positive controls. First, glutamatergic synapses formed by STN neurons were mapped using the sCRACm approach. In contrast to PPN synapses, STN synapses were found in both proximal and distal dendrites (Figure 3C, E). Next, RuBi-glutamate was uncaged (single-photon photolysis)

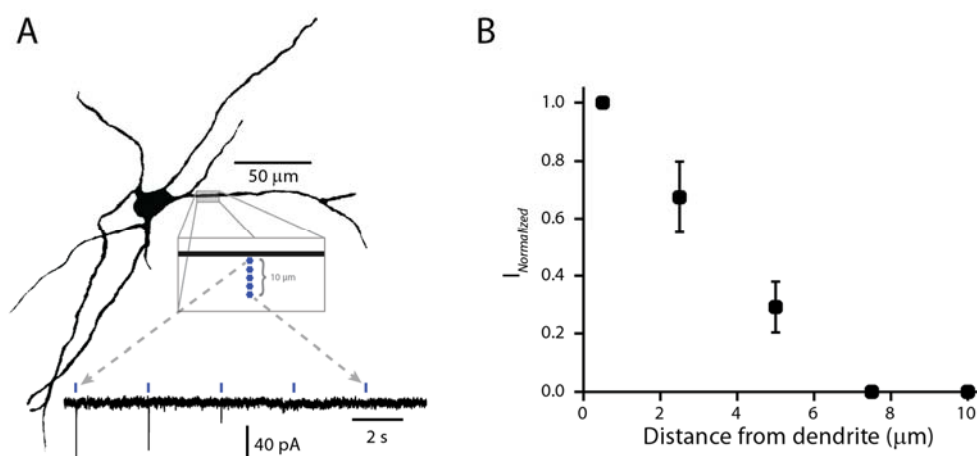


Figure 6. Validation of the spatial resolution for sCRACM functional mapping.

(A) Example reconstructed cell (Top). Five stimulation points were placed approximately 2 μm apart, starting next to and then moving away from (perpendicular to) the dendrite. Example recording (Bottom) of somatically recorded currents associated with each stimulation point. As the site of stimulation moved away from the dendrite, the amplitude of the response diminished. (B) Summary of normalized current amplitudes (normalized to amplitude of the current produced by the stimulus point closest to the dendrite) as a function of distance from the dendrite. As the point of stimulation moves away from the dendrite, response amplitude decays to zero. Data points are represented as mean ± standard deviation (n=4).

along the dendrite using a focused laser (473 nm) spot. Robust responses were evoked in both proximal and distal dendrites (Figure 3D,-E), arguing that there was a relatively uniform distribution of glutamatergic synapses throughout the SNc dendritic tree, in agreement with previous anatomical work (Henny et al., 2012). Thus, the apparent

preferential localization of PPN synapses on proximal dendrites does not reflect a limitation of the sCRACm approach or the inability to detect activation of glutamatergic synapses at distal dendritic locations.

PPN glutamatergic synapses were capable of spike patterning

Previous work has shown that proximal glutamatergic synapses onto SNc dopaminergic neurons are better able to drive spiking than more distal ones (Blythe et al., 2009). To determine the ability of proximal PPN synapses to drive patterned spiking, SNc dopaminergic neurons were recorded in the perforated patch mode and PPN axons stimulated optogenetically. The probability of evoking a spike in a SNc DA neuron rose rapidly with stimulus intensity (Figure 7). Using the lowest LED power that reliably evoked a spike (typically 6-10% of the LED maximum power), stimulus trains of varying length and frequency were delivered. In addition to regular trains, burst patterns recorded from SNc dopaminergic neurons *in vivo* were included (Grace and Bunney, 1984b). To ensure response fidelity for the higher-frequency (> 10 Hz) stimulation protocols, the opsin Chronos was used in a subset of these experiments (Klapoetke et al., 2014). Regardless of the protocol used, optical stimulation of PPN axons reliably evoked spikes throughout the stimulus train (Figure 8A-B), with the average spike frequency within the stimulus period being linearly related (with a slope of 1) to the stimulus frequency (Figure 8C).

To determine whether NMDARs contributed to the ability of PPN axons to drive burst spiking, a pharmacological approach was used. Surprisingly, application of the NMDAR antagonist CPP did not significantly alter the response to PPN stimulation at any frequency

(Figure 8D-F). In contrast, application of the AMPAR antagonist NBQX completely abolished responses (Figure 8D-F), indicating a dependence on AMPARs, but not NMDARs.

Frequently, PPN-evoked spikes were truncated in amplitude and had a more hyperpolarized threshold than spikes that were spontaneously generated (e.g., Fig 8B). These likely represent initial segment axonal (AIS) spikes that fail to invade the rest of the

Figure 7. Evoked-spike probability is related to stimulus intensity

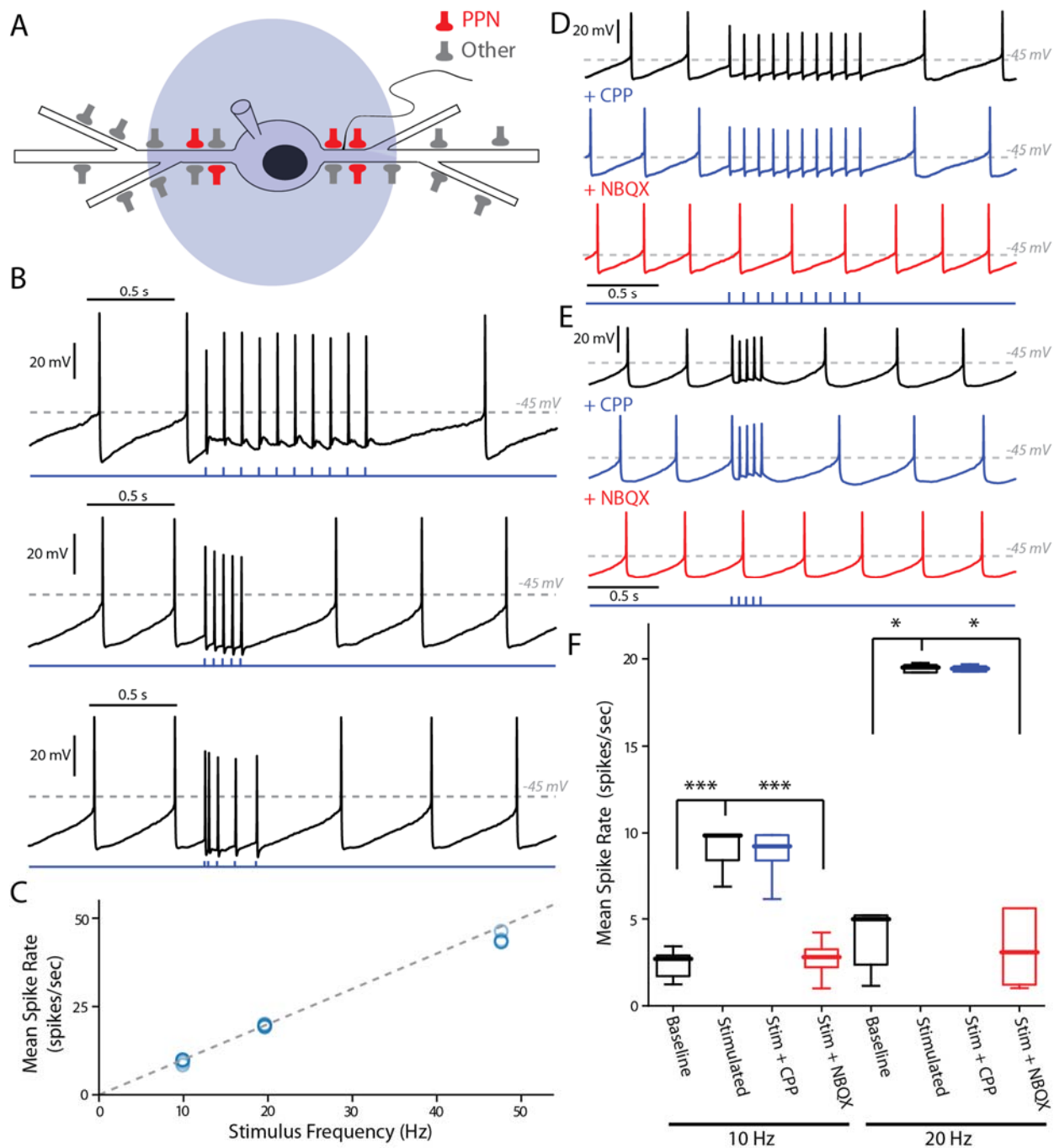
(A) Example traces from two cells. (Left) Showed no response to 2% LED stimulation, but higher stimulation intensities produced full spikes. (Right) In contrast, 2% and 4% LED stimulation produced graded excitatory post-synaptic potentials (EPSPS), while higher intensities produced full spikes. (B) Summary showing the probability of evoking a spike as a function of stimulus intensity, quantified as the fraction of cells (n=5) that responded with a full spike at a particular intensity. At intensities $\geq 6\%$ all cells reliably responded with a full spike upon stimulation.

Figure 8. PPN glutamatergic input is capable of generating burst firing in SNc DA neurons

(A) Full field blue-LED stimulation of ChR2-expressing PPN afferents was performed while recording spiking activity in SNc DA neurons using the perforated-patch configuration. (B) Example traces of different stimulation patterns: (Top) 10, 1ms stimuli with an inter-stimulus interval of 100 ms, (Middle) 5, 1 ms stimuli with an inter-stimulus interval of 50 ms, and (Bottom) 5, 1ms stimuli with inter-stimulus intervals of 20 ms, 50 ms, 100 ms, and 120 ms. In all cases spikes were reliably generated by the stimulation protocols. (C) Summary of the mean intra-stimulus spike frequency (spikes/s) as a function of the frequency of stimulation. The measured spike frequency was linearly related to the stimulation frequency in a near 1:1 relationship. (D) Example traces from a SNc DA neuron responding to the 10 stimuli, 10 Hz PPN ChR2 stimulation protocol before and after pharmacological manipulation. Application of the NMDAR antagonist, CPP (5 μ M), did not significantly attenuate the response to PPN stimulation, while application of the AMPA receptor antagonist, NBQX (10 μ M) completely abolished the evoked response. (E) Similar to (D), with the primary difference being the usage of the 5 stimuli, 20 Hz PPN stimulation protocol. As with (D), application of CPP failed to attenuate the response, while NBQX completely abolished the response. (F) Summary of pharmacological manipulation of SNc DA neuron firing pattern response to PPN stimulation. Both 10 Hz (9.03 ± 1.19 spikes/s, n=9) and 20Hz (19.53 ± 0.25 spikes/s, n=5) stimulation significantly increased firing rate in comparison to control (10 Hz stim: 2.40 ± 0.82 spikes/s, n=9, p=0.0001; 20 Hz stim: 3.43 ± 1.90 spikes/s, n=5, p=0.0117). CPP application failed to significantly decrease the response to stimulation (10 Hz stim: 8.81 ± 1.55 spikes/s, n=5, p=0.8413; 20 Hz stim: 19.49 ± 0.19 spikes/s, n=5, p=1.0). In contrast, NBQX application significantly attenuated the PPN evoked response (10 Hz stim: 2.71 ± 1.10 spikes/s, n=6, p=0.0008; 20 Hz stim: 2.73 ± 2.25 spikes/s, n=5, p=0.0234). Summaries are presented as mean \pm standard deviation. Statistical tests used were two-tailed Mann-Whitney tests with Holm-Bonferroni corrections for multiple comparisons. *** p < 0.001, * p < 0.05.

somato-dendritic (SD) region where the electrode was positioned (Grace and Bunney, 1980, 1983a, 1983b). Indeed, previous work has shown that antidromically-evoked AIS spikes often fail to generate full SD spikes in SNc DA neurons (Grace and Bunney, 1983b). The ability of AIS spikes to evoked full SD spikes should be dependent upon the excitability of the SD region, which should be determined by ongoing pacemaking. To test this

hypothesis, individual spikes were evoked by optical stimulation of PPN axons at different points in the pacemaking cycle (Figure 9A). When the stimulus occurred towards the end of normal pacemaking cycle, the evoked spikes were indistinguishable from spontaneously



occurring spikes (Fig 9A-B). In contrast, when spikes were evoked early in the oscillation,

just after a spontaneously occurring spike, they exhibit more hyperpolarized spike thresholds and reduced amplitudes, as evident in plots of the first derivative of membrane voltage (dV/dt) as a function of membrane voltage (mV) (Figure 9A, C). Plots of PPN-evoked spike threshold and amplitude as a function of the time from the preceding spike, normalized by the average interspike-interval (ISI) of the spikes preceding the stimulus (4 s worth of recording) revealed this relationship more clearly (Figure 9D-E). PPN-evoked spikes early in pacemaking cycle (i.e. near time = 0) had hyperpolarized thresholds and reduced amplitudes, whereas spikes evoked near the end of the pacemaking cycle were identical to spontaneously occurring spikes. Also, in agreement with previous work (Guzman et al., 2009), PPN-evoked spikes reset the pacemaking cycle, as indicated by a clustering of points around 1 when comparing the ISI between the evoked spike and the next spontaneously occurring spike to the mean ISI for the cell (Fig 9F).

Although PPN-evoked spikes were not strongly influenced by somatic conductances, they should be regulated by dendritic conductances because of the common dendritic location of the AIS (Blythe et al., 2009; Matsuda et al., 2009). One well described dendritic channel that slows repetitive spiking in SNc DA neurons is the small conductance, Ca^{2+} -activated K^+ channel (SK) (Ping and Shepard, 1996; Wolfart et al., 2001). Indeed, in addition to accelerating pacemaking rate, blocking SK channels with apamin increased the ability of PPN terminals expressing ChR2 to evoke faithful, repetitive (10 Hz) spiking at low stimulus intensities (Figure 10). Interestingly, PPN stimulation in the presence of apamin delayed the next spontaneously occurring spike, rather than simply resetting the pacemaking rhythm (Figure 10).

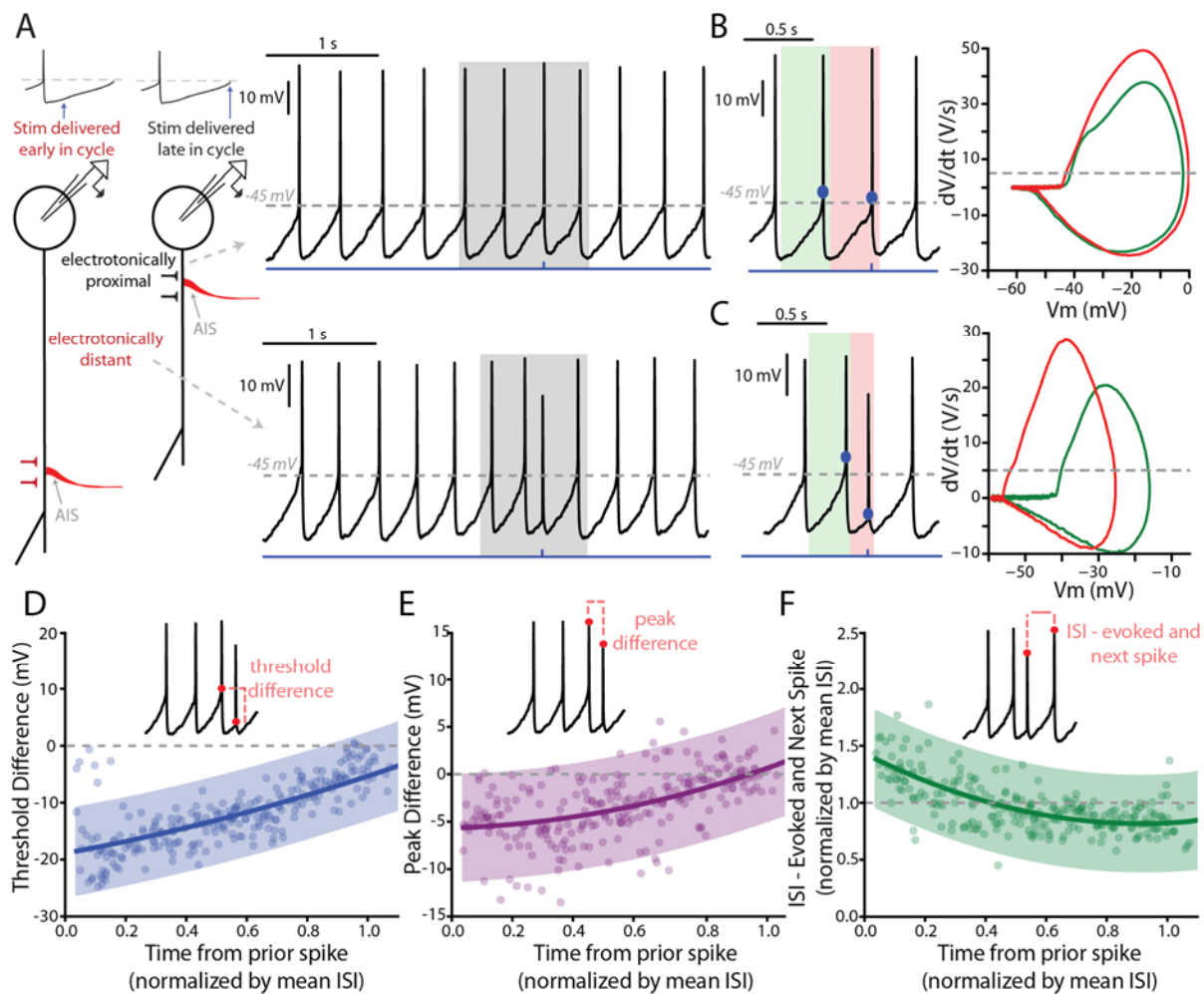


Figure 9. Features of PPN-evoked spikes depend on the phase of SNc DA neuron pacemaking cycle

(A) Schematic representation of two points in the pacemaking cycle. As the cell nears threshold towards the end of pacemaking cycle it “tightens up” in preparation of spiking. This manifests as an apparent shortening of the distance between the source of AP generation, the AIS, and the somatic recording electrode due to a longer length constant. Consequently, the evoked spike (Top) appears qualitatively similar to the spontaneously generated APs. In contrast, early in the oscillation cycle the cell is particularly “leaky”, resulting in a small length constant and consequently a spike that appears qualitatively different when recorded at the soma (Bottom). (B) Comparison of the PPN evoked spike (red) to the spike preceding the evoked spike (green). Representative spikes are expanded from the shaded region in A. Phase plots (Right), generated from respective green and red shaded regions (left), for the two spikes appear similar, with nearly identical thresholds (determined at the point when the dV/dt exceeds 5 V/S – i.e. the gray dashed line in the phase plot). (C) Similar to (B), with the primary difference being the point in the pacemaking cycle where the stimulus occurred. There is a significant shift in the threshold of the evoked spike, as observed by a leftward shift in its associated phase plot (Right, red). (D-F) Summaries of three properties of the evoked spike: threshold difference (in comparison to the preceding spike), peak difference (in comparison to the preceding spike), and inter-spike interval between evoked spike and the next spontaneously generated AP. Oscillation phase is represented as time to the stimulus from the preceding spike, normalized by the mean ISI for all the spikes preceding the stimulus (averaging window = 4 s). In (D) and (E) during the early phase of the oscillation (near $t=0$) there is a large deviation in measured spike threshold and spike peak in comparison to the preceding spike. This difference diminishes as t approaches 1. In (F), except for at the earliest time points the normalized ISI values largely cluster around 1, indicating a resetting of the pacemaking cycle. Fit lines are second-order polynomials, with shaded areas representing 95% confidence intervals.

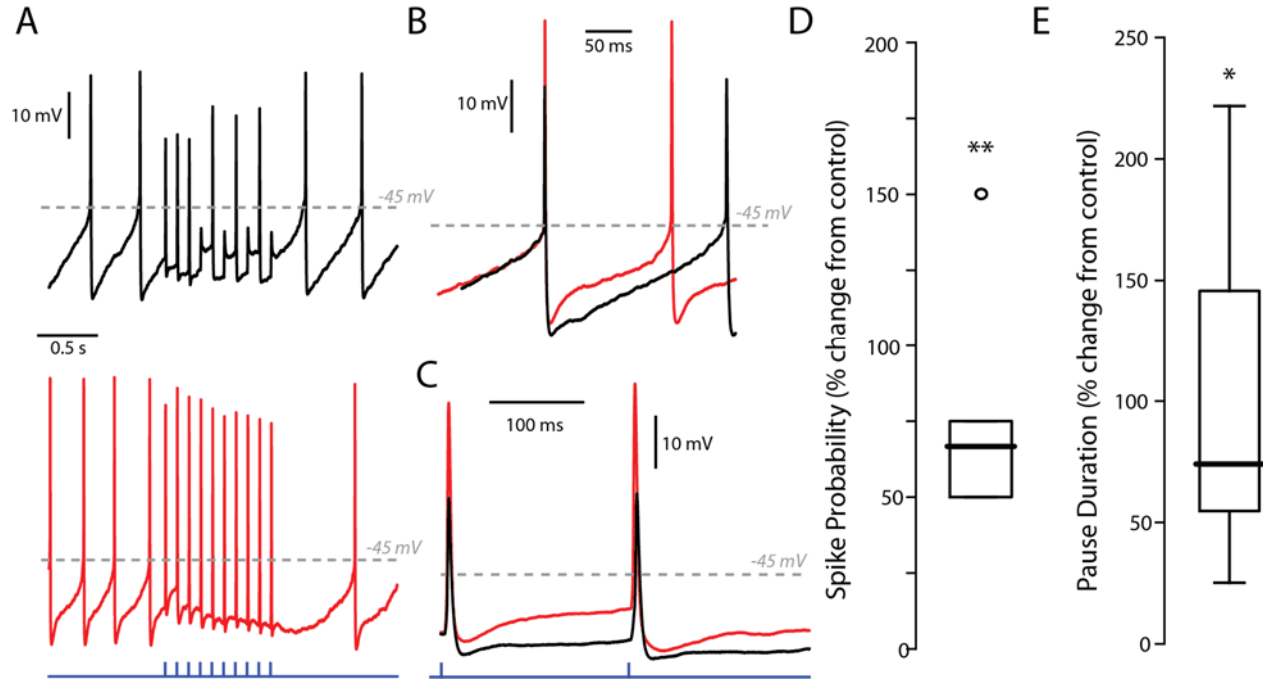


Figure 10. Effect of SK inhibition on PPN stimulation of SNc DA neurons

(A) Example traces of a stimulus train of 10 stimuli at 10 Hz with a low (5%) LED intensity before (black) and after (red) treatment with apamin (200 nM). Apamin treatment increased both the firing rate of the cell as well as the response to PPN stimulation. Apamin treatment also increased the pause between the last stimulus in the stimulus train and the next spontaneously occurring spike. (B) Enhanced example of a spontaneous spike before (black) and after (red) apamin treatment. As expected, apamin treatment produced an increase spike frequency and a decrease in the medium afterhyperpolarization (mAPH). (C) Enhanced example of an evoked spike before and after apamin treatment, again showing a decreased mAPH. (D) Summary after percent-change in spike probability as a result of apamin treatment at a 5% LED intensity. Spike probability was quantified as the number of full spikes divided by the total number of stimuli (10). Apamin significant increased the probability of evoking a spike ($78.34 \pm 41.50\%$; $n=5$; $p=0.0079$). Summary presented as mean \pm standard deviation. Statistical test used was a two-tailed Mann-Whitney test. ** $p < 0.01$. (E) Summary of percent-change in the duration of the pause in spiking between the last stimulus in the stimulus train and the next spontaneously occurring spike before and after apamin treatment. Apamin significant increased the duration of the pause ($104.29 \pm 79.29\%$; $n=5$; $p=0.0317$). Summary presented as mean \pm standard deviation. Statistical test used was a two-tailed Mann-Whitney test. * $p < 0.05$

PPN-evoked spikes propagated down the axon

As mentioned above, the AIS typically arises from a proximal dendrite in SNc DA neurons (Blythe et al., 2009; Matsuda et al., 2009), in the region where PPN synapses were found. Thus, it was possible that PPN-evoked spikes, even though they often appeared truncated at the soma, would be faithfully propagated down the axon. To test this hypothesis, paired recordings were performed from the soma and from the axon. First, a somatic whole cell recording was established and the cell filled with dye to allow visualization of the dendrites and axon. The axon was identified by the presence of a retraction ball (Atherton et al., 2008; Blythe et al., 2009). Once identified, a second pipette was used to record from the axon in a loose-seal configuration. Recordings were then simultaneously made of both spontaneous and evoked spikes from the soma and axon (Figure 11B-C). Spontaneously recorded somatic spikes invariably propagated into the axon, as expected. More importantly, PPN-evoked spikes were also invariably seen in the axon, regardless of the phase of the pacemaking cycle and the somatic appearance of the spike (Figure 11B-C). Plotting the instantaneous spike frequency within the axon as a function of the instantaneous spike frequency in the soma confirmed this relationship (Figure 11D-E). Failure of the somatically recorded spikes to invade the axon would lead to points below the linear trend line, but this was not seen as all somatic spikes showed corresponding axonal spikes (Figure 11D-E). This finding is in agreement with previous work showing that IS spikes alone are capable of triggering axonal firing (Grace and Bunney, 1983b).

A SNc dopaminergic neuron

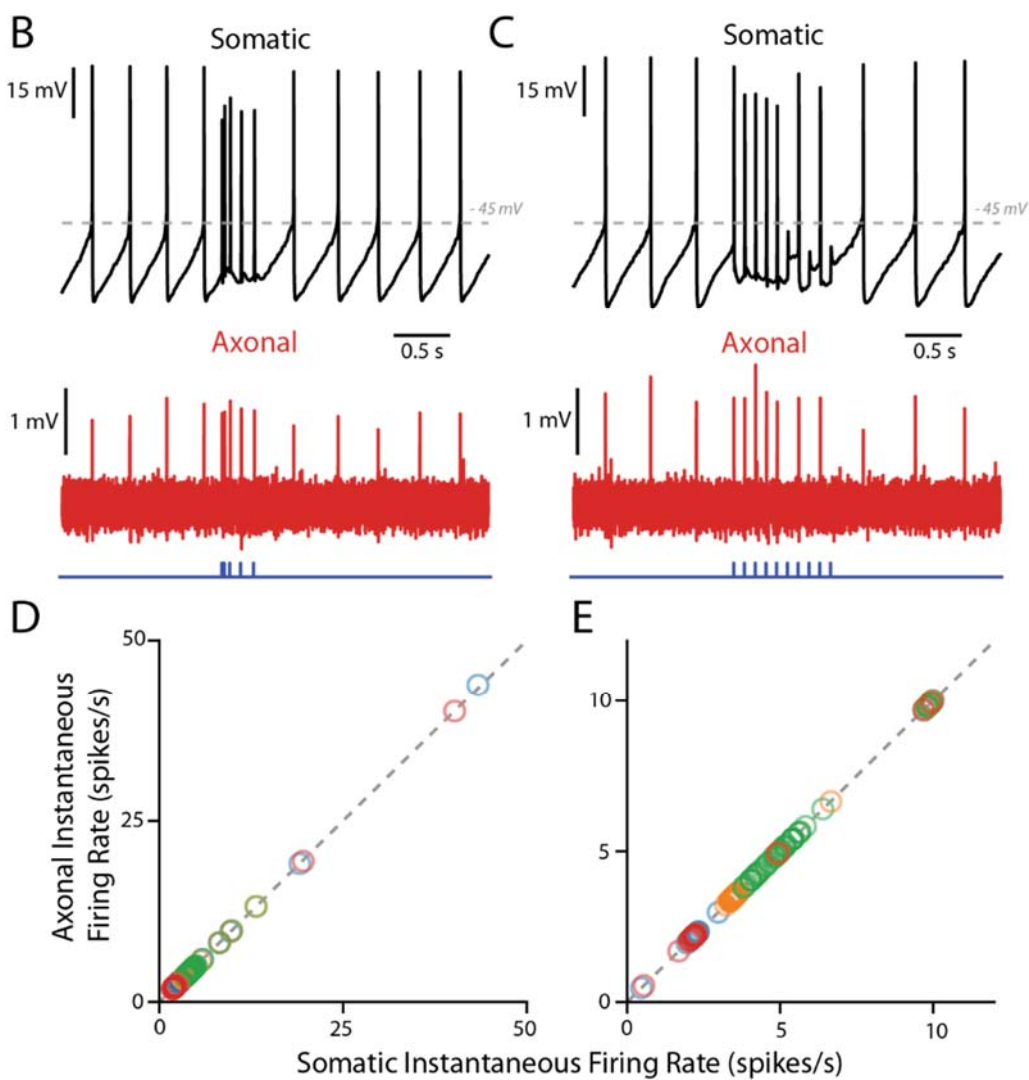
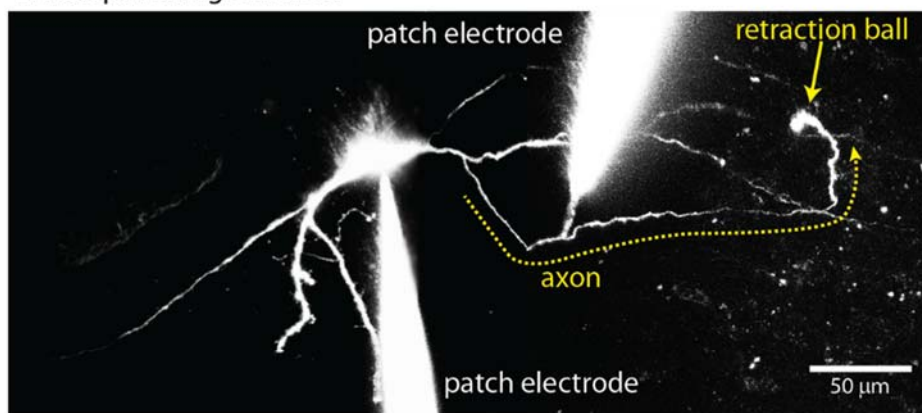


Figure 11. PPN-evoked spikes reliably invade the axon

(A) Reconstruction of an example cell where two recording electrodes are clearly visible. Paired recording were made in order to simultaneously measure evoked spikes at the soma and at the axon. Axons (yellow dashed line) were identified based upon the presence of a retraction ball (yellow arrow) following the filling of the cell with dye via the somatic electrode. After identification, loose-seal recordings were made of spike activity in the axon. (B) Example recording of somatic whole-cell (Top) and axonal loose-seal (Bottom) recordings of spontaneous and stimulated (5, 1 ms stimuli with variable inter-stimulus interval protocol) action potentials. Spikes recorded at the soma are mirrored by events in the axon. (C) Similar to (B), except for the application of a different stimulation protocol (10, 1 ms stimuli with an inter-stimulus interval of 100 ms) (D-E) Plot of the instantaneous spike rate (spikes/s) of APs recorded in the axon as a function of the instantaneous spike rate (spikes/s) of APs recorded in the soma. Points fall along a linear, 1:1 relationship (gray dashed lines), indicating reliable representation in the axonal recordings of spike events also recorded in the soma. (D) are data points from the variable inter-stimulus interval protocol; (E) are data points from the 10 Hz stimulation protocol. Different colors represent different cells (n=4).

Discussion

Burst spiking in SNc DA neurons is a critical signal for goal-directed behavior (Schultz, 2007; Tsai et al., 2009; Bromberg-Martin et al., 2010; Schultz, 2016a). While dependent upon synaptic activity (Grace and Bunney, 1984b; Overton and Clark, 1992; Smith and Grace, 1992), the cellular mechanisms dictating the temporal structure of the burst are poorly understood. The most widely held view is that bursts are produced by intrinsic oscillatory mechanisms engaged by activation of dendritic NMDARs (Lee and Tepper, 2009; Morikawa and Paladini, 2011; Paladini and Roeper, 2014). Our results expand this landscape to include an additional mechanism by which bursts can be generated. In particular, they show that bursts could be produced by patterned stimulation of PPN synapses formed on proximal dendrites near the AIS. Engagement of NMDARs was not necessary for burst generation in this case. Moreover, in contrast to the conventional model, this mechanism allows bursts to be generated and structured

independently of ongoing pacemaking activity or synaptic input to more distal dendrites, like that arising from tonic activity in pallidal and nigral GABAergic neurons. Being able to precisely control the timing and duration of bursts could prove to be important to movement control, particularly that triggered by external events.

PPN glutamatergic synapses target proximal dendrites

Our experiments provide the first characterization of the receptor complement at PPN glutamatergic and the sub-cellular distribution of these synapses on SNc DA neurons. Optogenetic approaches allowed the selective activation of axons originating in the PPN. Pharmacological tools allowed the receptor subtypes at these synapses to be determined. As in most adult glutamatergic synapses, the AMPARs at PPN synapses were Ca^{2+} -impermeable, as judged by their lack of rectification and insensitivity to philanthotoxin-74. Moreover, as expected from previous work examining NMDARs at unidentified synapses (Jones and Gibb, 2005; Brothwell et al., 2007; Suárez et al., 2010), the NMDARs at PPN synapses were GluN2B/D containing. More specifically, the magnitude of the NMDAR block achieved by ifenprodil was that expected of a triheteromeric, GluN2B/D containing receptor (Hatton and Paoletti, 2005; Huang and Gibb, 2014). The ability of the GluN2C/D potentiator (CIQ) to increase NMDAR currents further supports the proposition that triheteromeric GluNB/D containing receptors are present at this synapse (Jones and Gibb, 2005; Huang and Gibb, 2014).

Although the composition of ionotropic glutamate receptors at PPN synapses was expected, their sub-cellular distribution, as revealed by the sCRACM technique (Petreanu et al., 2009; Fieblinger et al., 2014), was not. In contrast to the broad distribution of postsynaptic glutamate receptors and STN synapses, PPN glutamatergic synapses were found only on proximal

dendrites. This location specificity places these synapses near the AIS, which typically arises from proximal portions of a primary dendrite (Blythe et al., 2009; Matsuda et al., 2009). It remains to be determined whether synapses made by other glutamatergic regions innervating the SNc (e.g., superior colliculus) have a similar distribution.

An alternative mechanism for burst generation

The positioning of PPN glutamatergic synapses on proximal dendrites near the AIS should maximize their ability to control spike generation. Indeed, at low optical stimulation intensities, SNc DA neurons faithfully followed the pattern of PPN stimulation, even at high frequencies. This behavior suggests that PPN synapses near the AIS are capable of driving spike generation independently of NMDARs. The AIS origin of the PPN evoked spikes was consistent with several features of the somatic recordings, including the dependence of the nominal spike threshold and amplitude on the phase of the pacemaking cycle and the faithful propagation of evoked spikes down the axon. Although focal optical stimulation of dendrites that did not bear the AIS might have evoked dendritic spikes that would have manifested greater dependence on the pacemaking cycle, it remains to be determined whether individual PPN axons have terminal fields that are restricted to a single dendrite or diverge to contact several dendrites, including the AIS bearing one.

The degree of PPN convergence on individual SNc DA neurons also is uncertain. Optogenetic stimulation artificially synchronizes spiking in PPN axons, producing a temporal summation of synaptic inputs that may not occur *in vivo*. This could lead to an over-estimation of the ability of PPN to control the patterning of SNc DA neuron spiking, particularly bursting. However, it is possible that individual SNc DA neurons are innervated by a small number of

PPN axons; in this case, synchronization of inputs becomes much less of a concern. The steep relationship between optical stimulus intensity and SNc DA neuron spike probability is consistent with this possibility. This kind of mapping between PPN and SNc would provide an explanation for the variability in SNc burst patterns observed *in vivo* (Grace and Bunney, 1984b; Hyland et al., 2002). However, to definitively answer this question, anatomical approaches will be needed. One possibility is single cell mapping experiments using tracer fills of individual PPN axons. Alternatively, a rabies-based retrograde tracing could be employed by generating a sparse starter populations within the SNc (Wickersham et al., 2013).

Regardless, these experiments demonstrate that PPN glutamatergic synapses are capable of determining the precise timing of SNc DA neuron spikes that are propagated down the axon to target structures, like the striatum. Moreover, PPN synapses were capable of driving precisely structured bursts, like those recorded *in vivo* (Grace and Bunney, 1984b). This result is consistent with previous studies showing that focal application of glutamate to proximal dendrites, as well as local electrical stimulation of glutamatergic axons, was capable of producing spike bursts (Blythe et al., 2007, 2009).

Thus, there appear to be two general mechanisms by which spike bursts can be generated in SNc DA neurons. In contrast to the PPN-driven mechanism, previous studies have shown that local application of glutamate can evoke bursts that depend upon activation of NMDARs (Johnson and Wu, 2004; Deister et al., 2009). *In vivo*, SNc DA neuron burst spiking can be attenuated by NMDAR antagonists (Charley et al., 1991; Overton and Clark, 1992; Smith and Grace, 1992; Chergui et al., 1993) or genetic deletion of NMDARs (Zweifel et al., 2009). Similarly, stimulation of the STN *in vivo* increases burst firing in SNc DA in an NMDA-dependent (Smith and Grace, 1992; Chergui et al., 1994). The bursts generated in this way

harness the intrinsic oscillatory mechanisms of dendrites (Deister et al., 2009; Kuznetsova et al., 2010; Ha and Kuznetsov, 2013). The dependence upon intrinsic oscillatory mechanisms will undoubtedly allow pacemaking and ongoing synaptic input, particularly GABAergic synaptic activity, to influence the timing of bursts, contrasting it with the ‘short-circuiting’ of these processes by PPN synapses. Another interesting feature of the NMDAR-dependent burst is its dependence upon the voltage-dependence of Mg^{2+} block. Using the dynamic clamp technique, Deister *et al.* (2009) showed that removal of NMDAR voltage sensitivity associated with Mg^{2+} block abolished burst firing. Given that tri-heteromeric GluN1-GluN2B-GluN2D NMDARs found at PPN synapses have lower Mg^{2+} sensitivity (Huang and Gibb, 2014), it could be that more distally located NMDARs have a different subunit composition that enhance their ability to promote bursts. Lastly, it is unclear to what extent extra-synaptic NMDARs play a role in burst generation. Given the differences in postsynaptic signaling by synaptic and extrasynaptic NMDARs (Hardingham and Bading, 2010; Paoletti et al., 2013), the differential engagement by the two different modes of burst generation could have important long-term consequences.

Functional consequences of PPN control of SNc

There are several lines of evidence suggesting that the PPN exerts a strong control over DA neuron spiking *in vivo*. For example, stimulation of the PPN *in vivo* produces a significant increase in bursting in ventral tegmental area (VTA) DA neurons and dopamine release in the nucleus accumbens (Floresco et al., 2003). Moreover, lesioning the PPN disrupts dopamine-dependent learning in a variety of behavioral tasks (Inglis et al., 2000; Alderson et al., 2008; Bortolanza et al., 2010; Jimenez-Martin et al., 2015; Syed et al., 2016). Recordings in behaving animals have shown that PPN neurons code for predicted reward value, reward magnitude and

stimulus salience (Pan and Hyland, 2005; Kobayashi and Okada, 2007; Okada et al., 2009; Norton et al., 2011; Okada and Kobayashi, 2013). Often, the activity in PPN precedes that in SNc (Pan and Hyland, 2005; Kobayashi and Okada, 2007; Okada et al., 2009), raising the possibility that signals from the PPN are critical for the computations performed by DA neurons.

In addition to reward signaling, recent work has implicated PPN glutamatergic neurons in the control of movement gated by the striatum (Roseberry et al., 2016). Our results show that this activity provides a potent excitation of SNc DA neurons that may be important to modulating striatal circuits controlling movement sequences. This inference is consistent with the observation that phasic activity in SNc DA neurons is temporally correlated not only with the outcomes of actions, but action itself (Howe and Dombeck, 2016). Precisely what is being coded by PPN activity influencing SNc and how this translates into the pattern of SNc spiking remains to be determined by *in vivo* experiments (Hong and Hikosaka, 2014). Nevertheless, it is tempting to speculate that the basal ganglia control of PPN glutamatergic neurons described by Roseberry *et al.* (2016) is fed back to the SNc and broadcast to the striatum, allowing complex movement sequences to be executed – a capacity that is lost in PD patients with degeneration of SNc DA neurons (Hernández et al., 2015).

Summary

Our studies identify a novel mechanism for burst generation in SNc DA neurons. Glutamatergic innervation of the SNc by the PPN was found to preferentially target proximal regions of the SNc dendritic tree, near where the AIS of these cells generally originates, placing these synapses in a favorable location to drive *spiking*. In contrast to the previously described mechanism involving the cooperation of intrinsic oscillatory activity with NMDAR activation to

generate bursts in SNc neurons, activation of PPN fibers was capable of directly patterning SNc neuron spiking independently of regular pacemaking activity and without the need to engage NMDARs. Further examination is required to determine whether this mechanism generalizes to other sources of glutamatergic input to SNc neurons. Nevertheless, this work indicates the PPN is a likely source of extrinsic control of SNc neuron firing *during* goal-directed behavior.

Future Directions

The work discussed here provides novel insight in to potential mechanisms for burst generation in SNc DA neurons. These findings raise a number of addition questions, however, regarding the interaction between PPN glutamatergic neurons and the SNc.

Does inhibition of PPN glutamatergic neuron firing attenuate spontaneous and reward-based bursting in SNc DA neurons?

A next logical step from the work presented here is an examination of how activity in PPN glutamatergic neurons affects SNc DA neurons *in vivo*. Several studies have shown that electrical stimulation of PPN *in vivo* is capable of eliciting burst firing in SNc neurons, which has been attributed at least in part in glutamatergic activity (Scarnati et al., 1984; Di Loreto et al., 1992; Lokwan et al., 1999; Hong and Hikosaka, 2014). These studies, however, fail to capture naturally occurring activity patterns within PPN glutamatergic neurons, therefore limiting the conclusions that can be drawn with regard to how PPN may govern SNc firing patterns. Furthermore, there is undoubtedly stimulation of not only glutamatergic but also cholinergic and potentially GABAergic input from the PPN to SNc neurons in these experimental paradigms, also making interpretation difficult. Similarly,

while studies have correlated activity patterns in the PPN with responses in the SNc, this work has not been able to distinguish between neurochemical subpopulations within the PPN (Pan and Hyland, 2005; Hong and Hikosaka, 2014).

One prediction from the data shown here is that disrupting PPN glutamatergic input to the SNc should produce a concomitant reduction in burst firing in the SNc. While lesions of the STN have been shown to reduce burst firing in the SNc (Smith and Grace, 1992), similar studies have not been performed for the PPN input to these cells. Lesioning the PPN, however, would not be an ideal choice given the mixed input from the PPN to the SNc. Rather, a more targeted strategy by which the input solely from PPN glutamatergic cells could be disrupted would be preferred. Chemogenetic approaches offer such an opportunity (Roth, 2016). Designer receptors exclusively activated by designer drugs (DREADDs)-based methods could be employed, whereby inhibitory muscarinic G-protein coupled receptors (GPCRs) that have been mutated to only respond to an exogenous ligand (CNO: clozapine-N-oxide) allow for dynamic control of neuronal activity through administration of said ligand (Krashes et al., 2011; Roth, 2016; Koga et al., 2017). Using a VGLUT2+ *Cre* line these DREADDs could exclusively expressed in PPN glutamatergic cells via intracranial injections in to the PPN of a *Cre*-dependent virus. Attenuation of firing within these cells could then be assessed in *in vivo* preparations monitoring firing patterns within the SNc in different behavioral contexts.

Does inhibition of PPN glutamatergic neurons disrupt learning?

Were inhibition of PPN glutamatergic neurons to lead to a reduction in burst activity in SNc DA neurons *in vivo*, the subsequent expectation would be a similar disruption in learning acquisition. A number of lesion studies have tested this hypothesis, with the general observation being that, indeed, lesioning the PPN impairs learning in classical and operant conditioning paradigms (Inglis et al., 2000; Alderson et al., 2008; Bortolanza et al., 2010; Jimenez-Martin et al., 2015; Syed et al., 2016). As discussed, though, lesions fail to provide information on how specific subpopulations in the PPN are involved in outcome measures.

Recent work using *in vivo* optogenetics has demonstrated that specific activation of PPN glutamatergic neurons is reinforcing (Yoo et al., 2016). PPN stimulation was shown to excite VTA DA neurons. Furthermore, when given the choice between two options (e.g. two nosepoke holes), animals preferred that which was paired with stimulation of PPN glutamatergic neurons (Yoo et al., 2016). The converse, however, has not been tested. In addition to the excitatory ChR2, optogenetic techniques allow for the silencing of neurons using archaerhodopsin or halorhodopsin (Han, 2012). *In vivo* recordings of the PPN has shown that they respond to behavior cues at shorter latency than DA neurons (Pan and Hyland, 2005). *Cre*-dependent expression of an inhibitory opsin in VGLUT2+ PPN neurons, using similar techniques described above, would allow for a directly inhibiting that response with high temporal precision. If firing in these cells is crucial to reinforcement learning, attenuation of their response to behavioral cues should block learning acquisition.

What learning-signals do PPN glutamatergic neurons encode?

Even if PPN glutamatergic neurons are shown to be a critical input to DA neurons for goal-directed behavior, it remains largely unclear what information these cells are providing to the SNc. As discussed, a number of studies have observed cells within the PPN that appear to encode signals corresponding to different components of reward signaling (Pan and Hyland, 2005; Kobayashi and Okada, 2007; Okada et al., 2009; Norton et al., 2011; Okada and Kobayashi, 2013); however, there exists substantial heterogeneity in the response profiles of PPN neurons with regards to sensory cues associated with reward. Unlike work characterizing different activity patterns in PPN subpopulations in response to changes in arousal state (Mena-Segovia et al., 2008; Boucetta and Jones, 2009; Roš et al., 2010), the reward-learning literature in PPN has largely studied the area without delving in to specifics about different populations within the PPN. It is likely, though, that the heterogeneity in observed in these cells is partly attributable to the neurochemical heterogeneity in cell populations in the PPN.

This could be attacked in multiple ways. One strategy would be to employ the techniques used in the PPN-arousal literature – namely, *in vivo* extracellular recording followed by juxtacellular labeling, allowing for post-hoc identification of cell type (Mena-Segovia et al., 2008; Boucetta and Jones, 2009; Roš et al., 2010). While this is likely the preferred method for studying the activity of single cells, an examination of the PPN glutamatergic population as a whole would also prove to be informative. *In vivo* imaging of large populations of neurons has been achieved using genetically-encoded calcium indicators (GECIs), particularly GCaMP (Chen et al., 2012; Zariwala et al., 2012; Dana et al., 2014). These can be targeted to specific populations of neurons using the *Cre*-driver

methods already described. *In vivo* imaging techniques have historically been limited to more superficial structures; recently, however, deeper brain areas have been imaged using implantable microendoscopes (Grewe et al., 2017). This technology has been paired with miniaturized, head-mounted fluorescent microscopy to allow for the recording of the activity in neural ensembles in awake behaving mice (Ghosh et al., 2011; Ziv et al., 2013; Grewe et al., 2017). Applied to the PPN, these techniques would allow for directly assessing how glutamatergic neurons respond when presented with salient stimuli, as well as how those responses change over the course of learning. The findings from this would have important implications for our understanding of how PPN neurons may be driving the activity of SNc DA neurons *in vivo*.

What implications do these findings have for other sources of glutamate to SNc DA neurons?

Our work indicates that synapses from the PPN and the STN have different spatial distributions in the dendritic tree of SNc neurons. This is potentially one explanation as to why previous work has shown that NMDAR activity is critical for STN-evoked burst firing in the SNc (Smith and Grace, 1992; Chergui et al., 1994), while our work, in agreement with others (Scarnati et al., 1984; Di Loreto et al., 1992; Lokwan et al., 1999), indicates that NMDAR activity is not a requirement for PPN glutamatergic input to drive SNc firing. Rather, it appears that preferential targeting of PPN input to proximal dendritic regions allows this input to directly pattern SNc DA neuron activity. An obvious question, then, is whether or not any of the other sources of glutamate to DA neurons have properties similar to that of PPN.

One potential candidate is the superior colliculus. Although preferentially activated by visual information, the SC, like the PPN, has been shown to respond to salient sensory cues (Comoli et al., 2003). Also like the PPN, the SC responds to these stimuli before the SNc, leading some to suggest that the SC is the source for short-latency visual information for the SNc (Comoli et al., 2003; Dommett et al., 2005). Finally, *in vivo* stimulation of the SC has been shown to increase burst firing in the SNc (Coizet et al., 2003). Despite these observations, *in vitro* studies have yet to be performed to assess the properties of this synapse.

Ultimately each of the major glutamatergic inputs to the SNc needs to be examined in greater detail. While a number of *in vivo* studies have been performed, many of the results provide a conflicting image on how glutamatergic input influences SNc neurons. Furthermore, *in vitro* data is largely lacking from this literature, as techniques allowing for the selective activation of specific inputs has only recently become available. More studies like the one completed here would aid in providing a more complete picture of what governs the activity of SNc DA neurons during action selection and reward-based learning.

Materials and Methods

Animals: Male and female C57Bl/6 or DAT-Cre/Ai14-tdTomato (on a C57Bl/6 background) mice were used. All experiments were performed in accordance with protocols reviewed and approved by the Northwestern Institutional Animal Care and Use Committee and NIH guidelines.

Stereotaxic Injections: Stereotaxic injections were performed when animals were between P16 and P25 days old. Animals were anesthetized with an isoflurane precision vaporizer (Smiths Medical PM, Inc., Norwell, MA) and placed in a stereotaxic frame (David Kopf Instruments, Tujunga, CA). The distance between bregma and lambda was measured and used to adjust the following stereotaxic coordinates: PPN – AP: -4.4, ML: 1.25, DV: 3.5; STN – AP: -1.8, ML: 1.4, DV: 4.5. A small hole was drilled using a micro drill bit (Fine Science Tools, Foster City, CA) and a calibrated glass pipette pulled on a P-97 Sutter Instruments (Novato, CA) puller was used to inject 40-60 nL of either AAV9.CAG.hChR2, AAV9.hSyn.hChR2, or AAV9.Syn.Chronos (Addgene 20938M, Addgene 26973P, or Addgene 62726, respectively, supplied by University of Pennsylvania Vector Core) at one of these locations. Animals were sacrificed 10-20 days post injection.

Slice preparation: Mice were anaesthetized with a mixture of ketamine (50 mg/kg) and xylazine (4.5 mg/kg) and intracardially perfused with ice-cold high-sucrose, high-magnesium artificial cerebrospinal fluid (aCSF) containing (in mM): 50 NaCl, 2.5 KCl, 25 NaHCO₃, 1.25 NaH₂PO₄, 1 CaCl₂, 10 MgCl₂, 25 glucose, pH 7.3 (~310 mOsm/L). The brain

was then removed, sectioned in to 220-275 μm coronal or parasagittal slices using a Leica VT1200 S vibratome (Wetzlar, Germany), and allowed to recover at room temperature for at least 30 minutes in aCSF containing (in mM): 82.5 NaCl, 2.5 KCl, 25 NaHCO₃, 1.25 NaH₂PO₄, 1.5 CaCl₂, 5.5 MgCl₂, 25 glucose, pH 7.3 (~310 mOsm/L). All solutions were oxygenated with a mixture of 95% O₂/5% CO₂.

Electrophysiology: Slices were transferred to a recording chamber continuously perfused with warm (33-35 C), oxygenated aCSF containing (in mM): 125 NaCl, 2.5 KCl, 25 NaHCO₃, 1.25 NaH₂PO₄, 2 CaCl₂, 1 MgCl₂, 25 glucose, pH 7.3 (~310 mOsm/L). Cells were visualized on an Olympus BX51 upright microscope equipped with an Olympus LUMPFL 60x1.0 NA water-dipping objective lens using a Thorlabs 1545M CMOS USB camera and Micro-Manager open source microscopy software (Edelstein et al., 2001). Stage movement, objective lens focus, and manipulator XYZ movement was controlled, respectively, by: FM-380 shifting stage, Olympus axial focus module, and manipulators (Luigs and Nuemann GmbH; Ratingen, Germany)

Patch pipettes were pulled from thick-walled borosilicate glass on a Sutter P-1000 puller. Pipette resistance was typically 3-4 M Ω , except for whole cell pacemaking and cell-attached axon recordings where pipette resistance typically was 8-15 M Ω . Several different internal solutions were used, depending on the experiment being performed. For whole-cell voltage-clamp experiments pipettes were filled with a cesium-based internal containing (in mM): 120 CsMeSO₃, 15 CsCl, 10 HEPES, 0.2 EGTA, 3 ATP-Mg, 0.3 GTP-Na, 10 TEA-Cl, 1.9 QX314-Cl. For whole-cell voltage-clamp calcium imaging experiments the same internal, absent EGTA, was supplemented with 100 μM Fluo-4 or Fura-2 and 25 μM Alexa

568. For whole-cell current-clamp experiments pipettes were filled with a potassium-based internal containing (in mM): 135 KMeSO₄, 5 KCl, 5 HEPES, 0.05 EGTA, 10 phosphocreatine-di(tris), 2 ATP-Mg, 0.5 GTP-Na as well as 25 μM Alexa 568. Perforated-patch experiments were performed with pipettes front-filled with a solution containing (in mM): 126 KMeSO₄, 14 KCl, 10 HEPES, 1 EGTA, 0.5 CaCl₂, 3MgCl₂ and then back filled with the same solution containing 20 μg/mL gramicidin-D. Loose-seal cell-attached recordings were made with pipettes filled with 145 mM NaCl, 10mM HEPES, and 25 μM Alexa 568 (ThermoFischer Scientific, Waltham, MA). All internals had a pH of 7.25-7.3 (with either 1 M CsOH, KOH, or NaOH) and an osmolarity of 280-300 mOsm/L.

Electrophysiological recordings were obtained using a Multiclamp 700B amplifier. Signals were filtered at 4-20 kHz and digitized at 10-50 kHz. For voltage clamp experiments access resistance was monitored throughout the experiment. Cells in which access deviated from baseline by more than 20% were discarded. For perforate patch experiments, cells were left to perforate until the spike height reached roughly 0 mV before data collection began. Rapid jumps in the observed voltage to positive (> 0mV) values were used as exclusion criterion due to break-in. The liquid junction potential for the cesium, potassium, and perforated internals in recording aCSF were 5.9 mV, 7 mV, and 5.1 mV respectively, and were corrected for during data analysis.

Pharmacology: A number of different pharmacological agents were used. Unless otherwise noted, drugs were purchased from R&D Systems (Minneapolis, MN) or Abcam (Cambridge, MA) and were prepared according to manufacturer instructions. They are listed here, along with their working concentration: NBQX (5 μM), (R)-CPP (5 μM),

SR95531 (10 μ M), mecamylamine hydrochloride (10 μ M), tetrodotoxin (1 μ M), 4-aminopyridine (100 μ M), apamin (200 nM), ifenprodil (5 μ M), TCN 201 (10 μ M), A 841720 (0.1 μ M), MTEP hydrochloride (0.5 μ M), philanthotoxin 74 (5 μ M), glycine (250 μ M), D-serine (250 μ M), CIQ (10 μ M; provided the Traynelis lab and Brandt Labs, Atlanta, GA).

2PLSM Imaging and photostimulation: Two-photon laser-scanning microscopy (2PLSM) was performed using an Ultima LSM system (Prairie Technologies, Middleton, WI). The 2P excitation source was a Chameleon-Ultra series tunable (690-1040 nm) Ti:sapphire laser system (Coherent Laser Group, Santa Clara, CA). Alexa and Fluo-4 dyes were excited using 820 nm (80 MHz pulse repetition frequency and \sim 140 fs pulse duration) excitation, while Fura-2 was imaged at 780nm. Laser power attenuation was achieved with two Pockels' cell electro-optic modulators (models M350-80-02-BK and M350-50-02-BK, Con Optics, Danbury, CT) controlled by PrairieView 5.0-5.3 software. The two cells were aligned in series to provide enhanced modulation range for fine control of the excitation dose (0.1% steps over five decades), to limit maximum power, and to serve as a rapid shutter during line scan acquisitions. The fluorescence emission was collected by non-de-scanned photomultiplier tubes (PMTs). Green channel (490-560 nm) signals were detected by a Hamamatsu H7422P-40 select GaAsP PMT, which was protected during blue laser exposures with a Uniblitz DSS10B-1-T-0 shutter (Vincent Associates). Red channel (580-630 nm) signals were detected by a Hamamatsu R3982 side on PMT. Cell visualization during laser scanning was made possible by a Dodt-tube-based transmission detector with a mirror routing the laser to a Hamamatsu R3982 side on PMT (Prairie Technologies; Middleton, WI). Scanning signals were sent and received by the PCI-NI6110 analog-to-

digital converter card in the system computer (National Instruments, Austin, TX). Scanned images were built up pixel by pixel (dwell time: 10-12 μ s), with PMT anode current to voltage conversion and sampling fixed in 0.4 μ s increments. For calcium imaging, line scans were performed along 5-10 μ m sections of dendrite (6 ms and 512 pixels per line). Cells were allowed to fill for a minimum of 30 minutes to allow for dye equilibration. Calcium fluorescence signals were background-subtracted and normalized by a baseline fluorescence (f_0). Calcium transients were quantified as the area under the transient.

One-photon (1P) photostimulation was performed using either a Prairie Aurora Launch (473 nm, 50 mW rated laser with AOTF intensity control) or a Prairie Helios laser launch (Coherent OBIS 473 nm laser). The launch was coupled to the Ultima scan head via a metal clad fiber optic cable. The launch optics were designed to provide \sim 1 μ m spot stimulation at the focal plan of the 60x/1.0NA objective lens; additional optics allowed for this spot size to be increased to \sim 10 μ m. Generally, a 1.0ND filter was employed to reduce the maximal power at the sample from \sim 18 mW to \sim 1.8 mW. Laser power was further controlled by the PrairieView software. A second pair of galvanometer mirrors within the Ultima scan head allowed for multiple stimulation points within the focal plane of interest. Full-field photostimulation was provided by either a pE-100 470 nm LED (CoolLED via Tek5 Systems, Yorktown Heights, NY) or an Excelitas Excite LED110 four-LED, coupled to scanning system via a Lumatec 3 mm liquid light guide via the Olympus BX-51 WIF rear epi-fluorescence port. For blue-light stimulation, a Chroma 39002 ET eGFP large (BX2) Olympus filter cube was used. The LED was remotely synchronized and activated by a TTL

signal from the PrairieView software. The maximum exposure field of view with the 60x/1.0NA objective lens was $\sim 415 \mu\text{m}$.

For sCRACM experiments, the point spread function of the blue laser was estimated by moving the nominal site of stimulation away from the dendrite (Figure 6). Laser power was calibrated based on this same procedure. For RuBi-glutamate uncaging experiments, RuBi-glutamate (2 mM) was superfused (0.4 ml/hr) using a system of syringe pumps (World Precision Instruments, Sarasota, FL) and a multi-barreled perfusion manifold fitted with a small-volume mixing tip that allowed rapid switching between solutions (Cell MicroControls, Norfolk, VA). In all photostimulation experiments, light pulses were limited to 1 ms, with the power calibrated based on achieving physiological responses within the scope of the respective experiment.

Fixed Tissue Preparation and Imaging: Fixed tissue was prepared by first perfusing anaesthetized animals with phosphate buffered saline (PBS, Sigma-Aldrich, St. Louis, MO) followed by 4% paraformaldehyde (PFA, diluted with PBS from 16% stock; Electron Microscopy Sciences, Hatfield, PA). The brain was then removed and allowed to further fix in PFA overnight, and then washed and stored in PBS. Brains were sectioned in to 100 μm parasagittal slices on a Leica VT1200 S vibratome. Sections were mounted on with ProLong Diamond (ThermoFischer Scientific, Waltham, MA) and imaged with an Olympus FV10i confocal laser scanning microscope.

Data Analysis and Statistics: Both electrophysiological and imaging data were analyzed using either GraphPad Prism (version 5.0, GraphPad Software), Fiji (Schindelin et al., 2012), or custom written python analysis scripts using a number of numerical python

packages: pandas (McKinney, 2010), SciPy (Jones et al., 2001), and statsmodels (Seabold and Perktold, 2010). Figures were created with matplotlib (Hunter, 2007) or GraphPad Prism and Adobe Illustrator. Data were summarized using box plots showing median values, first and third quartiles, and whiskers at 10th and 90th percentiles. Summary statistics are presented as mean \pm standard deviation. Sample n represents the number of neurons collected from brain slices from a minimum of three animals. Sample size was based on prior studies published from our lab and others using similar techniques (Blythe et al., 2009; Sanchez-Padilla et al., 2014). Statistical analysis was performed with either SciPy, statsmodels, or GraphPad Prism using non-parametric tests (Mann-Whitney U-test of significance or Wilcoxon signed rank test for between or within-subject design experiments, respectively) except where otherwise noted. To correct for multiple comparisons the Holm-Bonferroni method was used, with the reported p-values representing the adjusted p-value. Probability threshold for statistical significance was $P < 0.05$.

References

- Albin, R.L., Young, A.B., Penney, J.B., 1989. The functional anatomy of basal ganglia disorders. *Trends Neurosci.* 12, 366–375.
- Alderson, H.L., Brown, V.J., Latimer, M.P., Brasted, P.J., Robertson, A.H., Winn, P., 2002. The effect of excitotoxic lesions of the pedunclopontine tegmental nucleus on performance of a progressive ratio schedule of reinforcement. *Neuroscience* 112, 417–425.
- Alderson, H.L., Faulconbridge, L.F.H., Gregory, L.P., Latimer, M.P., Winn, P., 2003. Behavioural sensitisation to repeated d-amphetamine: effects of excitotoxic lesions of the pedunclopontine tegmental nucleus. *Neuroscience* 118, 311–315.
- Alderson, H.L., Jenkins, T.A., Kozak, R., Latimer, M.P., Winn, P., 2001. The effects of excitotoxic lesions of the pedunclopontine tegmental nucleus on conditioned place preference to 4%, 12% and 20% sucrose solutions. *Brain Res. Bull.* 56, 599–605.
- Alderson, H.L., Latimer, M.P., Blaha, C.D., Phillips, A.G., Winn, P., 2004. An examination of d-amphetamine self-administration in pedunclopontine tegmental nucleus-lesioned rats. *Neuroscience* 125, 349–358. doi:10.1016/j.neuroscience.2004.02.015
- Alderson, H.L., Latimer, M.P., Winn, P., 2008. A functional dissociation of the anterior and posterior pedunclopontine tegmental nucleus: excitotoxic lesions have differential effects on locomotion and the response to nicotine. *Brain Struct. Funct.* 213, 247–253. doi:10.1007/s00429-008-0174-4
- Alderson, H.L., Latimer, M.P., Winn, P., 2006. Intravenous self-administration of nicotine is altered by lesions of the posterior, but not anterior, pedunclopontine tegmental nucleus. *Eur. J. Neurosci.* 23, 2169–2175. doi:10.1111/j.1460-9568.2006.04737.x
- Amendola, J., Woodhouse, A., Martin-Eauclaire, M.-F., Goillard, J.-M., 2012. Ca²⁺/cAMP-Sensitive Covariation of IA and IH Voltage Dependences Tunes Rebound Firing in Dopaminergic Neurons. *J. Neurosci.* 32, 2166–2181. doi:10.1523/JNEUROSCI.5297-11.2012
- Andén, N.-E., Fuxe, K., Hamberger, B., Hökfelt, T., 1966. A Quantitative Study on the Nigro-Neostriatal Dopamine Neuron System in the Rat. *Acta Physiol. Scand.* 67, 306–312. doi:10.1111/j.1748-1716.1966.tb03317.x
- Atherton, J.F., Wokosin, D.L., Ramanathan, S., Bevan, M.D., 2008. Autonomous initiation and propagation of action potentials in neurons of the subthalamic nucleus. *J. Physiol.* 586, 5679–5700. doi:10.1113/jphysiol.2008.155861

- Balleine, B.W., Delgado, M.R., Hikosaka, O., 2007. The Role of the Dorsal Striatum in Reward and Decision-Making. *J. Neurosci.* 27, 8161–8165. doi:10.1523/JNEUROSCI.1554-07.2007
- Bamford, N.S., 2004. Dopamine Modulates Release from Corticostriatal Terminals. *J. Neurosci.* 24, 9541–9552. doi:10.1523/JNEUROSCI.2891-04.2004
- Baquet, Z.C., Williams, D., Brody, J., Smeyne, R.J., 2009. A comparison of model-based (2D) and design-based (3D) stereological methods for estimating cell number in the substantia nigra pars compacta (SNpc) of the C57BL/6J mouse. *Neuroscience* 161, 1082–1090. doi:10.1016/j.neuroscience.2009.04.031
- Barrot, M., Calza, L., Pozza, M., Le Moal, M., Piazza, P.V., 2000. Differential calbindin-immunoreactivity in dopamine neurons projecting to the rat striatal complex. *Eur. J. Neurosci.* 12, 4578–4582. doi:10.1111/j.1460-9568.2000.01349.x
- Bayer, H.M., Glimcher, P.W., 2005. Midbrain Dopamine Neurons Encode a Quantitative Reward Prediction Error Signal. *Neuron* 47, 129–141. doi:10.1016/j.neuron.2005.05.020
- Benes, F.M., 2001. Carlsson and the discovery of dopamine. *Trends Pharmacol. Sci.* 22, 46–47. doi:10.1016/S0165-6147(00)01607-2
- Beninato, M., Spencer, R.F., 1986. A cholinergic projection to the rat superior colliculus demonstrated by retrograde transport of horseradish peroxidase and choline acetyltransferase immunohistochemistry. *J. Comp. Neurol.* 253, 525–538. doi:10.1002/cne.902530409
- Bergman, H., Wichmann, T., Karmon, B., DeLong, M.R., 1994. The primate subthalamic nucleus. II. Neuronal activity in the MPTP model of parkinsonism. *J. Neurophysiol.* 72, 507–520.
- Bevan, M.D., Bolam, J.P., 1995. Cholinergic, GABAergic, and glutamate-enriched inputs from the mesopontine tegmentum to the subthalamic nucleus in the rat. *J. Neurosci.* 15, 7105–7120.
- Bevan, M.D., Magill, P.J., Terman, D., Bolam, J.P., Wilson, C.J., 2002. Move to the rhythm: oscillations in the subthalamic nucleus–external globus pallidus network. *Trends Neurosci.* 25, 525–531.
- Björklund, A., Dunnett, S.B., 2007. Dopamine neuron systems in the brain: an update. *Trends Neurosci.* Fifty years of dopamine research 30, 194–202. doi:10.1016/j.tins.2007.03.006

- Blythe, S.N., Atherton, J.F., Bevan, M.D., 2007. Synaptic Activation of Dendritic AMPA and NMDA Receptors Generates Transient High-Frequency Firing in Substantia Nigra Dopamine Neurons In Vitro. *J. Neurophysiol.* 97, 2837–2850. doi:10.1152/jn.01157.2006
- Blythe, S.N., Wokosin, D., Atherton, J.F., Bevan, M.D., 2009. Cellular Mechanisms Underlying Burst Firing in Substantia Nigra Dopamine Neurons. *J. Neurosci.* 29, 15531–15541. doi:10.1523/JNEUROSCI.2961-09.2009
- Bohnen, N.I., Muller, M.L.T.M., Koeppe, R.A., Studenski, S.A., Kilbourn, M.A., Frey, K.A., Albin, R.L., 2009. History of falls in Parkinson disease is associated with reduced cholinergic activity. *Neurology* 73, 1670–1676. doi:10.1212/WNL.0b013e3181c1ded6
- Bolam, J.P., Hanley, J.J., Booth, P.A.C., Bevan, M.D., 2000. Synaptic organisation of the basal ganglia. *J. Anat.* 196, 527–542.
- Bolam, J.P., Pissadaki, E.K., 2012. Living on the edge with too many mouths to feed: Why dopamine neurons die. *Mov. Disord.* 27, 1478–1483. doi:10.1002/mds.25135
- Bolam, J.P., Smith, Y., 1990. The GABA and substance P input to dopaminergic neurones in the substantia nigra of the rat. *Brain Res.* 529, 57–78. doi:10.1016/0006-8993(90)90811-0
- Bordas, C., Kovacs, A., Pal, B., 2015. The M-current contributes to high threshold membrane potential oscillations in a cell type-specific way in the pedunculopontine nucleus of mice. *Front. Cell. Neurosci.* 9. doi:10.3389/fncel.2015.00121
- Bortolanza, M., Wietzikoski, E.C., Boschen, S.L., Dombrowski, P.A., Latimer, M., MacLaren, D.A.A., Winn, P., Cunha, C.D., 2010. Functional disconnection of the substantia nigra pars compacta from the pedunculopontine nucleus impairs learning of a conditioned avoidance task. *Neurobiol. Learn. Mem.* 94, 229–239. doi:10.1016/j.nlm.2010.05.011
- Boucetta, S., Cissé, Y., Mainville, L., Morales, M., Jones, B.E., 2014. Discharge Profiles across the Sleep–Waking Cycle of Identified Cholinergic, GABAergic, and Glutamatergic Neurons in the Pontomesencephalic Tegmentum of the Rat. *J. Neurosci.* 34, 4708–4727. doi:10.1523/JNEUROSCI.2617-13.2014
- Boucetta, S., Jones, B.E., 2009. Activity Profiles of Cholinergic and Intermingled GABAergic and Putative Glutamatergic Neurons in the Pontomesencephalic Tegmentum of Urethane-Anesthetized Rats. *J. Neurosci.* 29, 4664–4674. doi:10.1523/JNEUROSCI.5502-08.2009

- Braithwaite, S.P., Paul, S., Nairn, A.C., Lombroso, P.J., 2006. Synaptic plasticity: one STEP at a time. *Trends Neurosci.* 29, 452–458. doi:10.1016/j.tins.2006.06.007
- Bromberg-Martin, E.S., Matsumoto, M., Hikosaka, O., 2010. Dopamine in Motivational Control: Rewarding, Aversive, and Alerting. *Neuron* 68, 815–834. doi:10.1016/j.neuron.2010.11.022
- Brothwell, S.L.C., Barber, J.L., Monaghan, D.T., Jane, D.E., Gibb, A.J., Jones, S., 2007. NR2B- and NR2D-containing synaptic NMDA receptors in developing rat substantia nigra pars compacta dopaminergic neurones. *J. Physiol.* 586, 739–750. doi:10.1113/jphysiol.2007.144618
- Bunney, B.S., Aghajanian, G.K., 1976. The precise localization of nigral afferents in the rat as determined by a retrograde tracing technique. *Brain Res.* 117, 423–435. doi:10.1016/0006-8993(76)90751-4
- Carlsson, A., 1959. The Occurrence, Distribution and Physiological Role of Catecholamines in the Nervous System. *Pharmacol. Rev.* 11, 490–493.
- Carpenter, M.B., Carleton, S.C., Keller, J.T., Conte, P., 1981. Connections of the subthalamic nucleus in the monkey. *Brain Res.* 224, 1–29. doi:10.1016/0006-8993(81)91113-6
- Carter, C.J., 1982. Topographical distribution of possible glutamatergic pathways from the frontal cortex to the striatum and substantia nigra in rats. *Neuropharmacology* 21 5, 379–83.
- Cepeda, C., Buchwald, N.A., Levine, M.S., 1993. Neuromodulatory actions of dopamine in the neostriatum are dependent upon the excitatory amino acid receptor subtypes activated. *Proc. Natl. Acad. Sci. U. S. A.* 90, 9576–9580.
- Chan, C.S., Guzman, J.N., Ilijic, E., Mercer, J.N., Rick, C., Tkatch, T., Meredith, G.E., Surmeier, D.J., 2007. “Rejuvenation” protects neurons in mouse models of Parkinson’s disease. *Nature* 447, 1081–1086. doi:10.1038/nature05865
- Chang, H.T., 1988. Substance P-dopamine relationship in the rat substantia nigra: a light and electron microscopy study of double immunocytochemically labeled materials. *Brain Res.* 448, 391–396. doi:10.1016/0006-8993(88)91284-X
- Chang, H.T., Kita, H., Kitai, S.T., 1984. The ultrastructural morphology of the subthalamic-nigral axon terminals intracellularly labeled with horseradish peroxidase. *Brain Res.* 299, 182–185. doi:10.1016/0006-8993(84)90805-9
- Charara, A., Parent, A., 1994. Brainstem dopaminergic, cholinergic and serotonergic afferents to the pallidum in the squirrel monkey. *Brain Res.* 640, 155–170.

- Charara, A., Smith, Y., Parent, A., 1996. Glutamatergic inputs from the pedunclopontine nucleus to midbrain dopaminergic neurons in primates: Phaseolus vulgaris-leucoagglutinin anterograde labeling combined with postembedding glutamate and GABA immunohistochemistry. *J. Comp. Neurol.* 364, 254–266.
- Charl y, P.J., Grenhoff, J., Chergui, K., Chapelle, B.D.L., Buda, M., Svensson, T.H., Chouvet, G., 1991. Burst firing of mesencephalic dopamine neurons is inhibited by somatodendritic application of kynurenate. *Acta Physiol. Scand.* 142, 105–112. doi:10.1111/j.1748-1716.1991.tb09134.x
- Chase, M.H., Morales, F.R., 1990. The atonia and myoclonia of active (REM) sleep. *Annu. Rev. Psychol.* 41, 557–584. doi:10.1146/annurev.ps.41.020190.003013
- Chase, M.H., Morales, F.R., Boxer, P.A., Fung, S.J., Soja, P.J., 1986. Effect of stimulation of the nucleus reticularis gigantocellularis on the membrane potential of cat lumbar motoneurons during sleep and wakefulness. *Brain Res.* 386, 237–244. doi:10.1016/0006-8993(86)90160-5
- Chen, Q., Cichon, J., Wang, W., Qiu, L., Lee, S.-J.R., Campbell, N.R., DeStefino, N., Goard, M.J., Fu, Z., Yasuda, R., Looger, L.L., Arenkiel, B.R., Gan, W.-B., Feng, G., 2012. Imaging Neural Activity Using Thy1-GCaMP Transgenic mice. *Neuron* 76, 297–308. doi:10.1016/j.neuron.2012.07.011
- Chergui, K., Akaoka, H., Charl y, P.J., Saunier, C.F., Buda, M., Chouvet, G., 1994. Subthalamic nucleus modulates burst firing of nigral dopamine neurones via NMDA receptors. *Neuroreport* 5, 1185–1188.
- Chergui, K., Charl y, P.J., Akaoka, H., Saunier, C.F., Brunet, J.-L., Buda, M., Svensson, T.H., Chouvet, G., 1993. Tonic Activation of NMDA Receptors Causes Spontaneous Burst Discharge of Rat Midbrain Dopamine Neurons In Vivo. *Eur. J. Neurosci.* 5, 137–144. doi:10.1111/j.1460-9568.1993.tb00479.x
- Cisek, P., Kalaska, J.F., 2010. Neural Mechanisms for Interacting with a World Full of Action Choices. *Annu. Rev. Neurosci.* 33, 269–298. doi:10.1146/annurev.neuro.051508.135409
- Clarke, P.B., Hommer, D.W., Pert, A., Skirboll, L.R., 1987. Innervation of substantia nigra neurons by cholinergic afferents from pedunclopontine nucleus in the rat: neuroanatomical and electrophysiological evidence. *Neuroscience* 23, 1011–1019.
- Coizet, V., Comoli, E., Westby, G.W.M., Redgrave, P., 2003. Phasic activation of substantia nigra and the ventral tegmental area by chemical stimulation of the superior colliculus: an electrophysiological investigation in the rat. *Eur. J. Neurosci.* 17, 28–40. doi:10.1046/j.1460-9568.2003.02415.x

- Comoli, E., Coizet, V., Boyes, J., Bolam, J.P., Canteras, N.S., Quirk, R.H., Overton, P.G., Redgrave, P., 2003. A direct projection from superior colliculus to substantia nigra for detecting salient visual events. *Nat. Neurosci.* 6, 974–980. doi:10.1038/nn1113
- Condé, H., Dormont, J.F., Farin, D., 1998. The role of the pedunclopontine tegmental nucleus in relation to conditioned motor performance in the cat II. Effects of reversible inactivation by intracerebral microinjections. *Exp. Brain Res.* 121, 411–418. doi:10.1007/s002210050475
- Cools, A.R., Rossum, J.M.V., 1976. Excitation-mediating and inhibition-mediating dopamine-receptors: A new concept towards a better understanding of electrophysiological, biochemical, pharmacological, functional and clinical data. *Psychopharmacologia* 45, 243–254. doi:10.1007/BF00421135
- Côté, P.-Y., Parent, A., 1992. Calbindin D-28k and choline acetyltransferase are expressed by different neuronal populations in pedunclopontine nucleus but not in nucleus basalis in squirrel monkeys. *Brain Res.* 593, 245–252.
- Cox, J., Pinto, L., Dan, Y., 2016. Calcium imaging of sleep–wake related neuronal activity in the dorsal pons. *Nat. Commun.* 7, ncomms10763. doi:10.1038/ncomms10763
- Dahlstroem, A., Fuxe, K., 1964. EVIDENCE FOR THE EXISTENCE OF MONOAMINE-CONTAINING NEURONS IN THE CENTRAL NERVOUS SYSTEM. I. DEMONSTRATION OF MONOAMINES IN THE CELL BODIES OF BRAIN STEM NEURONS. *Acta Physiol. Scand. Suppl.* SUPPL 232:1-55.
- Dana, H., Chen, T.-W., Hu, A., Shields, B.C., Guo, C., Looger, L.L., Kim, D.S., Svoboda, K., 2014. Thy1-GCaMP6 Transgenic Mice for Neuronal Population Imaging In Vivo. *PLOS ONE* 9, e108697. doi:10.1371/journal.pone.0108697
- Datta, S., 2007. Activation of Pedunclopontine Tegmental PKA Prevents GABA_B Receptor Activation–Mediated Rapid Eye Movement Sleep Suppression in the Freely Moving Rat. *J. Neurophysiol.* 97, 3841–3850. doi:10.1152/jn.00263.2007
- Datta, S., 2002. Evidence That REM Sleep Is Controlled by the Activation of Brain Stem Pedunclopontine Tegmental Kainate Receptor. *J. Neurophysiol.* 87, 1790–1798. doi:10.1152/jn.00763.2001
- Datta, S., Siwek, D.F., 2002. Single cell activity patterns of pedunclopontine tegmentum neurons across the sleep-wake cycle in the freely moving rats. *J. Neurosci. Res.* 70, 611–621. doi:10.1002/jnr.10405
- Datta, S., Siwek, D.F., 1997. Excitation of the Brain Stem Pedunclopontine Tegmentum Cholinergic Cells Induces Wakefulness and REM Sleep. *J. Neurophysiol.* 77, 2975–2988.

- Dautan, D., Hacıoğlu Bay, H., Bolam, J.P., Gerdjikov, T.V., Mena-Segovia, J., 2016a. Extrinsic Sources of Cholinergic Innervation of the Striatal Complex: A Whole-Brain Mapping Analysis. *Front. Neuroanat.* 10. doi:10.3389/fnana.2016.00001
- Dautan, D., Huerta-Ocampo, I., Witten, I.B., Deisseroth, K., Bolam, J.P., Gerdjikov, T., Mena-Segovia, J., 2014. A Major External Source of Cholinergic Innervation of the Striatum and Nucleus Accumbens Originates in the Brainstem. *J. Neurosci.* 34, 4509–4518. doi:10.1523/JNEUROSCI.5071-13.2014
- Dautan, D., Souza, A.S., Huerta-Ocampo, I., Valencia, M., Assous, M., Witten, I.B., Deisseroth, K., Tepper, J.M., Bolam, J.P., Gerdjikov, T.V., Mena-Segovia, J., 2016b. Segregated cholinergic transmission modulates dopamine neurons integrated in distinct functional circuits. *Nat. Neurosci.* 19, 1025–1033. doi:10.1038/nn.4335
- Day, M., Wokosin, D., Plotkin, J.L., Tian, X., Surmeier, D.J., 2008. Differential Excitability and Modulation of Striatal Medium Spiny Neuron Dendrites. *J. Neurosci.* 28, 11603–11614. doi:10.1523/JNEUROSCI.1840-08.2008
- Deignan, J., Luján, R., Bond, C., Riegel, A., Watanabe, M., Williams, J.T., Maylie, J., Adelman, J.P., 2012. SK2 and SK3 expression differentially affect firing frequency and precision in dopamine neurons. *Neuroscience* 217, 67–76. doi:10.1016/j.neuroscience.2012.04.053
- Deister, C.A., Teagarden, M.A., Wilson, C.J., Paladini, C.A., 2009. An Intrinsic Neuronal Oscillator Underlies Dopaminergic Neuron Bursting. *J. Neurosci.* 29, 15888–15897. doi:10.1523/JNEUROSCI.4053-09.2009
- DeLong, M.R., 1990. Primate models of movement disorders of basal ganglia origin. *Trends Neurosci.* 13, 281–285. doi:10.1016/0166-2236(90)90110-V
- Deniau, J.M., Hammond, C., Chevalier, G., Feger, J., 1978. Evidence for branched subthalamic nucleus projections to substantia nigra, entopeduncular nucleus and globus pallidus. *Neurosci. Lett.* 9, 117–121. doi:10.1016/0304-3940(78)90058-7
- Deurveilher, S., Hennevin, E., 2001. Lesions of the pedunclopontine tegmental nucleus reduce paradoxical sleep (PS) propensity: evidence from a short-term PS deprivation study in rats. *Eur. J. Neurosci.* 13, 1963–1976. doi:10.1046/j.0953-816x.2001.01562.x
- Di Loreto, S., Florio, T., Scarnati, E., 1992. Evidence that non-NMDA receptors are involved in the excitatory pathway from the pedunclopontine region to nigrostriatal dopaminergic neurons. *Exp. Brain Res.* 89, 79–86.
- Ding, S., Wei, W., Zhou, F.-M., 2011. Molecular and functional differences in voltage-activated sodium currents between GABA projection neurons and dopamine

- neurons in the substantia nigra. *J. Neurophysiol.* 106, 3019–3034.
doi:10.1152/jn.00305.2011
- Dommett, E., Coizet, V., Blaha, C.D., Martindale, J., Lefebvre, V., Walton, N., Mayhew, J.E.W., Overton, P.G., Redgrave, P., 2005. How Visual Stimuli Activate Dopaminergic Neurons at Short Latency. *Science* 307, 1476–1479. doi:10.1126/science.1107026
- Dormont, J.F., Condé, H., Farin, D., 1998. The role of the pedunculopontine tegmental nucleus in relation to conditioned motor performance in the cat. I. Context-dependent and reinforcement-related single unit activity. *Exp. Brain Res.* 121, 401–410.
- Dossi, R.C., Pare, D., Steriade, M., 1991. Short-lasting nicotinic and long-lasting muscarinic depolarizing responses of thalamocortical neurons to stimulation of mesopontine cholinergic nuclei. *J. Neurophysiol.* 65, 393–406.
- Dray, A., Davies, J., Oakley, N.R., Tongroach, P., Vellucci, S., 1978. The dorsal and medial raphe projections to the substantia nigra in the rat: Electrophysiological, biochemical and behavioural observations. *Brain Res.* 151, 431–442.
doi:10.1016/0006-8993(78)91077-6
- Dreyer, J.K., Herrik, K.F., Berg, R.W., Hounsgaard, J.D., 2010. Influence of Phasic and Tonic Dopamine Release on Receptor Activation. *J. Neurosci.* 30, 14273–14283.
doi:10.1523/JNEUROSCI.1894-10.2010
- Dugast, C., Suaud-Chagny, M.F., Gonon, F., 1994. Continuous in vivo monitoring of evoked dopamine release in the rat nucleus accumbens by amperometry. *Neuroscience* 62, 647–654.
- Dunah, A.W., Sirianni, A.C., Fienberg, A.A., Bastia, E., Schwarzschild, M.A., Standaert, D.G., 2004. Dopamine D1-Dependent Trafficking of Striatal *N*-Methyl-d-aspartate Glutamate Receptors Requires Fyn Protein Tyrosine Kinase but Not DARPP-32. *Mol. Pharmacol.* 65, 121–129. doi:10.1124/mol.65.1.121
- Edelstein, A., Amodaj, N., Hoover, K., Vale, R., Stuurman, N., 2001. Computer Control of Microscopes Using μ Manager, in: *Current Protocols in Molecular Biology*. John Wiley & Sons, Inc. doi:10.1002/0471142727.mb1420s92
- Edman, S., McKay, S., MacDonald, L.J., Samadi, M., Livesey, M.R., Hardingham, G.E., Wyllie, D.J.A., 2012. TCN 201 selectively blocks GluN2A-containing NMDARs in a GluN1 co-agonist dependent but non-competitive manner. *Neuropharmacology* 63, 441–449.
doi:10.1016/j.neuropharm.2012.04.027
- Féger, J., Robledo, P., 1991. The Effects of Activation or Inhibition of the Subthalamic Nucleus on the Metabolic and Electrophysiological Activities Within the Pallidal

- Complex and Substantia Nigra in the Rat. *Eur. J. Neurosci.* 3, 947–952. doi:10.1111/j.1460-9568.1991.tb00030.x
- Fibiger, H.C., Miller, J.J., 1977. An anatomical and electrophysiological investigation of the serotonergic projection from the dorsal raphe nucleus to the substantia nigra in the rat. *Neuroscience* 2, 975–987. doi:10.1016/0306-4522(77)90120-8
- Fieblinger, T., Graves, S.M., Sebel, L.E., Alcacer, C., Plotkin, J.L., Gertler, T.S., Chan, C.S., Heiman, M., Greengard, P., Cenci, M.A., Surmeier, D.J., 2014. Cell type-specific plasticity of striatal projection neurons in parkinsonism and L-DOPA-induced dyskinesia. *Nat. Commun.* 5, 5316. doi:10.1038/ncomms6316
- Fiorillo, C.D., Song, M.R., Yun, S.R., 2013. Multiphasic Temporal Dynamics in Responses of Midbrain Dopamine Neurons to Appetitive and Aversive Stimuli. *J. Neurosci.* 33, 4710–4725. doi:10.1523/JNEUROSCI.3883-12.2013
- Floresco, S.B., West, A.R., Ash, B., Moore, H., Grace, A.A., 2003. Afferent modulation of dopamine neuron firing differentially regulates tonic and phasic dopamine transmission. *Nat. Neurosci.* 6, 968–973. doi:10.1038/nn1103
- Flores-Hernández, J., Cepeda, C., Hernández-Echeagaray, E., Calvert, C.R., Jokel, E.S., Fienberg, A.A., Greengard, P., Levine, M.S., 2002. Dopamine Enhancement of NMDA Currents in Dissociated Medium-Sized Striatal Neurons: Role of D1 Receptors and DARPP-32. *J. Neurophysiol.* 88, 3010–3020. doi:10.1152/jn.00361.2002
- Florio, T., Scarnati, E., Confalone, G., Minchella, D., Galati, S., Stanzione, P., Stefani, A., Mazzone, P., 2007. High-frequency stimulation of the subthalamic nucleus modulates the activity of pedunculopontine neurons through direct activation of excitatory fibres as well as through indirect activation of inhibitory pallidal fibres in the rat. *Eur. J. Neurosci.* 25, 1174–1186. doi:10.1111/j.1460-9568.2007.05360.x
- Ford, B., Holmes, C.J., Mainville, L., Jones, B.E., 1995. GABAergic neurons in the rat pontomesencephalic tegmentum: Codistribution with cholinergic and other tegmental neurons projecting to the posterior lateral hypothalamus. *J. Comp. Neurol.* 363, 177–196. doi:10.1002/cne.903630203
- Fu, Y., Yuan, Y., Halliday, G., Rusznák, Z., Watson, C., Paxinos, G., 2012. A cytoarchitectonic and chemoarchitectonic analysis of the dopamine cell groups in the substantia nigra, ventral tegmental area, and retrorubral field in the mouse. *Brain Struct. Funct.* 217, 591–612. doi:10.1007/s00429-011-0349-2
- Furman, M., Zhan, Q., McCafferty, C., Lerner, B.A., Motelow, J.E., Meng, J., Ma, C., Buchanan, G.F., Witten, I.B., Deisseroth, K., Cardin, J.A., Blumenfeld, H., 2015. Optogenetic stimulation of cholinergic brainstem neurons during focal limbic seizures: Effects on cortical physiology. *Epilepsia* 56, e198–e202. doi:10.1111/epi.13220

- Futami, T., Takakusaki, K., Kitai, S.T., 1995. Glutamatergic and cholinergic inputs from the pedunculopontine tegmental nucleus to dopamine neurons in the substantia nigra pars compacta. *Neurosci. Res.* 21, 331–342.
- Fuxe, K., Ferré, S., Genedani, S., Franco, R., Agnati, L.F., 2007. Adenosine receptor–dopamine receptor interactions in the basal ganglia and their relevance for brain function. *Physiol. Behav., Karolinska Institutet - Neuroscience* 92, 210–217. doi:10.1016/j.physbeh.2007.05.034
- Galarraga, E., Hernández-lópez, S., Reyes, A., Barral, J., Bargas, J., 1997. Dopamine facilitates striatal Epsps through an L-type Ca²⁺ conductance. *Neuroreport* 8, 2183–2186.
- Garcia-Rill, E., Houser, C.R., Skinner, R.D., Smith, W., Woodward, D.J., 1987. Locomotion-inducing sites in the vicinity of the pedunculopontine nucleus. *Brain Res. Bull.* 18, 731–738.
- Garcia-Rill, E., Hyde, J., Kezunovic, N., Urbano, F.J., Petersen, E., 2015. The physiology of the pedunculopontine nucleus: implications for deep brain stimulation. *J. Neural Transm.* 122, 225–235. doi:10.1007/s00702-014-1243-x
- Garcia-Rill, E., Skinner, R.D., Miyazato, H., Homma, Y., 2001. Pedunculopontine stimulation induces prolonged activation of pontine reticular neurons. *Neuroscience* 104, 455–465. doi:10.1016/S0306-4522(01)00094-X
- Gardner, E.L., Ashby, C.R., 2000. Heterogeneity of the mesotelencephalic dopamine fibers: physiology and pharmacology. *Neurosci. Biobehav. Rev.* 24, 115–118. doi:10.1016/S0149-7634(99)00048-2
- Garris, P.A., Christensen, J.R.C., Rebec, G.V., Wightman, R.M., 1997. Real-Time Measurement of Electrically Evoked Extracellular Dopamine in the Striatum of Freely Moving Rats. *J. Neurochem.* 68, 152–161. doi:10.1046/j.1471-4159.1997.68010152.x
- Garris, P.A., Wightman, R.M., 1994. Different kinetics govern dopaminergic transmission in the amygdala, prefrontal cortex, and striatum: an in vivo voltammetric study. *J. Neurosci. Off. J. Soc. Neurosci.* 14, 442–450.
- Georges, F., Aston-Jones, G., 2002. Activation of Ventral Tegmental Area Cells by the Bed Nucleus of the Stria Terminalis: A Novel Excitatory Amino Acid Input to Midbrain Dopamine Neurons. *J. Neurosci.* 22, 5173–5187.
- Gerfen, C.R., 1992. The neostriatal mosaic: multiple levels of compartmental organization. *Trends Neurosci.* 15, 133–139. doi:10.1016/0166-2236(92)90355-C
- Gerfen, C.R., 1984. The neostriatal mosaic: compartmentalization of corticostriatal input and striatonigral output systems. *Nature* 311, 461–464. doi:10.1038/311461a0

- Gerfen, C.R., Baimbridge, K.G., Miller, J.J., 1985. The neostriatal mosaic: compartmental distribution of calcium-binding protein and parvalbumin in the basal ganglia of the rat and monkey. *Proc. Natl. Acad. Sci. U. S. A.* 82, 8780–8784.
- Gerfen, C.R., Engber, T.M., Mahan, L.C., Susel, Z., Chase, T.N., Monsma, F.J., Sibley, D.R., 1990. D1 and D2 dopamine receptor-regulated gene expression of striatonigral and striatopallidal neurons. *Science* 250, 1429–1432. doi:10.1126/science.2147780
- Gerfen, C.R., Surmeier, D.J., 2011. Modulation of Striatal Projection Systems by Dopamine. *Annu. Rev. Neurosci.* 34, 441–466. doi:10.1146/annurev-neuro-061010-113641
- Gerfen, C.R., Wilson, C.J., 1996. The basal ganglia. *Handb. Chem. Neuroanat., Integrated systems of the CNS, part III* 12, 371–468. doi:10.1016/S0924-8196(96)80004-2
- German, D.C., Manaye, K.F., 1993. Midbrain dopaminergic neurons (nuclei A8, A9, and A10): Three-dimensional reconstruction in the rat. *J. Comp. Neurol.* 331, 297–309.
- German, D.C., Manaye, K.F., Sonsalla, P.K., Brooks, B.A., 1992. Midbrain Dopaminergic Cell Loss in Parkinson's Disease and MPTP-Induced Parkinsonism: Sparing of Calbindin-D25k—Containing Cells. *Ann. N. Y. Acad. Sci.* 648, 42–62.
- Gertler, T.S., Chan, C.S., Surmeier, D.J., 2008. Dichotomous Anatomical Properties of Adult Striatal Medium Spiny Neurons. *J. Neurosci.* 28, 10814–10824. doi:10.1523/JNEUROSCI.2660-08.2008
- Gervais, J., Rouillard, C., 2000. Dorsal raphe stimulation differentially modulates dopaminergic neurons in the ventral tegmental area and substantia nigra. *Synapse* 35, 281–291. doi:10.1002/(SICI)1098-2396(20000315)35:4<281::AID-SYN6>3.0.CO;2-A
- Ghosh, K.K., Burns, L.D., Cocker, E.D., Nimmerjahn, A., Ziv, Y., Gamal, A.E., Schnitzer, M.J., 2011. Miniaturized integration of a fluorescence microscope. *Nat. Methods* 8, 871–878. doi:10.1038/nmeth.1694
- Gonon, F.G., 1988. Nonlinear relationship between impulse flow and dopamine released by rat midbrain dopaminergic neurons as studied by in vivo electrochemistry. *Neuroscience* 24, 19–28.
- González-Hernández, T., Rodríguez, M., 2000. Compartmental organization and chemical profile of dopaminergic and GABAergic neurons in the substantia nigra of the rat. *J. Comp. Neurol.* 421, 107–135. doi:10.1002/(SICI)1096-9861(20000522)421:1<107::AID-CNE7>3.0.CO;2-F
- Grace, A.A., Bunney, B.S., 1984a. The control of firing pattern in nigral dopamine neurons: single spike firing. *J. Neurosci.* 4, 2866–2876.

- Grace, A.A., Bunney, B.S., 1984b. The control of firing pattern in nigral dopamine neurons: burst firing. *J. Neurosci.* 4, 2877–2890.
- Grace, A.A., Bunney, B.S., 1983a. Intracellular and extracellular electrophysiology of nigral dopaminergic neurons--1. Identification and characterization. *Neuroscience* 10, 301–315.
- Grace, A.A., Bunney, B.S., 1983b. Intracellular and extracellular electrophysiology of nigral dopaminergic neurons—2. Action potential generating mechanisms and morphological correlates. *Neuroscience* 10, 317–331. doi:10.1016/0306-4522(83)90136-7
- Grace, A.A., Bunney, B.S., 1980. Nigral dopamine neurons: intracellular recording and identification with L-dopa injection and histofluorescence. *Science* 210, 654–656. doi:10.1126/science.7433992
- Grace, A.A., Onn, S.P., 1989. Morphology and electrophysiological properties of immunocytochemically identified rat dopamine neurons recorded in vitro. *J. Neurosci.* 9, 3463–3481.
- Granata, A.R., Kitai, S.T., 1989. Intracellular analysis of excitatory subthalamic inputs to the pedunculopontine neurons. *Brain Res.* 488, 57–72.
- Greengard, P., 2001. The Neurobiology of Slow Synaptic Transmission. *Science* 294, 1024–1030. doi:10.1126/science.294.5544.1024
- Greif, G.J., Lin, Y.J., Liu, J.C., Freedman, J.E., 1995. Dopamine-modulated potassium channels on rat striatal neurons: specific activation and cellular expression. *J. Neurosci.* 15, 4533–4544.
- Grewe, B.F., Gründemann, J., Kitch, L.J., Lecoq, J.A., Parker, J.G., Marshall, J.D., Larkin, M.C., Jercog, P.E., Grenier, F., Li, J.Z., Lüthi, A., Schnitzer, M.J., 2017. Neural ensemble dynamics underlying a long-term associative memory. *Nature* 543, 670–675. doi:10.1038/nature21682
- Grofová, I., 1975. The identification of striatal and pallidal neurons projecting to substantia nigra. *Brain Res.* 91, 286–291. doi:10.1016/0006-8993(75)90550-8
- Grofova, I., Deniau, J.M., Kitai, S.T., 1982. Morphology of the substantia nigra pars reticulata projection neurons intracellularly labeled with HRP. *J. Comp. Neurol.* 208, 352–368. doi:10.1002/cne.902080406
- Grofova, I., Keane, S., 1991. Descending brainstem projections of the pedunculopontine tegmental nucleus in the rat. *Anat. Embryol. (Berl.)* 184, 275–290.

- Grofova, I., Zhou, M., 1998. Nigral innervation of cholinergic and glutamatergic cells in the rat mesopontine tegmentum: light and electron microscopic anterograde tracing and immunohistochemical studies. *J. Comp. Neurol.* 395, 359–379.
- Guzman, J.N., Sanchez-Padilla, J., Chan, C.S., Surmeier, D.J., 2009. Robust Pacemaking in Substantia Nigra Dopaminergic Neurons. *J. Neurosci.* 29, 11011–11019. doi:10.1523/JNEUROSCI.2519-09.2009
- Guzman, J.N., Sanchez-Padilla, J., Wokosin, D., Kondapalli, J., Ilijic, E., Schumacker, P.T., Surmeier, D.J., 2010. Oxidant stress evoked by pacemaking in dopaminergic neurons is attenuated by DJ-1. *Nature* 468, 696–700. doi:10.1038/nature09536
- Ha, J., Kuznetsov, A., 2013. Interaction of NMDA Receptor and Pacemaking Mechanisms in the Midbrain Dopaminergic Neuron. *PLoS ONE* 8, e69984. doi:10.1371/journal.pone.0069984
- Haber, S.N., Lynd, E., Klein, C., Groenewegen, H.J., 1990. Topographic organization of the ventral striatal efferent projections in the rhesus monkey: An anterograde tracing study. *J. Comp. Neurol.* 293, 282–298. doi:10.1002/cne.902930210
- Hahn, J., Tse, T.E., Levitan, E.S., 2003. Long-Term K⁺ Channel-Mediated Dampening of Dopamine Neuron Excitability by the Antipsychotic Drug Haloperidol. *J. Neurosci.* 23, 10859–10866.
- Hall, W.C., Fitzpatrick, D., Klatt, L.L., Raczkowski, D., 1989. Cholinergic innervation of the superior colliculus in the cat. *J. Comp. Neurol.* 287, 495–514. doi:10.1002/cne.902870408
- Hallett, P.J., Spoelgen, R., Hyman, B.T., Standaert, D.G., Dunah, A.W., 2006. Dopamine D₁ Activation Potentiates Striatal NMDA Receptors by Tyrosine Phosphorylation-Dependent Subunit Trafficking. *J. Neurosci.* 26, 4690–4700. doi:10.1523/JNEUROSCI.0792-06.2006
- Hamani, C., Moro, E., Lozano, A.M., 2011. The pedunculopontine nucleus as a target for deep brain stimulation. *J. Neural Transm.* 118, 1461–1468. doi:10.1007/s00702-010-0547-8
- Hammond, C., Deniau, J.M., Rizk, A., Feger, J., 1978. Electrophysiological demonstration of an excitatory subthalamonigral pathway in the rat. *Brain Res.* 151, 235–244. doi:10.1016/0006-8993(78)90881-8
- Han, X., 2012. In Vivo Application of Optogenetics for Neural Circuit Analysis. *ACS Chem. Neurosci.* 3, 577–584. doi:10.1021/cn300065j

- Hardingham, G.E., Bading, H., 2010. Synaptic versus extrasynaptic NMDA receptor signalling: implications for neurodegenerative disorders. *Nat. Rev. Neurosci.* 11, 682–696. doi:10.1038/nrn2911
- Hardman, C.D., Henderson, J.M., Finkelstein, D.I., Horne, M.K., Paxinos, G., Halliday, G.M., 2002. Comparison of the basal ganglia in rats, marmosets, macaques, baboons, and humans: Volume and neuronal number for the output, internal relay, and striatal modulating nuclei. *J. Comp. Neurol.* 445, 238–255. doi:10.1002/cne.10165
- Hatton, C.J., Paoletti, P., 2005. Modulation of Triheteromeric NMDA Receptors by N-Terminal Domain Ligands. *Neuron* 46, 261–274. doi:10.1016/j.neuron.2005.03.005
- Hattori, T., Fibiger, H.C., McGeer, P.L., 1975. Demonstration of a pallido-nigral projection innervating dopaminergic neurons. *J. Comp. Neurol.* 162, 487–504. doi:10.1002/cne.901620406
- Häusser, M., Stuart, G., Racca, C., Sakmann, B., 1995. Axonal initiation and active dendritic propagation of action potentials in substantia nigra neurons. *Neuron* 15, 637–647.
- Hazrati, L.N., Parent, A., 1992. Projection from the deep cerebellar nuclei to the pedunculo-pontine nucleus in the squirrel monkey. *Brain Res.* 585, 267–271.
- Henley, J.M., Wilkinson, K.A., 2016. Synaptic AMPA receptor composition in development, plasticity and disease. *Nat. Rev. Neurosci.* 17, 337–350. doi:10.1038/nrn.2016.37
- Henny, P., Brown, M.T.C., Northrop, A., Faunes, M., Ungless, M.A., Magill, P.J., Bolam, J.P., 2012. Structural correlates of heterogeneous in vivo activity of midbrain dopaminergic neurons. *Nat. Neurosci.* 15, 613–619. doi:10.1038/nn.3048
- Hernández, L.F., Redgrave, P., Obeso, J.A., 2015. Habitual behavior and dopamine cell vulnerability in Parkinson disease. *Front. Neuroanat.* 9. doi:10.3389/fnana.2015.00099
- Hernández-Echeagaray, E., Starling, A.J., Cepeda, C., Levine, M.S., 2004. Modulation of AMPA currents by D2 dopamine receptors in striatal medium-sized spiny neurons: are dendrites necessary? *Eur. J. Neurosci.* 19, 2455–2463. doi:10.1111/j.0953-816X.2004.03344.x
- Hernández-López, S., Tkatch, T., Perez-Garci, E., Galarraga, E., Bargas, J., Hamm, H., Surmeier, D.J., 2000. D2 Dopamine Receptors in Striatal Medium Spiny Neurons Reduce L-Type Ca²⁺ Currents and Excitability via a Novel PLCβ1–IP3–Calcineurin-Signaling Cascade. *J. Neurosci.* 20, 8987–8995.

- Higley, M.J., Sabatini, B.L., 2010. Competitive regulation of synaptic Ca²⁺ influx by D2 dopamine and A2A adenosine receptors. *Nat. Neurosci.* 13, 958–966. doi:10.1038/nn.2592
- Hong, S., Hikosaka, O., 2014. Pedunculopontine tegmental nucleus neurons provide reward, sensorimotor, and alerting signals to midbrain dopamine neurons. *Neuroscience, The Ventral Tegmentum and Dopamine: A New Wave of Diversity* 282, 139–155. doi:10.1016/j.neuroscience.2014.07.002
- Horvitz, J.C., Stewart, T., Jacobs, B.L., 1997. Burst activity of ventral tegmental dopamine neurons is elicited by sensory stimuli in the awake cat. *Brain Res.* 759, 251–258. doi:10.1016/S0006-8993(97)00265-5
- Howe, M.W., Dombeck, D.A., 2016. Rapid signalling in distinct dopaminergic axons during locomotion and reward. *Nature* 535, 505–510. doi:10.1038/nature18942
- Huang, Z., Gibb, A.J., 2014. Mg²⁺ block properties of triheteromeric GluN1–GluN2B–GluN2D NMDA receptors on neonatal rat substantia nigra pars compacta dopaminergic neurones. *J. Physiol.* 592, 2059–2078. doi:10.1113/jphysiol.2013.267864
- Hunter, J.D., 2007. Matplotlib: A 2D Graphics Environment. *Comput. Sci. Eng.* 9, 90–95. doi:10.1109/MCSE.2007.55
- Hyland, B.I., Reynolds, J.N.J., Hay, J., Perk, C.G., Miller, R., 2002. Firing modes of midbrain dopamine cells in the freely moving rat. *Neuroscience* 114, 475–492. doi:10.1016/S0306-4522(02)00267-1
- Inglis, W.L., Olmstead, M.C., Robbins, T.W., 2000. Pedunculopontine tegmental nucleus lesions impair stimulus–reward learning in autoshaping and conditioned reinforcement paradigms. *Behav. Neurosci.* 114, 285.
- Iribe, Y., Moore, K., Pang, K.C., Tepper, J.M., 1999. Subthalamic stimulation-induced synaptic responses in substantia nigra pars compacta dopaminergic neurons in vitro. *J. Neurophysiol.* 82, 925–933.
- Jackson, A., Crossman, A.R., 1983. Nucleus tegmenti pedunculopontinus: efferent connections with special reference to the basal ganglia, studied in the rat by anterograde and retrograde transport of horseradish peroxidase. *Neuroscience* 10, 725–765.
- Jankovic, J., 2008. Parkinson’s disease: clinical features and diagnosis. *J. Neurol. Neurosurg. Psychiatry* 79, 368–376. doi:10.1136/jnnp.2007.131045
- Jimenez-Martin, J., Blanco-Lezcano, L., González-Fraguela, M.E., Díaz-Hung, M.-L., Serrano-Sánchez, T., Almenares, J.L., Francis-Turner, L., 2015. Effect of neurotoxic lesion of

- pedunculopontine nucleus in nigral and striatal redox balance and motor performance in rats. *Neuroscience* 289, 300–314.
doi:10.1016/j.neuroscience.2014.12.056
- Johnson, S.W., Wu, Y.-N., 2004. Multiple mechanisms underlie burst firing in rat midbrain dopamine neurons in vitro. *Brain Res.* 1019, 293–296.
doi:10.1016/j.brainres.2004.06.022
- Jones, B.E., 1991. Paradoxical sleep and its chemical/structural substrates in the brain. *Neuroscience* 40, 637–656. doi:10.1016/0306-4522(91)90002-6
- Jones, B.E., Yang, T.Z., 1985. The efferent projections from the reticular formation and the locus coeruleus studied by anterograde and retrograde axonal transport in the rat. *J. Comp. Neurol.* 242, 56–92. doi:10.1002/cne.902420105
- Jones, E., Oliphant, T., Peterson, P., others, 2001. SciPy: Open source scientific tools for Python.
- Jones, S., Gibb, A.J., 2005. Functional NR2B- and NR2D-containing NMDA receptor channels in rat substantia nigra dopaminergic neurones. *J. Physiol.* 569, 209–221.
doi:10.1113/jphysiol.2005.095554
- Kanazawa, I., Marshall, G.R., Kelly, J.S., 1976. Afferents to the rat substantia nigra studied with horseradish peroxidase, with special reference to fibres from the subthalamic nucleus. *Brain Res.* 115, 485–491. doi:10.1016/0006-8993(76)90364-4
- Kang, Y., Kitai, S.T., 1990. Electrophysiological properties of pedunculopontine neurons and their postsynaptic responses following stimulation of substantia nigra reticulata. *Brain Res.* 535, 79–95.
- Kawahara, Y., Ito, K., Sun, H., Kanazawa, I., Kwak, S., 2003. Low editing efficiency of GluR2 mRNA is associated with a low relative abundance of ADAR2 mRNA in white matter of normal human brain. *Eur. J. Neurosci.* 18, 23–33. doi:10.1046/j.1460-9568.2003.02718.x
- Kawano, M., Kawasaki, A., Sakata-Haga, H., Fukui, Y., Kawano, H., Nogami, H., Hisano, S., 2006. Particular subpopulations of midbrain and hypothalamic dopamine neurons express vesicular glutamate transporter 2 in the rat brain. *J. Comp. Neurol.* 498, 581–592. doi:10.1002/cne.21054
- Kebabian, J.W., 1978. Multiple classes of dopamine receptors in mammalian central nervous system: The involvement of dopamine-sensitive adenylyl cyclase. *Life Sci.* 23, 479–483. doi:10.1016/0024-3205(78)90157-1

- Kebabian, J.W., Greengard, P., 1971. Dopamine-Sensitive Adenyl Cyclase: Possible Role in Synaptic Transmission. *Science* 174, 1346–1349. doi:10.1126/science.174.4016.1346
- Khaliq, Z.M., Bean, B.P., 2010. Pacemaking in Dopaminergic Ventral Tegmental Area Neurons: Depolarizing Drive from Background and Voltage-Dependent Sodium Conductances. *J. Neurosci.* 30, 7401–7413. doi:10.1523/JNEUROSCI.0143-10.2010
- Kimm, T., Khaliq, Z.M., Bean, B.P., 2015. Differential Regulation of Action Potential Shape and Burst-Frequency Firing by BK and Kv2 Channels in Substantia Nigra Dopaminergic Neurons. *J. Neurosci.* 35, 16404–16417. doi:10.1523/JNEUROSCI.5291-14.2015
- Kita, H., Kitai, S.T., 1987. Efferent projections of the subthalamic nucleus in the rat: Light and electron microscopic analysis with the PHA-L method. *J. Comp. Neurol.* 260, 435–452. doi:10.1002/cne.902600309
- Klapoetke, N.C., Murata, Y., Kim, S.S., Pulver, S.R., Birdsey-Benson, A., Cho, Y.K., Morimoto, T.K., Chuong, A.S., Carpenter, E.J., Tian, Z., Wang, J., Xie, Y., Yan, Z., Zhang, Y., Chow, B.Y., Surek, B., Melkonian, M., Jayaraman, V., Constantine-Paton, M., Wong, G.K.-S., Boyden, E.S., 2014. Independent optical excitation of distinct neural populations. *Nat. Methods* 11, 338–346. doi:10.1038/nmeth.2836
- Kobayashi, K., Hoshino, K., Homma, S., Takagi, S., Norita, M., 2007. A possible monosynaptic pathway links the pedunculopontine tegmental nucleus to thalamostriatal neurons in the hooded rat. *Arch. Histol. Cytol.* 70, 207–214.
- Kobayashi, S., Nakamura, Y., 2003. Synaptic organization of the rat parafascicular nucleus, with special reference to its afferents from the superior colliculus and the pedunculopontine tegmental nucleus. *Brain Res.* 980, 80–91. doi:10.1016/S0006-8993(03)02921-4
- Kobayashi, S., Schultz, W., 2014. Reward Contexts Extend Dopamine Signals to Unrewarded Stimuli. *Curr. Biol.* 24, 56–62. doi:10.1016/j.cub.2013.10.061
- Kobayashi, Y., Inoue, Y., Yamamoto, M., Isa, T., Aizawa, H., 2002. Contribution of Pedunculopontine Tegmental Nucleus Neurons to Performance of Visually Guided Saccade Tasks in Monkeys. *J. Neurophysiol.* 88, 715–731.
- Kobayashi, Y., Okada, K.-I., 2007. Reward Prediction Error Computation in the Pedunculopontine Tegmental Nucleus Neurons. *Ann. N. Y. Acad. Sci.* 1104, 310–323. doi:10.1196/annals.1390.003
- Koga, K., Kanehisa, K., Kohro, Y., Shiratori-Hayashi, M., Tozaki-Saitoh, H., Inoue, K., Furue, H., Tsuda, M., 2017. Chemogenetic silencing of GABAergic dorsal horn interneurons

- induces morphine-resistant spontaneous nocifensive behaviours. *Sci. Rep.* 7, 4739. doi:10.1038/s41598-017-04972-3
- Koike, M., Iino, M., Ozawa, S., 1997. Blocking effect of 1-naphthyl acetyl spermine on Ca(2+)-permeable AMPA receptors in cultured rat hippocampal neurons. *Neurosci. Res.* 29, 27–36.
- Kornhuber, J., Kim, J.-S., Kornhuber, M.E., Kornhuber, H.H., 1984. The cortico-nigral projection: reduced glutamate content in the substantia nigra following frontal cortex ablation in the rat. *Brain Res.* 322, 124–126. doi:10.1016/0006-8993(84)91189-2
- Krashes, M.J., Koda, S., Ye, C., Rogan, S.C., Adams, A.C., Cusher, D.S., Maratos-Flier, E., Roth, B.L., Lowell, B.B., 2011. Rapid, reversible activation of AgRP neurons drives feeding behavior in mice. *J. Clin. Invest.* 121, 1424–1428. doi:10.1172/JCI46229
- Kravitz, A.V., Freeze, B.S., Parker, P.R.L., Kay, K., Thwin, M.T., Deisseroth, K., Kreitzer, A.C., 2010. Regulation of parkinsonian motor behaviours by optogenetic control of basal ganglia circuitry. *Nature* 466, 622–626. doi:10.1038/nature09159
- Kreitzer, A.C., Malenka, R.C., 2008. Striatal Plasticity and Basal Ganglia Circuit Function. *Neuron* 60, 543–554. doi:10.1016/j.neuron.2008.11.005
- Kreitzer, A.C., Malenka, R.C., 2007. Endocannabinoid-mediated rescue of striatal LTD and motor deficits in Parkinson's disease models. *Nature* 445, 643–647. doi:10.1038/nature05506
- Kroeger, D., Ferrari, L.L., Petit, G., Mahoney, C.E., Fuller, P.M., Arrigoni, E., Scammell, T.E., 2017. Cholinergic, Glutamatergic, and GABAergic Neurons of the Pedunculopontine Tegmental Nucleus Have Distinct Effects on Sleep/Wake Behavior in Mice. *J. Neurosci.* 37, 1352–1366. doi:10.1523/JNEUROSCI.1405-16.2016
- Kuznetsov, A.S., 2005. Transient High-Frequency Firing in a Coupled-Oscillator Model of the Mesencephalic Dopaminergic Neuron. *J. Neurophysiol.* 95, 932–947. doi:10.1152/jn.00691.2004
- Kuznetsova, A.Y., Huertas, M.A., Kuznetsov, A.S., Paladini, C.A., Canavier, C.C., 2010. Regulation of firing frequency in a computational model of a midbrain dopaminergic neuron. *J. Comput. Neurosci.* 28, 389–403. doi:10.1007/s10827-010-0222-y
- Lacey, M.G., Mercuri, N.B., North, R.A., 1989. Two cell types in rat substantia nigra zona compacta distinguished by membrane properties and the actions of dopamine and opioids. *J. Neurosci. Off. J. Soc. Neurosci.* 9, 1233–1241.

- Lai, Y.Y., Siegel, J.M., 1990. Muscle tone suppression and stepping produced by stimulation of midbrain and rostral pontine reticular formation. *J. Neurosci.* 10, 2727–2734.
- Lavoie, B., Parent, A., 1994a. Pedunclopontine nucleus in the squirrel monkey: cholinergic and glutamatergic projections to the substantia nigra. *J. Comp. Neurol.* 344, 232–241. doi:10.1002/cne.903440205
- Lavoie, B., Parent, A., 1994b. Pedunclopontine nucleus in the squirrel monkey: distribution of cholinergic and monoaminergic neurons in the mesopontine tegmentum with evidence for the presence of glutamate in cholinergic neurons. *J. Comp. Neurol.* 344, 190–209. doi:10.1002/cne.903440203
- Lavoie, B., Parent, A., 1994c. Pedunclopontine nucleus in the squirrel monkey: Projections to the basal ganglia as revealed by anterograde tract-tracing methods. *J. Comp. Neurol.* 344, 210–231. doi:10.1002/cne.903440204
- Lavoie, B., Parent, A., 1991. Dopaminergic neurons expressing calbindin in normal and parkinsonian monkeys. *Neuroreport* 2, 601–604.
- Le Moine, C., Normand, E., Bloch, B., 1991. Phenotypical characterization of the rat striatal neurons expressing the D1 dopamine receptor gene. *Proc. Natl. Acad. Sci. U. S. A.* 88, 4205–4209.
- Lee, C.R., Abercrombie, E.D., Tepper, J.M., 2004. Pallidal control of substantia nigra dopaminergic neuron firing pattern and its relation to extracellular neostriatal dopamine levels. *Neuroscience* 129, 481–489. doi:10.1016/j.neuroscience.2004.07.034
- Lee, C.R., Tepper, J.M., 2009. Basal Ganglia Control of Substantia Nigra Dopaminergic Neurons, in: Giovanni, G., Di Matteo, V., Esposito, E. (Eds.), *Birth, Life and Death of Dopaminergic Neurons in the Substantia Nigra*. Springer Vienna, Vienna, pp. 71–90.
- Leonard, C.S., Llinás, R., 1994. Serotonergic and cholinergic inhibition of mesopontine cholinergic neurons controlling rem sleep: An in vitro electrophysiological study. *Neuroscience* 59, 309–330. doi:10.1016/0306-4522(94)90599-1
- Leonard, C.S., Llinás, R., 1990. Electrophysiology of mammalian pedunclopontine and laterodorsal tegmental neurons in vitro: Implications for the control of REM sleep., in: *Brain Cholinergic System*. Oxford Science, Oxford, pp. 205–223.
- Lerner, T.N., Horne, E.A., Stella, N., Kreitzer, A.C., 2010. Endocannabinoid signaling mediates psychomotor activation by adenosine A2A antagonists. *J. Neurosci. Off. J. Soc. Neurosci.* 30, 2160–2164. doi:10.1523/JNEUROSCI.5844-09.2010

- Li, X., Qi, J., Yamaguchi, T., Wang, H.-L., Morales, M., 2013. Heterogeneous composition of dopamine neurons of the rat A10 region: molecular evidence for diverse signaling properties. *Brain Struct. Funct.* 218, 1159–1176. doi:10.1007/s00429-012-0452-z
- Liss, B., Roeper, J., 2001. ATP-sensitive potassium channels in dopaminergic neurons: transducers of mitochondrial dysfunction. *News Physiol. Sci.* 16, 214–216.
- Ljungberg, T., Apicella, P., Schultz, W., 1992. Responses of monkey dopamine neurons during learning of behavioral reactions. *J. Neurophysiol.* 67, 145–163.
- Lokwan, S.J.A., Overton, P.G., Berry, M.S., Clark, D., 1999. Stimulation of the pedunclopontine tegmental nucleus in the rat produces burst firing in A9 dopaminergic neurons. *Neuroscience* 92, 245–254.
- Lu, J., Sherman, D., Devor, M., Saper, C.B., 2006. A putative flip–flop switch for control of REM sleep. *Nature* 441, 589–594. doi:10.1038/nature04767
- Martinez-Gonzalez, C., Andel, J. van, Bolam, J.P., Mena-Segovia, J., 2014. Divergent motor projections from the pedunclopontine nucleus are differentially regulated in Parkinsonism. *Brain Struct. Funct.* 219, 1451–1462. doi:10.1007/s00429-013-0579-6
- Martinez-Gonzalez, C., Bolam, J.P., Mena-Segovia, J., 2011. Topographical Organization of the Pedunclopontine Nucleus. *Front. Neuroanat.* 5. doi:10.3389/fnana.2011.00022
- Martinez-Gonzalez, C., Wang, H.-L., Micklem, B.R., Bolam, J.P., Mena-Segovia, J., 2012. Subpopulations of cholinergic, GABAergic and glutamatergic neurons in the pedunclopontine nucleus contain calcium-binding proteins and are heterogeneously distributed. *Eur. J. Neurosci.* 35, 723–734. doi:10.1111/j.1460-9568.2012.08002.x
- Matsuda, W., Furuta, T., Nakamura, K.C., Hioki, H., Fujiyama, F., Arai, R., Kaneko, T., 2009. Single Nigrostriatal Dopaminergic Neurons Form Widely Spread and Highly Dense Axonal Arborizations in the Neostriatum. *J. Neurosci.* 29, 444–453. doi:10.1523/JNEUROSCI.4029-08.2009
- May, P.J., McHaffie, J.G., Stanford, T.R., Jiang, H., Costello, M.G., Coizet, V., Hayes, L.M., Haber, S.N., Redgrave, P., 2009. Tectonigral projections in the primate: a pathway for pre-attentive sensory input to midbrain dopaminergic neurons. *Eur. J. Neurosci.* 29, 575–587. doi:10.1111/j.1460-9568.2008.06596.x
- McCormick, D.A., 1993. Actions of acetylcholine in the cerebral cortex and thalamus and implications for function. *Prog. Brain Res.* 98, 303–308.

- McGeer, P.L., McGeer, E.G., Scherer, U., Singh, K., 1977. A glutamatergic corticostriatal path? *Brain Res.* 128, 369–373.
- McHaffie, J.G., Jiang, H., May, P.J., Coizet, V., Overton, P.G., Stein, B.E., Redgrave, P., 2006. A direct projection from superior colliculus to substantia nigra pars compacta in the cat. *Neuroscience* 138, 221–234. doi:10.1016/j.neuroscience.2005.11.015
- McKinney, W., 2010. Data Structures for Statistical Computing in Python, in: Walt, S. van der, Millman, J. (Eds.), *Proceedings of the 9th Python in Science Conference*. pp. 51–56.
- Mena-Segovia, J., Bolam, J.P., 2017. Rethinking the Pedunculo-pontine Nucleus: From Cellular Organization to Function. *Neuron* 94, 7–18. doi:10.1016/j.neuron.2017.02.027
- Mena-Segovia, J., Bolam, J.P., Magill, P.J., 2004. Pedunculo-pontine nucleus and basal ganglia: distant relatives or part of the same family? *Trends Neurosci.* 27, 585–588. doi:10.1016/j.tins.2004.07.009
- Mena-Segovia, J., Micklem, B.R., Nair-Roberts, R.G., Ungless, M.A., Bolam, J.P., 2009. GABAergic neuron distribution in the pedunculo-pontine nucleus defines functional subterritories. *J. Comp. Neurol.* 515, 397–408. doi:10.1002/cne.22065
- Mena-Segovia, J., Sims, H.M., Magill, P.J., Bolam, J.P., 2008. Cholinergic brainstem neurons modulate cortical gamma activity during slow oscillations. *J. Physiol.* 586, 2947–2960. doi:10.1113/jphysiol.2008.153874
- Mercuri, N.B., Bond, A., Calabresi, P., Stratta, F., Stefani, A., Bernardi, G., 1994. Effects of dihydropyridine calcium antagonists on rat midbrain dopaminergic neurones. *Br. J. Pharmacol.* 113, 831–838.
- Mesulam, M.-M., Geula, C., Bothwell, M.A., Hersh, L.B., 1989. Human reticular formation: Cholinergic neurons of the pedunculo-pontine and laterodorsal tegmental nuclei and some cytochemical comparisons to forebrain cholinergic neurons. *J. Comp. Neurol.* 283, 611–633. doi:10.1002/cne.902830414
- Mesulam, M.-M., Mufson, E.J., Levey, A.I., Wainer, B.H., 1984. Atlas of cholinergic neurons in the forebrain and upper brainstem of the macaque based on monoclonal choline acetyltransferase immunohistochemistry and acetylcholinesterase histochemistry. *Neuroscience* 12, 669–686. doi:10.1016/0306-4522(84)90163-5
- Mesulam, M.-M., Mufson, E.J., Wainer, B.H., Levey, A.I., 1983. Central cholinergic pathways in the rat: An overview based on an alternative nomenclature (Ch1–Ch6). *Neuroscience* 10, 1185–1201. doi:10.1016/0306-4522(83)90108-2

- Miller, W.C., DeLong, M.R., 1987. Altered Tonic Activity of Neurons in the Globus Pallidus and Subthalamic Nucleus in the Primate MPTP Model of Parkinsonism, in: *The Basal Ganglia II, Advances in Behavioral Biology*. Springer, Boston, MA, pp. 415–427. doi:10.1007/978-1-4684-5347-8_29
- Mitani, A., Ito, K., Hallanger, A.E., Wainer, B.H., Kataoka, K., McCarley, R.W., 1988. Cholinergic projections from the laterodorsal and pedunclopontine tegmental nuclei to the pontine gigantocellular tegmental field in the cat. *Brain Res.* 451, 397–402. doi:10.1016/0006-8993(88)90792-5
- Monsma, F.J., Mahan, L.C., McVittie, L.D., Gerfen, C.R., Sibley, D.R., 1990. Molecular cloning and expression of a D1 dopamine receptor linked to adenylyl cyclase activation. *Proc. Natl. Acad. Sci.* 87, 6723–6727.
- Monyer, H., Burnashev, N., Laurie, D.J., Sakmann, B., Seeburg, P.H., 1994. Developmental and regional expression in the rat brain and functional properties of four NMDA receptors. *Neuron* 12, 529–540. doi:10.1016/0896-6273(94)90210-0
- Mori, S., Nishimura, H., Kurakami, C., Yamamura, T., Aoki, M., 1978. Controlled locomotion in the mesencephalic cat: distribution of facilitatory and inhibitory regions within pontine tegmentum. *J. Neurophysiol.* 41, 1580–1591.
- Morikawa, H., Paladini, C.A., 2011. Dynamic regulation of midbrain dopamine neuron activity: intrinsic, synaptic, and plasticity mechanisms. *Neuroscience* 198, 95–111. doi:10.1016/j.neuroscience.2011.08.023
- Moruzzi, G., Magoun, H.W., 1949. Brain stem reticular formation and activation of the EEG. *Electroencephalogr. Clin. Neurophysiol.* 1, 455–473. doi:10.1016/0013-4694(49)90219-9
- Moss, J., Bolam, J.P., 2008. A Dopaminergic Axon Lattice in the Striatum and Its Relationship with Cortical and Thalamic Terminals. *J. Neurosci.* 28, 11221–11230. doi:10.1523/JNEUROSCI.2780-08.2008
- Moss, J., Bolam, P.J., 2009. The Relationship between Dopaminergic Axons and Glutamatergic Synapses in the Striatum: Structural Considerations, in: Iversen, L., Iversen, S., Dunnett, S., Bjorklund, A. (Eds.), *Dopamine Handbook*. Oxford University Press, pp. 49–60. doi:10.1093/acprof:oso/9780195373035.003.0005
- Motts, S.D., Schofield, B.R., 2009. Sources of cholinergic input to the inferior colliculus. *Neuroscience* 160, 103–114. doi:10.1016/j.neuroscience.2009.02.036
- Mullasseril, P., Hansen, K.B., Vance, K.M., Ogden, K.K., Yuan, H., Kurtkaya, N.L., Santangelo, R., Orr, A.G., Le, P., Vellano, K.M., Liotta, D.C., Traynelis, S.F., 2010. A subunit-selective

- potentiator of NR2C- and NR2D-containing NMDA receptors. *Nat. Commun.* 1, 90. doi:10.1038/ncomms1085
- Nair-Roberts, R.G., Chatelain-Badie, S.D., Benson, E., White-Cooper, H., Bolam, J.P., Ungless, M.A., 2008. Stereological estimates of dopaminergic, GABAergic and glutamatergic neurons in the ventral tegmental area, substantia nigra and retrorubral field in the rat. *Neuroscience* 152, 1024–1031. doi:10.1016/j.neuroscience.2008.01.046
- Naito, A., Kita, H., 1994. The cortico-nigral projection in the rat: an anterograde tracing study with biotinylated dextran amine. *Brain Res.* 637, 317–322. doi:10.1016/0006-8993(94)91252-1
- Nakamura, Y., Tokuno, H., Moriizumi, T., Kitao, Y., Kudo, M., 1989. Monosynaptic nigral inputs to the pedunclopontine tegmental nucleus neurons which send their axons to the medial reticular formation in the medulla oblongata. An electron microscopic study in the cat. *Neurosci. Lett.* 103, 145–150. doi:10.1016/0304-3940(89)90566-1
- Nakano, K., 2000. Neural circuits and topographic organization of the basal ganglia and related regions. *Brain Dev.* 22, 5–16.
- Nedergaard, S., Flatman, J.A., Engberg, I., 1993. Nifedipine- and omega-conotoxin-sensitive Ca²⁺ conductances in guinea-pig substantia nigra pars compacta neurones. *J. Physiol.* 466, 727–747.
- Nelson, E. I., Liang, C.-L., Sinton, C. m., German, D. c., 1996. Midbrain dopaminergic neurons in the mouse: Computer-assisted mapping. *J. Comp. Neurol.* 369, 361–371. doi:10.1002/(SICI)1096-9861(19960603)369:3<361::AID-CNE3>3.0.CO;2-3
- Neuhoff, H., Neu, A., Liss, B., Roeper, J., 2002. Ih channels contribute to the different functional properties of identified dopaminergic subpopulations in the midbrain. *J. Neurosci.* 22, 1290–1302.
- Nicola, S.M., Malenka, R.C., 1998. Modulation of Synaptic Transmission by Dopamine and Norepinephrine in Ventral but not Dorsal Striatum. *J. Neurophysiol.* 79, 1768–1776.
- Nicola, S.M., Surmeier, D.J., Malenka, R.C., 2000. Dopaminergic modulation of neuronal excitability in the striatum and nucleus accumbens. *Annu. Rev. Neurosci.* 23, 185–215.
- Nomoto, K., Schultz, W., Watanabe, T., Sakagami, M., 2010. Temporally Extended Dopamine Responses to Perceptually Demanding Reward-Predictive Stimuli. *J. Neurosci.* 30, 10692–10702. doi:10.1523/JNEUROSCI.4828-09.2010
- Norton, A.B.W., Jo, Y.S., Clark, E.W., Taylor, C.A., Mizumori, S.J.Y., 2011. Independent neural coding of reward and movement by pedunclopontine tegmental nucleus neurons

- in freely navigating rats. *Eur. J. Neurosci.* 33, 1885–1896. doi:10.1111/j.1460-9568.2011.07649.x
- Oakman, S.A., Faris, P.L., Cozzari, C., Hartman, B.K., 1999. Characterization of the extent of pontomesencephalic cholinergic neurons' projections to the thalamus: comparison with projections to midbrain dopaminergic groups. *Neuroscience* 94, 529–547.
- Oakman, S.A., Faris, P.L., Kerr, P.E., Cozzari, C., Hartman, B.K., 1995. Distribution of pontomesencephalic cholinergic neurons projecting to substantia nigra differs significantly from those projecting to ventral tegmental area. *J. Neurosci.* 15, 5859–5869.
- Okada, K., Toyama, K., Inoue, Y., Isa, T., Kobayashi, Y., 2009. Different Pedunclopontine Tegmental Neurons Signal Predicted and Actual Task Rewards. *J. Neurosci.* 29, 4858–4870. doi:10.1523/JNEUROSCI.4415-08.2009
- Okada, K.-I., Kobayashi, Y., 2013. Reward prediction-related increases and decreases in tonic neuronal activity of the pedunclopontine tegmental nucleus. *Front. Integr. Neurosci.* 7. doi:10.3389/fnint.2013.00036
- Olson, P.A., 2005. G-Protein-Coupled Receptor Modulation of Striatal CaV1.3 L-Type Ca²⁺ Channels Is Dependent on a Shank-Binding Domain. *J. Neurosci.* 25, 1050–1062. doi:10.1523/JNEUROSCI.3327-04.2005
- Olszewski, J., Baxter, D., 1982. *Cytoarchitecture of the Human Brain Stem*. Karger.
- Onali, P., Olanas, M.C., Gessa, G.L., 1985. Characterization of dopamine receptors mediating inhibition of adenylate cyclase activity in rat striatum. *Mol. Pharmacol.* 28, 138–145.
- Oorschot, D.E., 1996. Total number of neurons in the neostriatal, pallidal, subthalamic, and substantia nigral nuclei of the rat basal ganglia: A stereological study using the cavalieri and optical disector methods. *J. Comp. Neurol.* 366, 580–599. doi:10.1002/(SICI)1096-9861(19960318)366:4<580::AID-CNE3>3.0.CO;2-0
- Overton, P., Clark, D., 1992. Iontophoretically administered drugs acting at the N-methyl-D-aspartate receptor modulate burst firing in A9 dopamine neurons in the rat. *Synapse* 10, 131–140.
- Overton, P.G., Clark, D., 1997. Burst firing in midbrain dopaminergic neurons. *Brain Res. Rev.* 25, 312–334. doi:10.1016/S0165-0173(97)00039-8
- Pahapill, P.A., Lozano, A.M., 2000. The pedunclopontine nucleus and Parkinson's disease. *Brain J. Neurol.* 123 (Pt 9), 1767–1783.

- Paladini, C.A., Celada, P., Tepper, J.M., 1999. Striatal, pallidal, and pars reticulata evoked inhibition of nigrostriatal dopaminergic neurons is mediated by GABAA receptors in vivo. *Neuroscience* 89, 799–812. doi:10.1016/S0306-4522(98)00355-8
- Paladini, C.A., Roeper, J., 2014. Generating bursts (and pauses) in the dopamine midbrain neurons. *Neuroscience, The Ventral Tegmentum and Dopamine: A New Wave of Diversity* 282, 109–121. doi:10.1016/j.neuroscience.2014.07.032
- Pan, W.-X., Hyland, B.I., 2005. Pedunculopontine Tegmental Nucleus Controls Conditioned Responses of Midbrain Dopamine Neurons in Behaving Rats. *J. Neurosci.* 25, 4725–4732. doi:10.1523/JNEUROSCI.0277-05.2005
- Pan, W.-X., Schmidt, R., Wickens, J.R., Hyland, B.I., 2005. Dopamine Cells Respond to Predicted Events during Classical Conditioning: Evidence for Eligibility Traces in the Reward-Learning Network. *J. Neurosci.* 25, 6235–6242. doi:10.1523/JNEUROSCI.1478-05.2005
- Paoletti, P., Bellone, C., Zhou, Q., 2013. NMDA receptor subunit diversity: impact on receptor properties, synaptic plasticity and disease. *Nat. Rev. Neurosci.* 14, 383–400. doi:10.1038/nrn3504
- Parent, M., Descarries, L., 2008. Acetylcholine innervation of the adult rat thalamus: Distribution and ultrastructural features in dorsolateral geniculate, parafascicular, and reticular thalamic nuclei. *J. Comp. Neurol.* 511, 678–691. doi:10.1002/cne.21868
- Pawlak, V., Kerr, J.N.D., 2008. Dopamine Receptor Activation Is Required for Corticostriatal Spike-Timing-Dependent Plasticity. *J. Neurosci.* 28, 2435–2446. doi:10.1523/JNEUROSCI.4402-07.2008
- Petreaanu, L., Mao, T., Sternson, S.M., Svoboda, K., 2009. The subcellular organization of neocortical excitatory connections. *Nature* 457, 1142–1145. doi:10.1038/nature07709
- Petzold, A., Valencia, M., Pál, B., Mena-Segovia, J., 2015. Decoding brain state transitions in the pedunculopontine nucleus: cooperative phasic and tonic mechanisms. *Front. Neural Circuits* 9. doi:10.3389/fncir.2015.00068
- Ping, H.X., Shepard, P.D., 1999. Blockade of SK-type Ca²⁺-activated K⁺ channels uncovers a Ca²⁺-dependent slow afterdepolarization in nigral dopamine neurons. *J. Neurophysiol.* 81, 977–984.
- Ping, H.X., Shepard, P.D., 1996. Apamin-sensitive Ca(2+)-activated K⁺ channels regulate pacemaker activity in nigral dopamine neurons. *Neuroreport* 7, 809–814.

- Poulsen, M.H., Lucas, S., Strømgaard, K., Kristensen, A.S., 2014. Evaluation of PhTX-74 as Subtype-Selective Inhibitor of GluA2-Containing AMPA Receptors. *Mol. Pharmacol.* 85, 261–268. doi:10.1124/mol.113.089961
- Puopolo, M., Raviola, E., Bean, B.P., 2007. Roles of Subthreshold Calcium Current and Sodium Current in Spontaneous Firing of Mouse Midbrain Dopamine Neurons. *J. Neurosci.* 27, 645–656. doi:10.1523/JNEUROSCI.4341-06.2007
- Ramírez-Latorre, J.A., 2012. Functional Upregulation of Ca²⁺-Activated K⁺ Channels in the Development of Substantia Nigra Dopamine Neurons. *PLoS ONE* 7, e51610. doi:10.1371/journal.pone.0051610
- Redgrave, P., Mitchell, I.J., Dean, P., 1987. Descending projections from the superior colliculus in rat: a study using orthograde transport of wheatgerm-agglutinin conjugated horseradish peroxidase. *Exp. Brain Res.* 68, 147–167.
- Redgrave, P., Rodriguez, M., Smith, Y., Rodriguez-Oroz, M.C., Lehericy, S., Bergman, H., Agid, Y., DeLong, M.R., Obeso, J.A., 2010. Goal-directed and habitual control in the basal ganglia: implications for Parkinson's disease. *Nat. Rev. Neurosci.* 11, 760–772. doi:10.1038/nrn2915
- Retchless, B.S., Gao, W., Johnson, J.W., 2012. A single GluN2 subunit residue controls NMDA receptor channel properties via intersubunit interaction. *Nat. Neurosci.* 15, 406–413. doi:10.1038/nn.3025
- Reynolds, J.N.J., Hyland, B.I., Wickens, J.R., 2001. A cellular mechanism of reward-related learning. *Nature* 413, 67–70. doi:10.1038/35092560
- Ribak, C.E., Vaughn, J.E., Roberts, E., 1980. Gabaergic nerve terminals decrease in the substantia nigra following hemitranssections of the striatonigral and pallidonigral pathways. *Brain Res.* 192, 413–420. doi:10.1016/0006-8993(80)90893-8
- Rinne, J.O., Ma, S.Y., Lee, M.S., Collan, Y., Røyttä, M., 2008. Loss of cholinergic neurons in the pedunculopontine nucleus in Parkinson's disease is related to disability of the patients. *Parkinsonism Relat. Disord.* 14, 553–557. doi:10.1016/j.parkreldis.2008.01.006
- Robledo, P., Féger, J., 1990. Excitatory influence of rat subthalamic nucleus to substantia nigra pars reticulata and the pallidal complex: electrophysiological data. *Brain Res.* 518, 47–54. doi:10.1016/0006-8993(90)90952-8
- Rolland, A.-S., Tandé, D., Herrero, M.-T., Luquin, M.-R., Vazquez-Claverie, M., Karachi, C., Hirsch, E.C., François, C., 2009. Evidence for a dopaminergic innervation of the pedunculopontine nucleus in monkeys, and its drastic reduction after MPTP

- intoxication: Dopaminergic innervation of the lower brainstem. *J. Neurochem.* 110, 1321–1329. doi:10.1111/j.1471-4159.2009.06220.x
- Romo, R., Schultz, W., 1990. Dopamine neurons of the monkey midbrain: contingencies of responses to active touch during self-initiated arm movements. *J. Neurophysiol.* 63, 592–606.
- Roš, H., Magill, P.J., Moss, J., Bolam, J.P., Mena-Segovia, J., 2010. Distinct types of non-cholinergic pedunculopontine neurons are differentially modulated during global brain states. *Neuroscience* 170, 78–91. doi:10.1016/j.neuroscience.2010.06.068
- Roseberry, T.K., Lee, A.M., Lalive, A.L., Wilbrecht, L., Bonci, A., Kreitzer, A.C., 2016. Cell-Type-Specific Control of Brainstem Locomotor Circuits by Basal Ganglia. *Cell* 164, 526–537. doi:10.1016/j.cell.2015.12.037
- Roth, B.L., 2016. DREADDs for Neuroscientists. *Neuron* 89, 683–694. doi:10.1016/j.neuron.2016.01.040
- Rye, D.B., Lee, H.J., Saper, C.B., Wainer, B.H., 1988. Medullary and spinal efferents of the pedunculopontine tegmental nucleus and adjacent mesopontine tegmentum in the rat. *J. Comp. Neurol.* 269, 315–341. doi:10.1002/cne.902690302
- Rye, D.B., Saper, C.B., Lee, H.J., Wainer, B.H., 1987. Pedunculopontine tegmental nucleus of the rat: cytoarchitecture, cytochemistry, and some extrapyramidal connections of the mesopontine tegmentum. *J. Comp. Neurol.* 259, 483–528. doi:10.1002/cne.902590403
- Sah, P., Faber, E.S.L., Armentia, M.L.D., Power, J., 2003. The Amygdaloid Complex: Anatomy and Physiology. *Physiol. Rev.* 83, 803–834. doi:10.1152/physrev.00002.2003
- Saitoh, K., Hattori, S., Song, W.-J., Isa, T., Takakusaki, K., 2003. Nigral GABAergic inhibition upon cholinergic neurons in the rat pedunculopontine tegmental nucleus. *Eur. J. Neurosci.* 18, 879–886. doi:10.1046/j.1460-9568.2003.02825.x
- Sanchez-Padilla, J., Guzman, J.N., Ilijic, E., Kondapalli, J., Galtieri, D.J., Yang, B., Schieber, S., Oertel, W., Wokosin, D., Schumacker, P.T., Surmeier, D.J., 2014. Mitochondrial oxidant stress in locus coeruleus is regulated by activity and nitric oxide synthase. *Nat. Neurosci.* 17, 832–840. doi:10.1038/nn.3717
- Sarpal, D., Koenig, J.I., Adelman, J.P., Brady, D., Prendeville, L.C., Shepard, P.D., 2004. Regional distribution of SK3 mRNA-containing neurons in the adult and adolescent rat ventral midbrain and their relationship to dopamine-containing cells. *Synapse* 53, 104–113. doi:10.1002/syn.20042

- Satoh, K., Fibiger, H.C., 1986. Cholinergic neurons of the laterodorsal tegmental nucleus: efferent and afferent connections. *J. Comp. Neurol.* 253, 277–302.
- Scarnati, E., Campana, E., Pacitti, C., 1984. Pedunculo-pontine-evoked excitation of substantia nigra neurons in the rat. *Brain Res.* 304, 351–361.
- Scarnati, E., Proia, A., Campana, E., Pacitti, C., 1986. A microiontophoretic study on the nature of the putative synaptic neurotransmitter involved in the pedunculo-pontine-substantia nigra pars compacta excitatory pathway of the rat. *Exp. Brain Res.* 62, 470–478.
- Scarnati, E., Proia, A., Di Loreto, S., Pacitti, C., 1987. The reciprocal electrophysiological influence between the nucleus tegmenti pedunculo-pontinus and the substantia nigra in normal and decorticated rats. *Brain Res.* 423, 116–124.
- Schiffmann, Desdouits, Menu, Greengard, Vincent, J.-D., Vanderhaeghen, J.-J., Girault, J.-A., 1998. Modulation of the voltage-gated sodium current in rat striatal neurons by DARPP-32, an inhibitor of protein phosphatase. *Eur. J. Neurosci.* 10, 1312–1320. doi:10.1046/j.1460-9568.1998.00142.x
- Schindelin, J., Arganda-Carreras, I., Frise, E., Kaynig, V., Longair, M., Pietzsch, T., Preibisch, S., Rueden, C., Saalfeld, S., Schmid, B., Tinevez, J.-Y., White, D.J., Hartenstein, V., Eliceiri, K., Tomancak, P., Cardona, A., 2012. Fiji: an open-source platform for biological-image analysis. *Nat. Methods* 9, 676–682. doi:10.1038/nmeth.2019
- Schofield, B.R., Motts, S.D., 2009. Projections from auditory cortex to cholinergic cells in the midbrain tegmentum of guinea pigs. *Brain Res. Bull.* 80, 163–170. doi:10.1016/j.brainresbull.2009.06.015
- Schultz, W., 2016a. Reward functions of the basal ganglia. *J. Neural Transm.* 123, 679–693. doi:10.1007/s00702-016-1510-0
- Schultz, W., 2016b. Dopamine reward prediction error coding. *Dialogues Clin. Neurosci.* 18, 23–32.
- Schultz, W., 2007. Multiple Dopamine Functions at Different Time Courses. *Annu. Rev. Neurosci.* 30, 259–288. doi:10.1146/annurev.neuro.28.061604.135722
- Schultz, W., 2002. Getting Formal with Dopamine and Reward. *Neuron* 36, 241–263. doi:10.1016/S0896-6273(02)00967-4
- Schultz, W., 1998. Predictive Reward Signal of Dopamine Neurons. *J. Neurophysiol.* 80, 1–27.

- Schultz, W., Apicella, P., Ljungberg, T., 1993. Responses of monkey dopamine neurons to reward and conditioned stimuli during successive steps of learning a delayed response task. *J. Neurosci.* 13, 900–913.
- Schultz, W., Dayan, P., Montague, P.R., 1997. A Neural Substrate of Prediction and Reward. *Science* 275, 1593–1599. doi:10.1126/science.275.5306.1593
- Seabold, J.S., Perktold, J., 2010. Statsmodels: Econometric and Statistical Modeling with Python, in: Proceedings of the 9th Python in Science Conference.
- Segev, D., Korngreen, A., 2007. Kinetics of two voltage-gated K⁺ conductances in substantia nigra dopaminergic neurons. *Brain Res.* 1173, 27–35. doi:10.1016/j.brainres.2007.08.006
- Semba, K., Fibiger, H.C., 1992. Afferent connections of the laterodorsal and the pedunclopontine tegmental nuclei in the rat: A retro-and antero-grade transport and immunohistochemical study. *J. Comp. Neurol.* 323, 387–410.
- Senogles, S.E., 1994. The D2 dopamine receptor isoforms signal through distinct Gi alpha proteins to inhibit adenylyl cyclase. A study with site-directed mutant Gi alpha proteins. *J. Biol. Chem.* 269, 23120–23127.
- Sesack, S.R., Deutch, A.Y., Roth, R.H., Bunney, B.S., 1989. Topographical organization of the efferent projections of the medial prefrontal cortex in the rat: an anterograde tract-tracing study with Phaseolus vulgaris leucoagglutinin. *J. Comp. Neurol.* 290, 213–242. doi:10.1002/cne.902900205
- Shen, W., Flajolet, M., Greengard, P., Surmeier, D.J., 2008. Dichotomous Dopaminergic Control of Striatal Synaptic Plasticity. *Science* 321, 848–851. doi:10.1126/science.1160575
- Shepard, P.D., Bunney, B.S., 1991. Repetitive firing properties of putative dopamine-containing neurons in vitro: regulation by an apamin-sensitive Ca²⁺-activated K⁺ conductance. *Exp. Brain Res.* 86, 141–150.
- Shepard, P.D., Bunney, B.S., 1988. Effects of apamin on the discharge properties of putative dopamine-containing neurons in vitro. *Brain Res.* 463, 380–384.
- Shik, M.L., Severin, F.V., Orlovskii, G.N., 1966. [Control of walking and running by means of electric stimulation of the midbrain]. *Biofizika* 11, 659–666.
- Shouse, M.N., Siegel, J.M., 1992. Pontine regulation of REM sleep components in cats: integrity of the pedunclopontine tegmentum (PPT) is important for phasic events but unnecessary for atonia during REM sleep. *Brain Res.* 571, 50–63. doi:10.1016/0006-8993(92)90508-7

- Skinner, R.D., Kinjo, N., Henderson, V., Garcia-Rill, E., 1990a. Locomotor projections from the pedunculopontine nucleus to the spinal cord. *Neuroreport* 1, 183–186.
- Skinner, R.D., Kinjo, N., Ishikawa, Y., Biedermann, J.A., Garcia-Rill, E., 1990b. Locomotor projections from the pedunculopontine nucleus to the medioventral medulla. *Neuroreport* 1, 207–210.
- Smiley, J.F., Williams, S.M., Szigeti, K., Goldman-Rakic, P.S., 1992. Light and electron microscopic characterization of dopamine-immunoreactive axons in human cerebral cortex. *J. Comp. Neurol.* 321, 325–335. doi:10.1002/cne.903210302
- Smith, I.D., Grace, A.A., 1992. Role of the subthalamic nucleus in the regulation of nigral dopamine neuron activity. *Synapse* 12, 287–303.
- Smith, Y., Bevan, M.D., Shink, E., Bolam, J.P., 1998. Microcircuitry of the direct and indirect pathways of the basal ganglia. *Neuroscience* 86, 353–387.
- Smith, Y., Charara, A., Parent, A., 1996. Synaptic innervation of midbrain dopaminergic neurons by glutamate-enriched terminals in the squirrel monkey. *J. Comp. Neurol.* 364, 231–253. doi:10.1002/(SICI)1096-9861(19960108)364:2<231::AID-CNE4>3.0.CO;2-6
- Smith, Y., Hazrati, L.-N., Parent, A., 1990. Efferent projections of the subthalamic nucleus in the squirrel monkey as studied by the PHA-L anterograde tracing method. *J. Comp. Neurol.* 294, 306–323.
- Smith, Y., Paré, D., Deschênes, M., Parent, A., Steriade, M., 1988. Cholinergic and non-cholinergic projections from the upper brainstem core to the visual thalamus in the cat. *Exp. Brain Res.* 70, 166–180.
- Snyder, G.L., Allen, P.B., Fienberg, A.A., Valle, C.G., Haganir, R.L., Nairn, A.C., Greengard, P., 2000. Regulation of Phosphorylation of the GluR1 AMPA Receptor in the Neostriatum by Dopamine and Psychostimulants *In Vivo*. *J. Neurosci.* 20, 4480–4488.
- Spann, B.M., Grofova, I., 1991. Nigropedunculopontine projection in the rat: An Anterograde tracing study with phaseolus vulgaris-leucoagglutinin (PHA-L). *J. Comp. Neurol.* 311, 375–388. doi:10.1002/cne.903110308
- Spann, B.M., Grofova, I., 1989. Origin of ascending and spinal pathways from the nucleus tegmenti pedunculopontinus in the rat. *J. Comp. Neurol.* 283, 13–27. doi:10.1002/cne.902830103

- Steinfels, G.F., Heym, J., Strecker, R.E., Jacobs, B.L., 1983. Behavioral correlates of dopaminergic unit activity in freely moving cats. *Brain Res.* 258, 217–228. doi:10.1016/0006-8993(83)91145-9
- Steininger, T.L., Rye, D.B., Wainer, B.H., 1992. Afferent projections to the cholinergic pedunclopontine tegmental nucleus and adjacent midbrain extrapyramidal area in the albino rat. I. Retrograde tracing studies. *J. Comp. Neurol.* 321, 515–543. doi:10.1002/cne.903210403
- Steininger, T.L., Wainer, B.H., Blakely, R.D., Rye, D.B., 1997. Serotonergic dorsal raphe nucleus projections to the cholinergic and noncholinergic neurons of the pedunclopontine tegmental region: a light and electron microscopic anterograde tracing and immunohistochemical study. *J. Comp. Neurol.* 382, 302–322.
- Steriade, M., 1996. Arousal--Revisiting the Reticular Activating System. *Science* 272, 225–225. doi:10.1126/science.272.5259.225
- Steriade, M., 1993. Cholinergic blockage of network- and intrinsically generated slow oscillations promotes waking and REM sleep activity patterns in thalamic and cortical neurons. *Prog. Brain Res.* 98, 345–355.
- Steriade, M., Datta, S., Pare, D., Oakson, G., Dossi, R.C., 1990a. Neuronal activities in brainstem cholinergic nuclei related to tonic activation processes in thalamocortical systems. *J. Neurosci.* 10, 2541–2559.
- Steriade, M., Dossi, R.C., Paré, D., Oakson, G., 1991. Fast oscillations (20-40 Hz) in thalamocortical systems and their potentiation by mesopontine cholinergic nuclei in the cat. *Proc. Natl. Acad. Sci.* 88, 4396–4400. doi:10.1073/pnas.88.10.4396
- Steriade, M., Pare, D., Datta, S., Oakson, G., Dossi, R.C., 1990b. Different cellular types in mesopontine cholinergic nuclei related to ponto-geniculo-occipital waves. *J. Neurosci.* 10, 2560–2579.
- Steriade, M., Paré, D., Parent, A., Smith, Y., 1988. Projections of cholinergic and non-cholinergic neurons of the brainstem core to relay and associational thalamic nuclei in the cat and macaque monkey. *Neuroscience* 25, 47–67.
- Suárez, F., Zhao, Q., Monaghan, D.T., Jane, D.E., Jones, S., Gibb, A.J., 2010. Functional heterogeneity of NMDA receptors in rat substantia nigra pars compacta and reticulata neurones: Substantia nigra NMDA receptor heterogeneity. *Eur. J. Neurosci.* 32, 359–367. doi:10.1111/j.1460-9568.2010.07298.x
- Sugimoto, T., Hattori, T., 1984. Organization and efferent projections of nucleus tegmenti pedunclopontinus pars compacta with special reference to its cholinergic aspects. *Neuroscience* 11, 931–946. doi:10.1016/0306-4522(84)90204-5

- Sun, X., Zhao, Y., Wolf, M.E., 2005. Dopamine Receptor Stimulation Modulates AMPA Receptor Synaptic Insertion in Prefrontal Cortex Neurons. *J. Neurosci.* 25, 7342–7351. doi:10.1523/JNEUROSCI.4603-04.2005
- Surmeier, D.J., Bargas, J., Hemmings, H.C., Nairn, A.C., Greengard, P., 1995. Modulation of calcium currents by a D1 dopaminergic protein kinase/phosphatase cascade in rat neostriatal neurons. *Neuron* 14, 385–397. doi:10.1016/0896-6273(95)90294-5
- Surmeier, D.J., Ding, J., Day, M., Wang, Z., Shen, W., 2007. D1 and D2 dopamine-receptor modulation of striatal glutamatergic signaling in striatal medium spiny neurons. *Trends Neurosci.* 30, 228–235. doi:10.1016/j.tins.2007.03.008
- Surmeier, D.J., Kitai, S.T., 1993. D1 and D2 dopamine receptor modulation of sodium and potassium currents in rat neostriatal neurons. *Prog. Brain Res.* 99, 309–324.
- Surmeier, D.J., Song, W.-J., Yan, Z., 1996. Coordinated expression of dopamine receptors in neostriatal medium spiny neurons. *J. Neurosci.* 16, 6579–6591.
- Syed, A., Baker, P.M., Ragozzino, M.E., 2016. Pedunculopontine tegmental nucleus lesions impair probabilistic reversal learning by reducing sensitivity to positive reward feedback. *Neurobiol. Learn. Mem.* 131, 1–8. doi:10.1016/j.nlm.2016.03.010
- Takakusaki, K., Chiba, R., Nozu, T., Okumura, T., 2016. Brainstem control of locomotion and muscle tone with special reference to the role of the mesopontine tegmentum and medullary reticulospinal systems. *J. Neural Transm.* 123, 695–729. doi:10.1007/s00702-015-1475-4
- Takakusaki, K., Shiroyama, T., Kitai, S.T., 1997. Two types of cholinergic neurons in the rat tegmental pedunculopontine nucleus: electrophysiological and morphological characterization. *Neuroscience* 79, 1089–1109.
- Takakusaki, K., Shiroyama, T., Yamamoto, T., Kitai, S.T., 1996. Cholinergic and noncholinergic tegmental pedunculopontine projection neurons in rats revealed by intracellular labeling. *J. Comp. Neurol.* 371, 345–361. doi:10.1002/(SICI)1096-9861(19960729)371:3<345::AID-CNE1>3.0.CO;2-2
- Tepper, J.M., Martin, L.P., Anderson, D.R., 1995. GABAA receptor-mediated inhibition of rat substantia nigra dopaminergic neurons by pars reticulata projection neurons. *J. Neurosci.* 15, 3092–3103.
- Thompson, J.A., Felsen, G., 2013. Activity in mouse pedunculopontine tegmental nucleus reflects action and outcome in a decision-making task. *J. Neurophysiol.* 110, 2817–2829. doi:10.1152/jn.00464.2013

- Tobler, P.N., Dickinson, A., Schultz, W., 2003. Coding of Predicted Reward Omission by Dopamine Neurons in a Conditioned Inhibition Paradigm. *J. Neurosci.* 23, 10402–10410.
- Tsai, H.-C., Zhang, F., Adamantidis, A., Stuber, G.D., Bonci, A., de Lecea, L., Deisseroth, K., 2009. Phasic Firing in Dopaminergic Neurons Is Sufficient for Behavioral Conditioning. *Science* 324, 1080–1084. doi:10.1126/science.1168878
- Tulloch, I.F., Arbuthnott, G.W., Wright, A.K., 1978. Topographical organization of the striatonigral pathway revealed by anterograde and retrograde neuroanatomical tracing techniques. *J. Anat.* 127, 425–441.
- Usunoff, K., Romansky, K., Malinov, G., Ivanov, D., Blagov, Z., Galabov, G., 1982. Electron microscopic evidence for the existence of a corticonigral tract in the cat. *J. Hirnforsch.* 23, 23–29.
- Vallone, D., Picetti, R., Borrelli, E., 2000. Structure and function of dopamine receptors. *Neurosci. Biobehav. Rev.* 24, 125–132. doi:10.1016/S0149-7634(99)00063-9
- Van Der Kooy, D., Hattori, T., 1980. Single subthalamic nucleus neurons project to both the globus pallidus and substantia nigra in rat. *J. Comp. Neurol.* 192, 751–768. doi:10.1002/cne.901920409
- Van Dort, C.J., Zachs, D.P., Kenny, J.D., Zheng, S., Goldblum, R.R., Gelwan, N.A., Ramos, D.M., Nolan, M.A., Wang, K., Weng, F.-J., Lin, Y., Wilson, M.A., Brown, E.N., 2015. Optogenetic activation of cholinergic neurons in the PPT or LDT induces REM sleep. *Proc. Natl. Acad. Sci.* 112, 584–589. doi:10.1073/pnas.1423136112
- Vertes, R.P., 1991. A PHA-L analysis of ascending projections of the dorsal raphe nucleus in the rat. *J. Comp. Neurol.* 313, 643–668. doi:10.1002/cne.903130409
- Vilchis, C., Bargas, J., Ayala, G.X., Galván, E., Galarraga, E., 1999. Ca²⁺ channels that activate Ca²⁺-dependent K⁺ currents in neostriatal neurons. *Neuroscience* 95, 745–752. doi:10.1016/S0306-4522(99)00493-5
- Wang, H.-L., Morales, M., 2009. Pedunclopontine and laterodorsal tegmental nuclei contain distinct populations of cholinergic, glutamatergic and GABAergic neurons in the rat. *Eur. J. Neurosci.* 29, 340–358. doi:10.1111/j.1460-9568.2008.06576.x
- Wang, Z., Kai, L., Day, M., Ronesi, J., Yin, H.H., Ding, J., Tkatch, T., Lovinger, D.M., Surmeier, D.J., 2006. Dopaminergic Control of Corticostriatal Long-Term Synaptic Depression in Medium Spiny Neurons Is Mediated by Cholinergic Interneurons. *Neuron* 50, 443–452. doi:10.1016/j.neuron.2006.04.010

- Washburn, M.S., Numberger, M., Zhang, S., Dingledine, R., 1997. Differential Dependence on GluR2 Expression of Three Characteristic Features of AMPA Receptors. *J. Neurosci.* 17, 9393–9406.
- Watabe-Uchida, M., Zhu, L., Ogawa, S.K., Vamanrao, A., Uchida, N., 2012. Whole-Brain Mapping of Direct Inputs to Midbrain Dopamine Neurons. *Neuron* 74, 858–873. doi:10.1016/j.neuron.2012.03.017
- Weinberger, M., Hamani, C., Hutchison, W.D., Moro, E., Lozano, A.M., Dostrovsky, J.O., 2008. Pedunclopontine nucleus microelectrode recordings in movement disorder patients. *Exp. Brain Res.* 188, 165–174. doi:10.1007/s00221-008-1349-1
- White, F.J., 1996. Synaptic Regulation of Mesocorticolimbic Dopamine Neurons. *Annu. Rev. Neurosci.* 19, 405–436. doi:10.1146/annurev.ne.19.030196.002201
- Wickens, J.R., Arbuthnott, G.W., 2005. Chapter IV Structural and functional interactions in the striatum at the receptor level. *Handb. Chem. Neuroanat., Dopamine* 21, 199–236. doi:10.1016/S0924-8196(05)80008-9
- Wickersham, I.R., Sullivan, H.A., Seung, H.S., 2013. Axonal and subcellular labelling using modified rabies viral vectors. *Nat. Commun.* 4. doi:10.1038/ncomms3332
- Wightman, R.M., Robinson, D.L., 2002. Transient changes in mesolimbic dopamine and their association with “reward.” *J. Neurochem.* 82, 721–735. doi:10.1046/j.1471-4159.2002.01005.x
- Williams, J.A., Comisarow, J., Day, J., Fibiger, H.C., Reiner, P.B., 1994. State-dependent release of acetylcholine in rat thalamus measured by in vivo microdialysis. *J. Neurosci.* 14, 5236–5242.
- Williams, K., 1993. Ifenprodil discriminates subtypes of the N-methyl-D-aspartate receptor: selectivity and mechanisms at recombinant heteromeric receptors. *Mol. Pharmacol.* 44, 851–859.
- Williams, M.N., Faull, R.L., 1985. The striatonigral projection and nigrotectal neurons in the rat. A correlated light and electron microscopic study demonstrating a monosynaptic striatal input to identified nigrotectal neurons using a combined degeneration and horseradish peroxidase procedure. *Neuroscience* 14, 991–1010.
- Wilson, C.J., Callaway, J.C., 2000. Coupled oscillator model of the dopaminergic neuron of the substantia nigra. *J. Neurophysiol.* 83, 3084–3100.
- Wilson, D.I.G., MacLaren, D.A.A., Winn, P., 2009. Bar pressing for food: differential consequences of lesions to the anterior versus posterior pedunclopontine. *Eur. J. Neurosci.* 30, 504–513. doi:10.1111/j.1460-9568.2009.06836.x

- Wolfart, J., Neuhoff, H., Franz, O., Roeper, J., 2001. Differential expression of the small-conductance, calcium-activated potassium channel SK3 is critical for pacemaker control in dopaminergic midbrain neurons. *J. Neurosci.* 21, 3443–3456.
- Woolf, N.J., Butcher, L.L., 1986. Cholinergic systems in the rat brain: III. Projections from the pontomesencephalic tegmentum to the thalamus, tectum, basal ganglia, and basal forebrain. *Brain Res. Bull.* 16, 603–637.
- Wright, A.L., Vissel, B., 2012. The essential role of AMPA receptor GluR2 subunit RNA editing in the normal and diseased brain. *Front. Mol. Neurosci.* 5. doi:10.3389/fnmol.2012.00034
- Wyllie, D.J.A., Livesey, M.R., Hardingham, G.E., 2013. Influence of GluN2 subunit identity on NMDA receptor function. *Neuropharmacology, Glutamate Receptor-Dependent Synaptic Plasticity* 74, 4–17. doi:10.1016/j.neuropharm.2013.01.016
- Xiao, C., Cho, J.R., Zhou, C., Treweek, J.B., Chan, K., McKinney, S.L., Yang, B., Gradinaru, V., 2016. Cholinergic Mesopontine Signals Govern Locomotion and Reward through Dissociable Midbrain Pathways. *Neuron* 90, 333–347. doi:10.1016/j.neuron.2016.03.028
- Yamaguchi, T., Wang, H.-L., Li, X., Ng, T.H., Morales, M., 2011. Mesocorticolimbic Glutamatergic Pathway. *J. Neurosci.* 31, 8476–8490. doi:10.1523/JNEUROSCI.1598-11.2011
- Yamaguchi, T., Wang, H.-L., Morales, M., 2013. Glutamate neurons in the substantia nigra compacta and retrorubral field. *Eur. J. Neurosci.* 38, 3602–3610. doi:10.1111/ejn.12359
- Yetnikoff, L., Lavezzi, H.N., Reichard, R.A., Zahm, D.S., 2014. An update on the connections of the ventral mesencephalic dopaminergic complex. *Neuroscience, The Ventral Tegmentum and Dopamine: A New Wave of Diversity* 282, 23–48. doi:10.1016/j.neuroscience.2014.04.010
- Yin, H.H., Mulcare, S.P., Hilário, M.R.F., Clouse, E., Holloway, T., Davis, M.I., Hansson, A.C., Lovinger, D.M., Costa, R.M., 2009. Dynamic reorganization of striatal circuits during the acquisition and consolidation of a skill. *Nat. Neurosci.* 12, 333–341. doi:10.1038/nn.2261
- Yoo, J.H., Zell, V., Wu, J., Punta, C., Ramajayam, N., Shen, X., Faget, L., Lilascharoen, V., Lim, B.K., Hnasko, T.S., 2016. Activation of pedunclopontine glutamate neurons is reinforcing. *J. Neurosci.* 3082–16. doi:10.1523/JNEUROSCI.3082-16.2016
- Zahm, D.S., Cheng, A.Y., Lee, T.J., Ghobadi, C.W., Schwartz, Z.M., Geisler, S., Parsely, K.P., Gruber, C., Veh, R.W., 2011. Inputs to the midbrain dopaminergic complex in the rat,

with emphasis on extended amygdala-recipient sectors. *J. Comp. Neurol.* 519, 3159–3188. doi:10.1002/cne.22670

Zariwala, H.A., Borghuis, B.G., Hoogland, T.M., Madisen, L., Tian, L., De Zeeuw, C.I., Zeng, H., Looger, L.L., Svoboda, K., Chen, T.-W., 2012. A Cre-Dependent GCaMP3 Reporter Mouse for Neuronal Imaging In Vivo. *J. Neurosci.* 32, 3131–3141. doi:10.1523/JNEUROSCI.4469-11.2012

Ziv, Y., Burns, L.D., Cocker, E.D., Hamel, E.O., Ghosh, K.K., Kitch, L.J., Gamal, A.E., Schnitzer, M.J., 2013. Long-term dynamics of CA1 hippocampal place codes. *Nat. Neurosci.* 16, 264–266. doi:10.1038/nn.3329

Zweifel, L.S., Parker, J.G., Lobb, C.J., Rainwater, A., Wall, V.Z., Fadok, J.P., Darvas, M., Kim, M.J., Mizumori, S.J., Paladini, C.A., 2009. Disruption of NMDAR-dependent burst firing by dopamine neurons provides selective assessment of phasic dopamine-dependent behavior. *Proc. Natl. Acad. Sci.* 106, 7281–7288.

Appendix A: Additional Projects

Transient Activation of GABA_B Receptors Suppresses SK Channel Currents in Substantia Nigra Pars Compacta Dopaminergic Neurons

Authors: Estep, C.M., Galtieri, D.J., Zampese, E., Goldberg, J.A., Brichta, L., Greengard, P., Surmeier

Status: Published (2016), PLOS ONE 11, e0169044. doi:10.1371/journal.pone.0169044

Summary:

This project examined the effect of transient GABA_B receptor activation on pacemaking activity in SNc DA neurons. In contrast to prolonged GABA_B activation, which produces a well described suppression of firing through K_{ir}3 channel activity, transient stimulation of GABA_B receptors, achieved through photolysis of RuBi-GABA, increased spike rate and irregularity. This was found to be mediated by suppression of SK channels, likely through inhibition of adenylate-cyclase and the subsequent reduction in PKA activity.

Contribution:

My primary contribution to this work was validation of the experimental findings, particularly of the observation that transient GABA_B receptor activation increased spike rate and irregularity. Perforated-patch recordings were performed before and after photolysis of RuBi-GABA, and the subsequent changes in firing pattern were analyzed. I also performed pilot studies with focal 1P excitation of RuBi-GABA in different portions of the SNc dendritic tree to assess any potential differences in regional expression of GABA_B receptors. Additionally, the software packages discussed in Appendix B were critical for the

data analysis performed in in this paper. I also contributed to the writing and revising of the manuscript.

Calcium Entry and α -Synuclein Inclusions Elevate Dendritic Mitochondrial Oxidant Stress in Dopaminergic Neurons

Authors: Dryanovski, D.I., Guzman, J.N., Xie, Z., Galtieri, D.J., Volpicelli-Daley, L.A., Lee, V.M.-Y., Miller, R.J., Schumacker, P.T., Surmeier, D.J.

Status: Published (2013), The Journal of Neuroscience 33, 10154–10164.
doi:10.1523/JNEUROSCI.5311-12.2013

Summary:

This study examined the interaction between mitochondrial oxidant stress, calcium entry, and Lewy-body aggregates in cultured SNc DA neurons. Prior work from our lab had shown that calcium entry through L-type VGCCs significantly contributed to oxidant stress in SNc DA neurons (Guzman et al., 2010). This study extended those findings by showing that dendritic compartments showed higher mitochondrial stress than somatic compartments, with mitochondrial stress in dendritic compartments increasing with distance from the soma. Furthermore, it was shown that α -synuclein Lewy-body aggregates increased mitochondrial stress in these same compartments by elevating cytosolic reactive-oxidant species formation.

Contribution:

I contributed both 2PLSM calcium imaging data and 2P mitochondrial roGFP imaging data to this study. I performed 2PLSM imaging to validate the presence of calcium oscillations in the cultured DA neurons and to compare them to those observed in SNc DA neurons recorded in *ev vivo* brain slices. I also collected the 2P roGFP data from different

compartments (somatic vs. dendritic) in SNc and VTA DA neurons in *ev vivo* brain slices, showing elevated stress in SNc dendrites in comparison to the somatic region.

Mitochondrial oxidant stress in locus coeruleus is regulated by activity and nitric oxide synthase

Authors: Sanchez-Padilla, J., Guzman, J.N., Ilijic, E., Kondapalli, J., Galtieri, D.J., Yang, B., Schieber, S., Oertel, W., Wokosin, D., Schumacker, P.T., Surmeier, D.J.

Status: Published (2014), Nature Neuroscience 17, 832–840. doi:10.1038/nn.3717

Summary:

This study assessed mechanisms of vulnerability in locus coeruleus (LC) neurons. Like the SNc, the LC is known to degenerate in PD. This study examined the basic physiology of these cells and found that, like the SNc, they possess L-type VGCCs that significantly contribute to mitochondrial oxidant stress. It was also shown that nitric oxide production through a mitochondrial form of nitric oxide synthase (NOS) contributed to mitochondrial stress. This NOS was further shown to be stimulated by calcium entry through L-type channels.

Contribution:

I contributed data measuring the effect of the NOS inhibitor L-N^G-nitroarginine methyl ester (L-NAME) on mitochondrial stress in SNc DA neurons, which was used as a comparison to the effect of L-NAME application on mitochondrial stress in LC neurons. I also contributed to the 2PLSM calcium imaging data used to calculate intrinsic calcium buffering capacity in LC neurons described in this study.

Chronic isradipine treatment lowers calcium-dependent mitochondrial stress and damage in dopaminergic neurons at risk in Parkinson's disease

Authors: Guzman, J., Ilijic, E., Yang, B., Sanchez-Padilla, J., Wokosin, D., Galtieri, D.J., Kondapalli, J., Schumacker, P.T., Surmeier, D.J.

Status: Being revised, The Journal of Clinical Investigation

Summary:

This study examined the effect of chronic treatment of the L-type calcium channel inhibitor, isradipine, on calcium transients and mitochondrial stress in SNc DA neurons. Previous work has shown that inhibition of L-type channels abolishes dendritic calcium oscillations and reduces mitochondrial oxidant stress in SNc neurons (Guzman et al., 2009, 2010). The present study extends this finding by chronically administering isradipine via osmotic pumps for 7-10 days. Fura-2 2PLSM calcium imaging was used to quantify the amplitude of the observed calcium oscillations in units of nanomolars of calcium. It was observed that sub-micromolar levels of isradipine reduced the calcium oscillations, particularly the sub-threshold component. Mitochondrial oxidant stress as well as mitochondrial turnover were also shown to be lowered by chronic isradipine treatment.

Contribution:

I primarily contributed validation data showing that chronic isradipine treatment did not alter the intrinsic properties of SNc DA neurons. Animals were implanted with osmotic pumps to continuously deliver either saline or isradipine for 7-10 days. Perforated patch recordings were then performed to assess changes in basal firing rate, current-frequency relationship, and I_H . No significant effects on these intrinsic properties were found as a

result of the isradipine treatment. I also contributed to the validation of the Fura-2 imaging technique used throughout this study.

Appendix B: Development of Analysis Tools

In addition to the experimental work completed over the course of my dissertation, a significant portion of my time in the Surmeier lab has been devoted to developing analysis tools for the lab. The overarching goals driving this have been twofold: addressing both points of inefficiency as well as outright gaps in the data workflows of lab members and increasing transparency in the process of data being transformed from a raw form to that of a finished figure. Over time, in collaboration with Drs. Chad Estep and David Wokosin, a library of both general and task-specific tools has been generated. These were all created in Python, using a variety of libraries within the PyData ecosystem and have been made publicly available through the Surmeier lab Github repository (github.com/surmeierlab). The major projects are outlined below, along with a description of the needs they were meant to fill.

Why Python?

A conscious decision was made at the start of this process to develop these tools in Python rather than other available options, particularly MATLAB. While both Python and MATLAB offer similar capabilities for mathematical operations, including data structures allowing for vectorized operations (inherent to MATLAB; through the numpy package in Python), Python is a far more mature language from a software development standpoint. This becomes a non-trivial point when developing tools that extend beyond simple analysis scripts. For example, MATLAB limits any individual function file to only one external

callable function, resulting in many small files, each corresponding to a single function, that would more ideally be organized into a single unit. This becomes incredibly cumbersome when a project grows beyond a few files, especially when multiple users are involved. The Python package system is far more streamlined, allowing for the logical organization of functions into modules that are easy to distribute amongst users. Individual functions, whole modules, or whole packages can then be imported as needed. The fact that all MATLAB functions share the same global namespace further complicates large projects.

Python, being first and foremost a general purpose programming language, also has a broad array of tools beyond numerical operations. For example, Python offers far more capabilities for working with non-numerical data types (such as strings), which was an important consideration for parsing the metadata files generated by our 2PLSM systems. It also provides access to a number of graphical interface and data visualization libraries, both of which proved incredibly useful for the tools developed here. Python itself, as well as the various libraries written in Python that we ultimately ended up using in building these packages, are all also open source, meaning that the underlying code is freely available for examination. This is not true for MATLAB, where much of the code, including many of the built-in algorithms, are proprietary. Ultimately all of these factors contributed to the decision to develop these tools in Python.

Neurphys

Neurphys is a general purpose analysis package for working with data generated either with pClamp (Molecular Devices) or Prairie View 5.0+ (Bruker, formerly Prairie Technologies) acquisition software. It implements separate import modules, *read_abf* and

read_pv, for *.abf files (pClamp) and Prairie View data folders. The former utilizes the neo Python package (<https://pythonhosted.org/neo/io.html>) for interfacing with *.abf files. The latter parses the metadata contained within the configuration XML files in the specified folders to identify the data files within the folder that need to be read. Ultimately both import functions collapse the data in to a standard format – a multidimensional pandas DataFrame, where repetitions (sweeps) are the additional dimension. For example, a data file containing ten sweeps, with data columns from voltage, current, and stimulus channels will produce a DataFrame with columns time, primary (voltage), secondary (current), and channel_1 (unless given a specified name in the acquisition software), and indexes of sweep001 through sweep010 as an additional index level. The logic behind this is that once data from different sources (i.e. pClamp vs. Prairie View) are standardized, a single set of analysis functions can be written that can be used regardless of the data source.

Data generated on the 2PLSM systems have two added layers of complexity that have to be dealt with during import step. One is that there are potentially multiple transforms to the data that need to be done to organize the data and convert it to meaningful values. Unlike pClamp, Prairie View saves each individual sweep as a separate *.csv file. Each of these has to be read in to generate the final DataFrame. Furthermore, the values stored in these files represent raw voltages read from the National Instruments 6052 card. These must be converted to

o the appropriate voltage or current values based on information in the associated metadata files. Second, the Prairie View systems generate both neurophysiological as well as 2PLSM imaging data. In particular, line scan data generates a second set of *.csv files

that also need to be read in to their own DataFrame. The *read_pv* module handles this by returning a dictionary with corresponding “voltage recording” and “linescan” keys, which can be used to access the respective DataFrames. The dictionary also contains a “file attributes” key that contains all of the read-in metadata for each respective file, should it need to be referenced at some point during analysis.

As mentioned, the benefit of having a standardized data structure is that a single set of analysis functions can then be written for data generated by pClamp or Prairie View. In addition to the data import modules, Neurphys contains several analysis modules that cover many of the typical experiments performed by our lab. They are, briefly:

utilities: contains a number of helper functions that cover baselining traces, finding a peak, calculating the decay of a transient, and smoothing (simple running average)

synaptics: contains functions to analyze synaptic currents (amplitude, decay) and PPR data

membrane: calculates membrane properties (tau, membrane capacitance, membrane and access resistance), based on fits performed on the transients from a square voltage step

pacemaking: contains functions for detecting a series of peaks, baselining cell-attached / loose-seal current-clamp recordings, calculating either instantaneous frequency or ISI, and generating a phase plot.

oscillation: contains functions for evaluating oscillatory activity (power spectrum, kernel-density estimates)

calcium: functions for converting 2PLSM calcium imaging data to calcium concentration, based on methods developed in the Surmeier lab

nuplot: contains series of functions for plotting raw neurophysiological data and summary data (e.g. boxplots) in the styles standard to the Surmeier lab.

PVDataTools

In 2013 Prairie View 5.0 was released. This greatly expanded the Prairie View imaging suite to include both modules for photostimulation as well as for recording neurophysiological data. Prior to this, Prairie View only handled the imaging acquisition portion of our 2PLSM systems. The neurophysiological and photostimulation capabilities were provided through integration of the Prairie View software with WinFluor (John Dempster, Strathclyde University, Scotland). WinFluor provided the necessary means by which to control the MultiClamp amplifier (e.g. seal test, voltage and current protocols) and synchronize the acquisition of electrophysiological data with imaging data. In addition to the acquisition tools WinFluor provided, it also came with a series of basic data visualization and analysis tools that were crucial to performing experiments on the 2PLSM systems. With the transition to 5.0, however, these tools were lost, as WinFluor does not support the data generated by the new modules. While Prairie View 5.0 offered new acquisition tools, it did not provide any associated analysis functionality. Nor were the visualization tools it provided adequate, as they were both tied directly to the 2PLSM systems and, while in use, occluded data acquisition (i.e. while viewing collected data, new data could not be acquired in parallel).

PVDataTools was therefore developed to meet the experimental needs of the 2PLSM users. In particular, its main purpose is to provide a way to easily import and visualize newly acquired data (Figure A1). The interface, built with the Python bindings for the Qt

application framework, organizes folders based on recording channels, with the ability to plot individual sweeps or a series of sweeps. Plotting is accomplished through the PyQtGraph library (<http://www.pyqtgraph.org/>). Both neurophysiological and 2PLSM imaging data is supported (Figure A1). The *Data Viewer* module provides some simple tools, such as the ability to baseline, average, and smooth traces as well as calculate values over a region. The interface is designed to be similar to that of pClamp, with markers indexing in to plotted traces and providing a means to select regions to analyze (Figure A1).

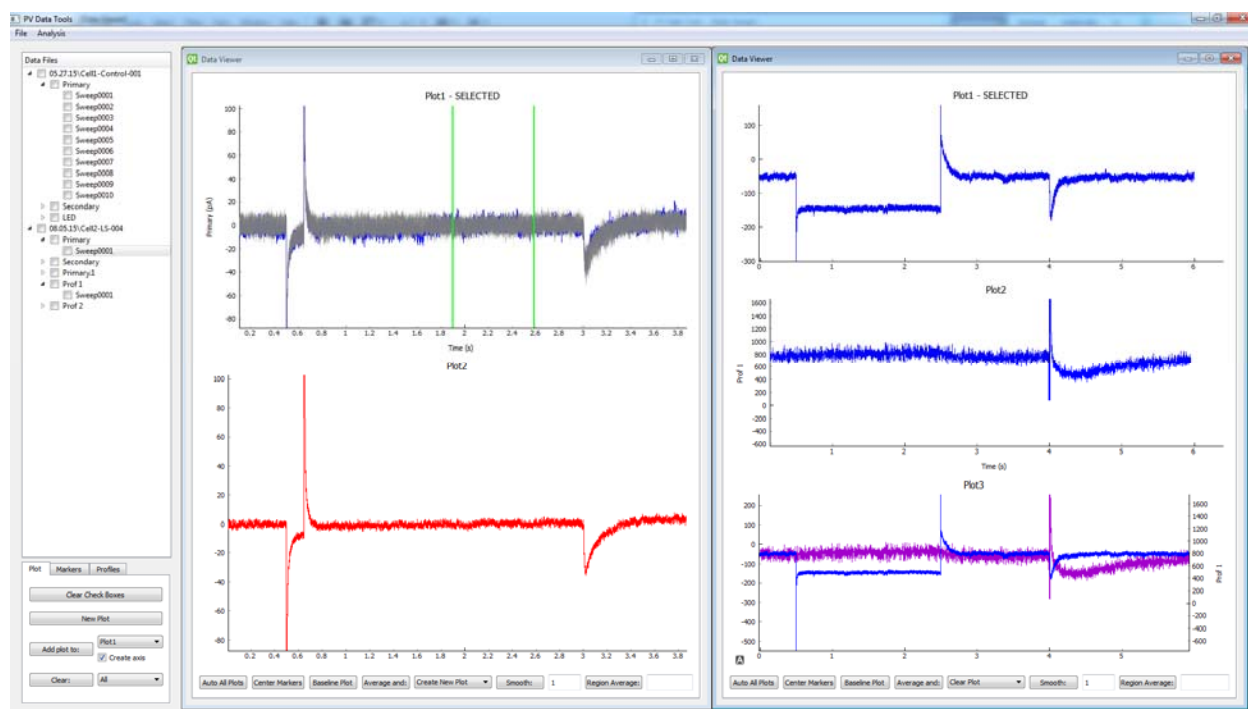
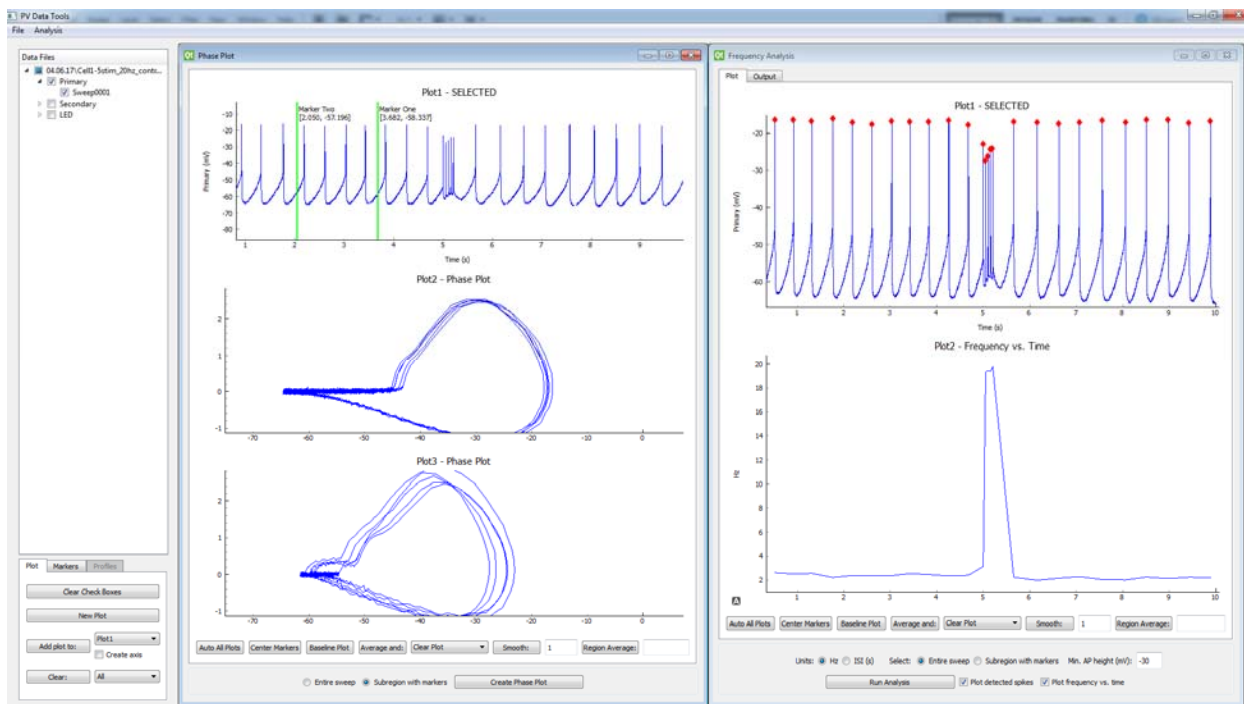


Figure A1. Data visualization with PVDDataTools

Imported data is organized in to a tree structure. Multiple *Data Viewer* windows can be opened, with the interface changing to match the currently selected window. (Left) *Data Viewer* shows sweeps of voltage-clamp recordings of an evoked current that have been baselined using the region between the green markers. The red trace on the bottom is the average of the traces above. (Right) *Data Viewer* shows current and 2PLSM calcium-imaging data plotted separately and then, on the bottom, plotted on the same plot.

Traces with dissimilar axes, such as current and imaging data, can also be visualized on the same plot by creating an addition axis.

Secondary to its main purpose as a visualization tool, PVDDataTools also provides a number of analysis modules covering many of the functions provided by Neurphys. In particular, analysis modules exist for analyzing membrane properties, evoked synaptic events (both single events and trains, including PPR), and pacemaking (phase plot and frequency analysis; Figure A2).



Two different analysis modules are provided that cover pacemaking activity. (Left) Phase plots were generated from the selected region between the two markers (top phase plot) and from the region of stimulated spikes (bottom phase plot). (Right) Detected spikes, based on a minimum threshold, and plotted and marked with a red marker (top plot). The instantaneous firing rate is shown in the lower plot. The Output tab (not shown) provides the actual column of analyzed values, along with the calculated average firing rate.

PyMinis

One of the standard experiments performed by the lab is the collection of either spontaneous miniature synaptic currents (minis) or asynchronously evoked (through strontium replacement of calcium in the aCSF) minis. While software packages, such as Mini Analysis (Synaptosoft, Fort Lee, NJ), for the identification and analysis of these events exists, few offer a simple, intuitive interface for both automatically and manually identifying minis. Furthermore, a desired feature that was lacking was the ability to fit and subtract the large, synchronous release event present in the evoked-minis experiment (e.g. Figure A3, left). PyMinis was therefore created with these needs in mind. It supports data collected by both pClamp and Prairie View. The user can optionally perform a bi-exponential fit on a particular region of the recorded data and have the fit subtracted prior

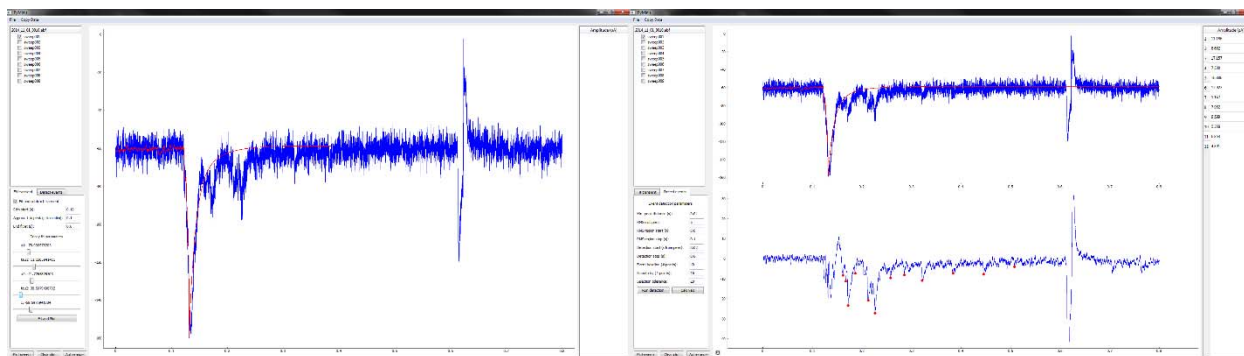


Figure A3. PyMinis workflow

(Left) A trace from an evoked-minis experiment is shown. The red line represents the calculated fit for the transient. An initial fit is generated automatically, and then the parameters – amplitude 1 (a_1), tau 1, amplitude 2 (a_2), tau 2, and offset (c) – are modified by the user to more accurately fit the transient. (Right) The transient is then subtracted from the original trace (top). The trace is filtered and miniature events detected based on the user-defined parameters. Detected events are marked by red marked (bottom). Incorrect markers can be removed, while missed events can be marked by the user. The amplitudes of the events are then reported.

to running event detection. The parameters of this fit are made available for manual tweaking through a series of sliders (Figure A3, left). Events are detected based on user-defined parameters relating to event amplitude with respect to the root mean square (RMS) of the noise. Additionally, single peaks can be selected or de-selected by the user by simply right or double-left clicking on the either unmarked or marked event (Figure A3, right). Once the correct events have been marked, their amplitudes are calculated and displayed.

Miscellaneous

On several occasions, smaller applications were built with the intention of providing a more efficient means by which to analyze a regularly-performed experiment. Two examples of these are presented below.

Calcium Oscillation Analysis

One of the major areas of studies for the lab is the enhanced vulnerability of neuron populations in PD. As part of this, experiments examining calcium oscillations in the dendrites of pacemaking cells are often performed. Recently the lab has developed techniques using Fura-2 to quantify, in units of calcium concentration, the magnitude of these events. This is done by first hyperpolarizing cells to generate a maximum fluorescence value, and then converting the raw fluorescence values of the recording of interest in to a calcium concentration with nanomolars as the unit using the equation:

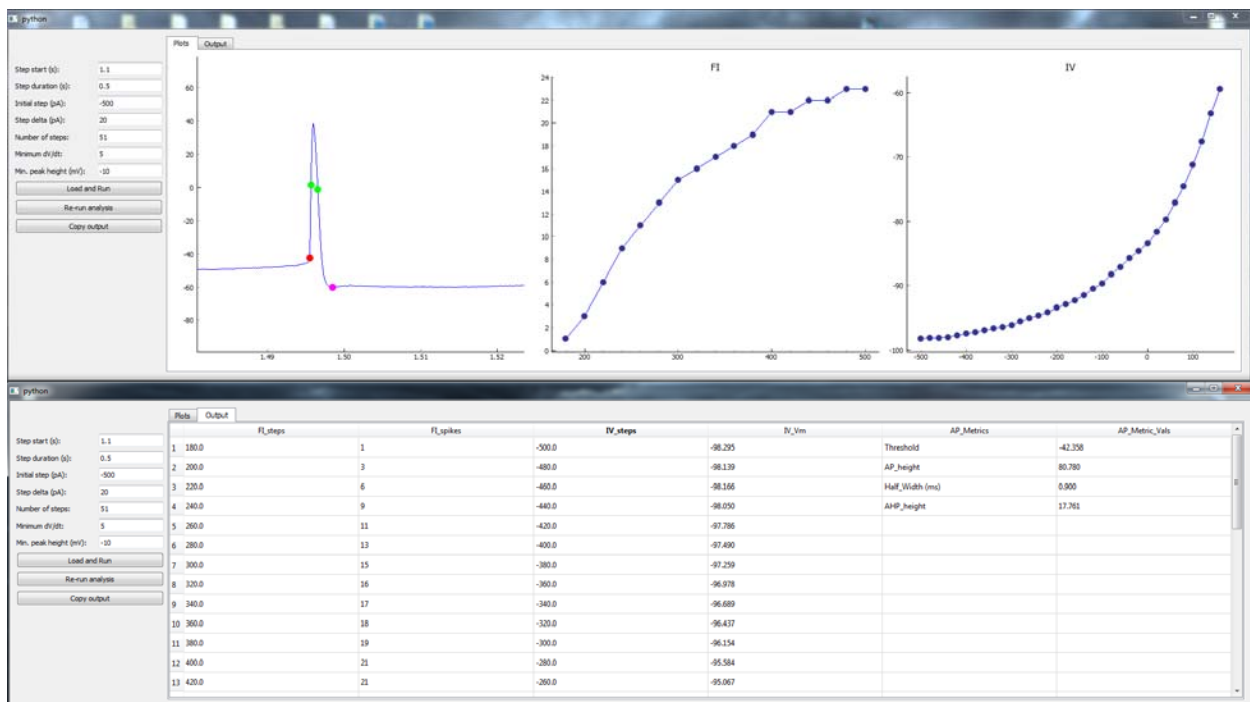
$$[\text{Ca}^{2+}] = \frac{K_d * 1 - f / f_{max}}{f / f_{max} - 1 / R_f}$$

An application was built to first perform this conversation based on the user specifying a calibration file, followed by analysis of each of the individual oscillations in an associated

recording file. The steps in the analysis are plotted, and a data table with the output measures for each oscillation is generated (Figure A4).

Frequency-Current and Current-Voltage Analysis

Another often performed experiment in the lab is to apply a series of hyperpolarizing and depolarizing current steps to a cell in order to generate, respectively, current-voltage (IV) and frequency-current (FI) plots. This provides information about the intrinsic properties of the cell. Additionally, the first spike produced is often analyzed to determine spike waveform properties such as half-width and threshold. An application was built to generate the IV, FI, and action potential metrics from a file containing a series of current steps. The user provides information about the current step protocol (i.e. number



amplitude (pink marker), AP height, and half-width (green markers). (Middle) An FI curve is plotted, where the first step is defined as the step where the first spike occurs. (Right). All other steps are used to generate an IV. (Bottom) The values for the FI, IV, and action potential metrics are provided in a table.

of steps, initial step amplitude, current delta between steps), along with the desired voltage-change per unit time (dV/dt) for determining threshold. The application uses the negative steps preceding the detection of the first spike for generating the IV, while any steps after a spike is detected (including that step) are used for the FI. Action potential height is defined as the difference between the peak of the AP and threshold, while the AHP height is defined as the difference between the peak of the AHP and threshold. The half-width is calculated from the nearest points to the half-height (i.e. half the AP height) on the rising and falling phases of the action potential.